

Imaging development and plasticity in the mouse visual system

Dissertation

zur Erlangung des Grades eines Doktors
der Naturwissenschaften

der Fakultät für Biologie
der Ludwig-Maximilians-Universität München

vorgelegt

von

Sonja Hofer

München, Mai 2006

Erstgutachter: PD Dr. Mark Hübener

Zweitgutachter: Prof. Dr. Benedikt Grothe

Tag der mündlichen Prüfung: 22.06.2006

Ehrenwörtliche Versicherung:

Ich versichere hiermit ehrenwörtlich, dass ich die Dissertation mit dem Titel „Imaging development and plasticity in the mouse visual system“ selbständig und ohne unerlaubte Beihilfe angefertigt habe. Ich habe mich dabei keiner anderen als der von mir ausdrücklich bezeichneten Hilfen und Quellen bedient.

Erklärung:

Hiermit erkläre ich, dass ich mich nicht anderweitig einer Doktorprüfung ohne Erfolg unterzogen habe. Die Dissertation wurde in ihrer jetzigen oder ähnlichen Form bei keiner anderen Hochschule eingereicht und hat noch keinen sonstigen Prüfungszwecken gedient.

München, den 23.05.2006

Sonja Hofer

Acknowledgements

First and foremost I wish to thank PD Dr. Mark Hübener for being such a great, caring and helpful supervisor. Besides creating a wonderful working atmosphere, he, even in the most stressful situations, always took the time to listen and help, to give advice and to thoroughly discuss scientific and personal issues. I continuously felt warmly and cheerfully guided and at the same time enjoyed the freedom to develop my own ideas and work independently.

I am also very grateful to Prof. Dr. Tobias Bonhoeffer for giving me the opportunity to accomplish my PhD thesis in his excellent laboratory. I always felt assured of his generous support and warm encouragement. I was time and time again impressed by his amazing skill to negotiate his busy schedule, as he always found the time for valuable counsel, advice and discussion.

I would like to thank the members of my thesis committee, Prof. Dr. Benedikt Grothe, Prof. Dr. Martin Korte and Prof. Dr. Axel Borst for fruitful discussions and helpful suggestions.

I am thankful to Volker Staiger who, besides relieving me of the hated task of solution making, is always extremely competent and very patient towards any kind of question or problem. Thanks also to Max Sperling for his help with programming and general computer problems.

Special thanks to the ‘in vivo’ gang for shared sorrows, encouraging conversations, wonderful tap dances and highly enriched Monday afternoons, and to the girls from the ‘Blocksberg’ for always having an open ear and a cheery comment, it is a pleasure to share room with you.

I really enjoyed the good spirits in the Bonhoeffer department. Thanks to everybody for the very nice time, enjoyable lunches and coffee breaks, relaxing sports activities and especially all the tasty cakes, which often saved my day.

My deep gratitude goes to my family for making all this possible, always standing behind me and spoiling me in the kindest way.

All my thanks and love to Thomas Mrsic-Flögel for simply being everything I could possibly ever ask for.

Table of contents

Table of contents	1
Summary	3
Abbreviations	5
1. Introduction	6
1.1. The mouse visual system	7
1.2. Visual system development	9
1.3. Ocular dominance plasticity in mouse visual cortex.....	13
1.4. Summary of aims	23
2. Altered map of visual space in the superior colliculus of mice lacking early retinal waves	25
2.1. Abstract	25
2.2. Introduction.....	26
2.3. Material and Methods.....	27
2.4. Results.....	29
2.4.1. Imaging intrinsic signals in the SC.....	29
2.4.2. Stimulus mapping reveals broader activations in the SC of $\beta 2^{-/-}$ mice.....	30
2.4.3. Mapping functional retinotopy in the SC	32
2.4.4. Gross retinotopic organization is altered in the SC of $\beta 2^{-/-}$ mice	34
2.4.5. Size, elongation and orientation of response patches vary systematically along the SC	36
2.5. Discussion.....	39
2.5.1. Mapping intrinsic signals in the SC.....	39
2.5.2. Local topography is functionally less refined in $\beta 2^{-/-}$ mice	39
2.5.3. Coarse retinotopy is altered in $\beta 2^{-/-}$ mice.....	40
2.5.4. General implications for activity-dependent map formation.....	42
3. Prior experience enhances plasticity in adult visual cortex	43
3.1. Abstract	43
3.2. Introduction.....	44

3.3. Material and Methods	45
3.4. Results	48
3.4.1. Imaging of mouse binocular visual cortex	48
3.4.2. Determining OD shifts with intrinsic optical imaging.....	50
3.4.3. Critical period MD facilitates OD plasticity in adults	51
3.4.4. Adult MD experience facilitates subsequent OD plasticity.....	53
3.4.5. The facilitatory effect of prior MD is eye specific	57
3.5. Discussion	59
3.5.1. Intrinsic signal imaging of OD plasticity.....	59
3.5.2. Strength of eye representation after juvenile and adult MD	60
3.5.3. Facilitation of adult OD plasticity by prior MD experience	61
3.5.4. Specific trace in the visual cortex	62
3.5.5. General implications.....	63
4. Monocular deprivation induces bidirectional scaling of eye-specific responses in primary visual cortex.....	65
4.1. Abstract.....	65
4.2. Introduction	66
4.3. Material and Methods	68
4.4. Results	71
4.4.1. Mapping ocular dominance with in vivo calcium imaging	71
4.4.2. Bidirectional changes of eye-specific responses induced by MD	73
4.4.3. Orientation selectivity in mouse visual cortex after MD	79
4.5. Discussion	82
4.5.1. Imaging calcium transients in mouse binocular visual cortex.....	82
4.5.2. Organization and specificity of functional properties	83
4.5.3. Homeostatic OD plasticity.....	84
4.5.4. MD-induced changes in orientation tuning	86
4.5.5. General conclusions	87
5. Overview and Outlook	89
6. References	94
Publications based on the work in this thesis	114
Curriculum vitae.....	115

Summary

Neuronal activity, both intrinsically generated and sensory-evoked, is known to play an important role in the development of the brain. Sensory experiences continue to exert a strong influence on the functional connectivity of neuronal circuits, especially in the cerebral cortex, allowing for learning and adaptation to an ever changing environment. The visual system provides a convenient and well established model to study both development and experience-dependent plasticity of neuronal circuits. The aim of this thesis is to employ the mouse visual system to explore how neuronal activity influences the formation of brain circuits and mediates their experience-dependent modification later in life.

In the first part of this thesis (Chapter 2), I examined the role of retinal activity in the formation of topographic maps in a target region of retinal ganglion cells. It is generally assumed that in order to obtain such highly precise and ordered maps during development, spontaneous patterns of neuronal activity are crucial for the refinement of connections. Applying intrinsic signal imaging to mouse superior colliculus (SC), I confirmed this assumption by showing that functional connectivity is less precise in transgenic mice with disrupted patterns of retinal ganglion cell activity. In comparison to normal mice, visual stimuli activated larger, less defined regions in the SC in mice lacking early retinal waves. Surprisingly, I also found that the overall topographic organization was affected by the lack of correlated spiking in the retina. Although the rough retinotopic organization was maintained, the map showed substantial distortion, indicating that patterned retinal activity before eye-opening plays a more important role in topographic map formation than previously thought.

Later in development, sensory-evoked activity is equally influential in shaping functional connectivity, since altered sensory input induces strong changes in cortical circuitry. Closure of one eye for a few days (monocular deprivation, MD), for instance, substantially changes cortical responsiveness to the two eyes, shifting ocular dominance (OD) towards the non-deprived eye. This paradigm therefore provides a powerful model system for experience-dependent plasticity. In Chapter 3, I used intrinsic signal imaging to assess the magnitude of cortical responses evoked by stimulation of the two eyes in order to explore OD plasticity in

mouse visual cortex. I confirmed recent, debated findings in demonstrating strong MD-induced plasticity in adult animals, which was mediated by partly different mechanisms than in juvenile mice. I also found that restoring binocular vision after MD led to full recovery of eye-specific responses at all ages. Interestingly, the prior experience of altered sensory input seemed to be somehow preserved in cortical circuits, such that subsequent cortical adaptation to the same experience was improved. A second MD resulted in much faster and more persistent OD shifts. This enhancement of plasticity was highly specific, as it was only observed for repeated deprivation of the same eye, indicating that a lasting trace was established in cortical connections by the initial experience.

In Chapter 4, I explored OD plasticity in greater detail by monitoring network activity at the level of individual neurons with *in vivo* two-photon imaging of calcium signals. Monitoring calcium transients associated with neuronal activity in up to hundred cells simultaneously, enabled me to examine MD-induced changes in the functional properties of each neuron independently. I found that, in general, deprived eye responses were weakened and non-deprived eye responses strengthened after MD in juvenile mice, as was expected from previous population response measurements. Neurons still dominated by deprived-eye inputs, however, did not lose their responsiveness, but rather exhibited enhanced responses following MD. This strongly suggests that homeostatic plasticity acted on these cells during deprivation and caused an up-scaling of their responsiveness, while neurons also receiving substantial input from the non-deprived eye shifted their responsiveness towards that eye. Both competitive and homeostatic processes therefore seem to operate during OD plasticity, depending on the distribution of functional inputs in individual cells.

In conclusion, the work presented in this thesis provides further insight into the role of activity-dependent mechanisms in determining and shaping functional connectivity in the brain.

Abbreviations

BDNF	brain-derived neurotrophic factor
CamKII	Ca ²⁺ /Calmodulin-dependent kinase II
cAMP	cyclic adenosine-5'-monophosphate
CREB	Ca ²⁺ /cAMP-responsive element binding protein
dLGN	dorsal lateral geniculate nucleus
Erk	extracellular-signal regulated kinase
GABA	gamma-aminobutyric acid
GAD	glutamic acid decarboxylase
LGN	lateral geniculate nucleus
LTP	long-term potentiation
LTD	long-term depression
MD	monocular deprivation
MF	magnification factor
mGluR2	metabotropic glutamate receptor type 2
nAChR	nicotinic acetylcholine receptor
NMDA	N-methyl-D-aspartate
PKA	cAMP-dependent protein kinase
OD	ocular dominance
OSI	orientation selectivity index
RGC	retinal ganglion cell
SC	superior colliculus
STDP	spike-timing dependent plasticity
tPA	tissue plasminogen activator
TTX	tetrodotoxin
V1	primary visual cortex
VEP	visually evoked potential

1. Introduction

One of the most important tasks our brain has to master is the processing and interpretation of sensory information, and the subsequent execution of adequate behaviours. A highly complex network of several brain regions, their neuronal circuits and interconnections provides the substrate for these processes. How the trillion of functionally meaningful connections in the brain are formed during development and how they are shaped and modified later by learning and experience is one of the most exciting questions in neuroscience research.

Early brain development is mostly achieved through genetically predefined processes, governed by the differential expression of molecules in space and time. These molecules serve to guide migrating cells, steer outgrowing axons, or specify topographic maps. In general, however, a hardwired system emerging only from such intrinsic cues would probably be sufficient for simple organisms that merely rely on reflexes and predefined chains of actions and reactions. But in order to accomplish more complex behaviours and flexible reactions to environmental challenges, external cues and experiences should take their part in setting up and shaping a precisely connected nervous system. Thus, particularly in higher-order organisms, experience and learning play an important role in development and throughout life. Despite great effort, the detailed mechanisms that mediate learning and the formation of memories are still far from being understood. This is largely due to the fact that learning of certain skills or tasks is a very complex process, often involving interactions between several brain areas. Therefore, relatively simple and standardized model systems are often used to study experience-dependent plasticity and learning.

Sensory systems are highly amenable for investigating the role of experience in regulating the development and plasticity of neuronal circuits *in vivo*. Compared to brain networks involved in higher cognitive functions, sensory pathways are much better understood and easier to manipulate. In the 1960s, Nobel Prize winners David Hubel and Torsten Wiesel pioneered this research by studying experience-dependent plasticity in the mammalian visual system. They found that alterations of the sensory input lead to strong adaptive changes in cortical

circuits (Wiesel and Hubel 1963). Over the last decades a large number of studies in many different vertebrate species have added to our knowledge about the formation and plasticity of neuronal maps and circuits. Recently, however, research has increasingly concentrated on the mouse as an experimental animal. With the expanding repertoire of transgenic and knockout techniques that became available for the mouse in recent years, this species offers great advantages over other mammals for studying the cellular and molecular mechanisms of development and plasticity. Since I have used the mouse visual system to address such questions in my thesis, I will now present a brief introduction into the visual system of this species.

1.1. The mouse visual system

Before the establishment of the mouse as the mammalian model organism for genetic manipulations, this species was largely neglected by visual neuroscientists. Being a nocturnal animal, the mouse predominantly relies on other sensory cues like olfactory and tactile information and is often thought to have a simple visual system with rather poor vision. Though it is true that the visual acuity of the mouse is considerably lower than that of higher mammals (about 0.5 cycles/degree, compared to about 6 cycles/degree in the cat and up to 80 cycles/degree in certain primate species, Gianfranceschi et al. 1999), mice undoubtedly use, and sometimes even preferentially rely on visual information (Etienne et al. 1996). Mice can be trained rapidly on visual tasks (Prusky and Douglas 2003); in fact, in all studies using the popular Morris water maze (Morris 1984) to study memory function in mice, visual cues are used by the animal to find the hidden platform.

Importantly, the mouse visual system shares most of the principal features with visual systems of higher mammals. The main visual pathway consists of projections from the retina to the dorsal lateral geniculate nucleus (LGN) in the thalamus, from where the sensory information is relayed to the primary visual cortex (Fig. 1.1), and further on to several secondary visual areas for higher-order processing. Retinal ganglion cell (RGC) axons also project to other target areas, including the superior colliculus (SC) in the midbrain, which receives multiple sensory inputs and is involved in orienting in space and the generation of eye- and head movements.

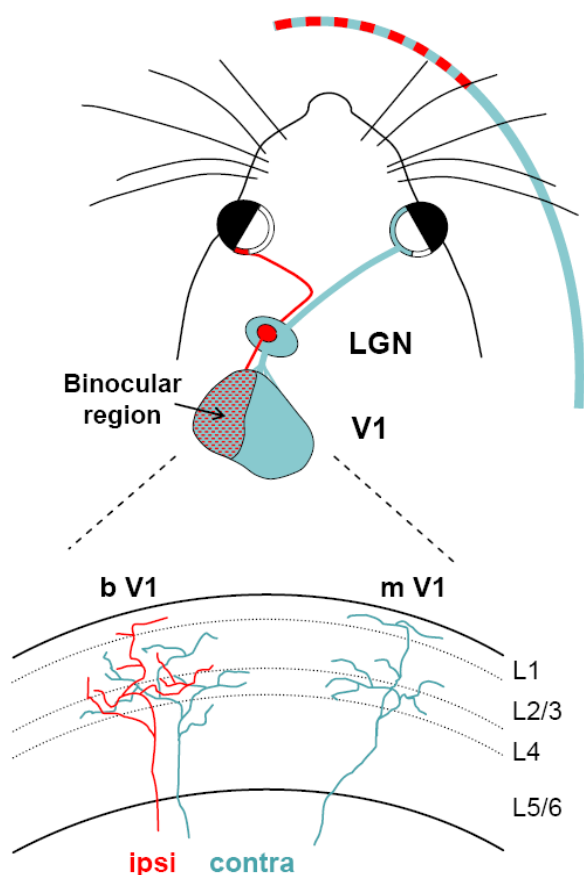


Figure 1.1. A schematic of the mouse visual system.

Most retinal ganglion cell axons (turquoise) project to the contralateral lateral geniculate nucleus (LGN). From there visual information is passed on to the primary visual cortex (V1). A small eye-specific region in the LGN and subsequently, the lateral third of V1, are additionally innervated by ipsilateral projections from the temporal retina (red). Although neurons in the binocular region of V1 are dominated by contralateral eye input, most neurons respond to both eyes. Thalamocortical axons from the LGN arborise not only within layer 4 (L4) but also in superficial layers (L1-3). bV1: binocular V1, mV1: monocular V1.

The different stages of visual processing all contain a continuous representation of visual space, a so called retinotopic map. The spatial information of the image is thereby preserved, such that adjacent points in the visual field activate neurons at adjacent positions in these structures. As in most other mammals, the visual field of the mouse contains a notable binocular region which is seen by both eyes (Dräger 1975, Wagor et al. 1980). While the majority of RGC axons cross over to the other hemisphere at the optic chiasm, a small fraction of RGCs from the temporal retina project to the ipsilateral hemisphere, to allow for binocular processing of corresponding visual information from the central visual field in higher visual areas, e.g. for depth perception (Fig. 1.1). In the SC and LGN, the inputs from both eyes are still completely separated in eye-specific regions (Rossi et al. 2001). The mouse primary visual cortex (V1), however, contains a binocular region, where the large majority of cells respond to stimulation of either eye, although the contralateral input is mostly dominant.

The binocular region comprises about one third of V1 (Dräger 1975, Wagor et al. 1980, Gordon and Stryker 1996), a surprisingly large portion, considering that only 3-5% of the RGC axons project ipsilaterally (Williams et al. 2003). How this discrepancy arises is unclear, but it is conceivable that the ipsilateral eye representation in the visual cortex could be strengthened by callosal projections, connecting the two hemispheres.

The visual cortex of higher mammals such as cats or monkeys shows a highly ordered organization of many response properties. It is composed of small columnar units extending through the six cortical layers, in which neurons share similar stimulus preferences. For instance, cortical cells preferentially responding to one or the other eye are grouped together, leading to alternating ocular dominance (OD) columns (Hubel and Wiesel 1977, LeVay et al. 1978). Likewise, neurons preferring similar stimulus orientations or directions are clustered in orientation and direction columns (Bonhoeffer and Grinvald 1991, Weliky et al. 1996). In contrast, in mice as well as in other rodent species, no pronounced columnar organization has been demonstrated so far in the visual cortex (Metin et al. 1988, Schuett et al. 2002, Van Hooser et al. 2005). Nonetheless, individual neurons exhibit functional properties similar to higher mammals: Most cells prefer edge- or bar-like stimuli rather than circular spots, with a significant fraction of neurons being sharply tuned to different stimulus orientations and directions. In fact, all major functional classes of neurons described for higher mammals can also be found in the mouse (Dräger 1975, Mangini and Pearlman 1980, Metin et al. 1988). Receptive field sizes, however, are considerably larger in mouse visual cortex (Metin et al. 1988, Grubb and Thompson 2003), which partially explains the substantially lower visual acuity in this species.

1.2. Visual system development

Since the early stages of visual processing in vertebrates are well described both anatomically and functionally, they serve as popular model systems to study the development of neural networks, especially to address the role of sensory experience versus genetically predefined cues in setting up functional circuits. Whereas there is general consent that the early stages of development like the generation and specification of cells and brain areas, cell migration and directed axon growth are guided by molecular cues, the importance of internal versus external

factors for the recognition and specific innervation of the appropriate target neurons is still strongly debated. Studies on visual system development have particularly concentrated on two processes: The formation of topographic maps with their complex ordered representation of sensory space, and the segregation of inputs from the two eyes in eye-specific layers or regions in the target area.

Retinotopic map formation

Most knowledge about the mechanisms of topographic map formation has been obtained from studying the developing retinotectal system. Extensive research of how retinal ganglion cells find their appropriate target in the optic tectum (or the superior colliculus in mammals) has led to the concept that the basic topographic order is achieved by molecular guidance cues, while activity-dependent mechanisms provide subsequent refinement of connections in order to obtain a highly precise retinotopic map. Essentially confirming Sperry's chemoaffinity hypothesis (Sperry 1963), it was found that cell surface molecules, expressed in a complementary and graded fashion in the retina and its target regions, act as positional labels by mediating repulsion or attraction of outgrowing retinal axons (Cheng et al. 1995, Drescher et al. 1995). Members of the Eph receptor family and their ephrin ligands seem to play an especially important role. The mapping of the anterior-posterior axis in the tectum, for instance, is tightly controlled by matched expression gradients of EphA receptors in the retina and ephrins in the tectum mediating axon repulsion (Flanagan and Vanderhaeghen 1998, McLaughlin et al. 2003a). Equally, axon attraction based on EphB/EphrinB interactions seems to guide medio-lateral patterning (Hindges et al. 2002). Eph receptors and ephrins have been found to act quite universally, not only mediating intra-areal organization in various target regions (Feldheim et al. 1998, Cang et al. 2005a), but also controlling inter-areal specificity (Dufour et al. 2003). More recently, additional factors have been demonstrated to be required for topographic map formation (Brown et al. 2000, Mui et al. 2002, Schmitt et al. 2006).

In birds and mammals, the molecular cues governing map formation do not seem to directly guide RGC growth cones, but rather mediate specific interstitial branching (Yates et al. 2001, McLaughlin et al. 2003b) in the appropriate termination zone (TZ). RGC growth cones invade the target region quite generously and show extensive overshoot. Precise topography develops

subsequently by large-scale retraction, stabilisation of appropriate branches and further selective arborisation (Fig. 1.2, McLaughlin et al. 2003b, Ruthazer et al. 2003).

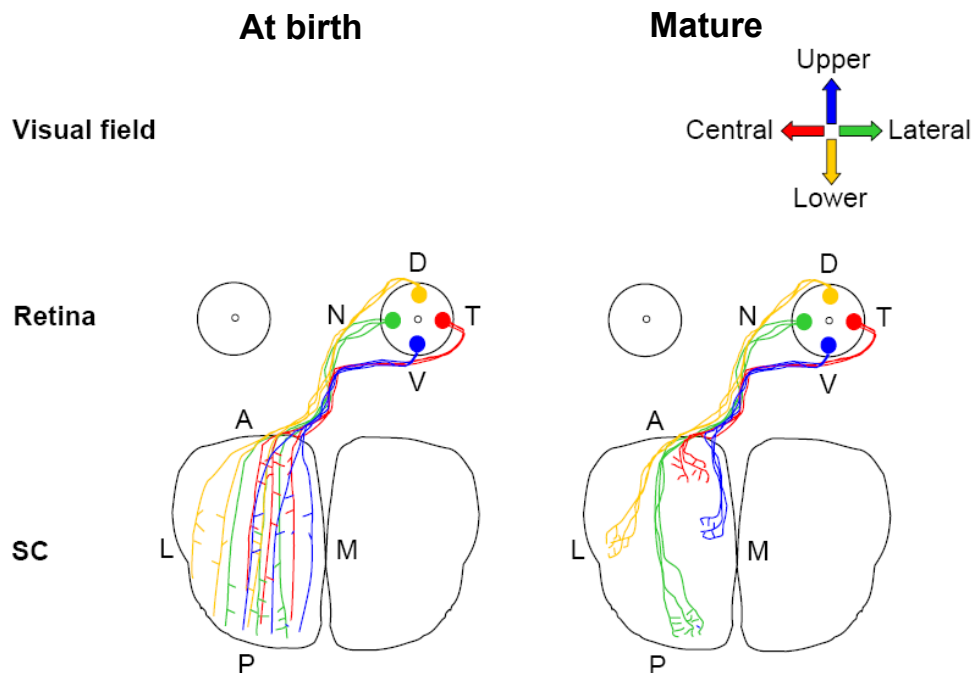


Figure 1.2. Development of the retinotopic map in the mouse SC. Large-scale remodelling takes place during the development of retinocollicular projections. Initially RGC axons invade the entire extent of the SC, and overshoot their future target region (left, at birth). RGC axon refinement then proceeds by elimination of inappropriate branches and selective branching within the final termination zone, leading to the mature retinotopic map (right).

If RGC activity is blocked, however, termination zones remain large and the connectivity unrefined (Kobayashi et al. 1990, Simon et al. 1992). Thus, map refinement is believed to depend on activity-dependent mechanisms. The formation of most retinotopic maps is complete long before vision starts to drive neuronal networks, and hence is unlikely to be shaped by sensory experience. Earlier in development, however, patterned neuronal activity arises intrinsically in different brain regions (McCormick et al. 1995, Yuste et al. 1995), best described for the retina, where spontaneous waves of activity cause highly correlated spiking of neighbouring RGCs, whereas RGCs from distant retinal regions (or the two eyes) show no correlations in their spiking patterns (Galli and Maffei 1988, Meister et al. 1991, Wong et al. 1995). These retinal waves are perfectly suited to refine retinotopic maps in the retinal target

regions through Hebbian mechanisms, by strengthening of correlated inputs and weakening of uncorrelated inputs.

Recently, several interrelated studies provided strong evidence supporting this idea. Retinal waves are initially mediated by cholinergic transmission from starburst amacrine cells (Feller et al. 1996, Wong 1999, Zheng et al. 2006). Mice deficient for the $\beta 2$ subunit of the nicotinic acetylcholine receptor ($\beta 2^{-/-}$ mice) lack early retinal waves, but show normal levels of ganglion cell activity (Bansal et al. 2000, McLaughlin et al. 2003b). This disruption of correlated retinal activity patterns leads to much broader, less refined projections of RGC axons both in the SC (McLaughlin et al. 2003b) and the LGN (Grubb et al. 2003). Consequently, $\beta 2^{-/-}$ mice also show abnormal functional properties of neurons in both target regions (Grubb et al. 2003, Chandrasekaran et al. 2005). These results strongly suggest that neuronal activity does not simply play a permissive role in map formation, but that it directly instructs map refinement by correlation-based rules. The resumption of correlated RGC activity in $\beta 2^{-/-}$ later on, when retinal waves start to be mediated by glutamate, does not essentially improve the phenotype (McLaughlin et al. 2003b, Grubb et al. 2003), indicating that the early period of correlated spiking is especially important. Recently, formation of the orderly projection from LGN to visual cortex has been suggested to equally depend on retinal waves, since geniculocortical mapping is also imprecise in $\beta 2^{-/-}$ mice (Cang et al. 2005b). While the role of correlated spiking for map-refinement is therefore quite well established, it is completely unresolved if neuronal activity is also important for the overall retinotopic organization. This question will be addressed in the first part of my thesis (Chapter 2).

Eye-specific segregation in the LGN

In the LGN as well as in the SC the inputs from both eyes terminate in separate eye-specific layers or regions. During development, RGC axons from the eyes are strongly overlapping (Linden et al. 1981), and the gradual segregation of left and right eye afferents is a classical example for the strong influence of neuronal activity on circuit development. Complete blockade of early RGC activity prevents eye-specific segregation in the LGN (Penn et al. 1998) and altering the level of activity in one eye leads to size changes of the eye specific target regions (Stellwagen and Shatz 2002), indicating that the development of eye-specific regions is an activity-dependent, competitive process. The formation of ordered eye-specific layers at

invariant positions, e.g. in the ferret LGN, however, suggests that molecular guidance cues are also involved in determining the rough position of eye-specific RGC axon termination (Sanes and Yamagata 1999). A recent study showed that gradients of EphA receptors and ephrinA ligands mediate appropriate targeting of eye-specific projections (Huberman et al. 2005). If after the blockade of retinal spiking, patterned RGC activity is resumed later, inputs from the eyes can still completely segregate; however, they do not form ordered eye-specific layers, but show a patchy distribution (Huberman et al. 2002). Lamination mediating cues therefore seem to be restricted to earlier periods, whereas segregation of inputs is activity dependent.

It is still disputed if neuronal activity plays an instructive, correlation-based role in eye input segregation. Disrupting correlated RGC activity by specific depletion of cholinergic amacrine cells in the ferret retina does not affect ocular segregation in the LGN (Huberman et al. 2003). However, this might well be due to some remaining correlated firing of RGCs in this study, since disruption of patterned retinal spiking in the $\beta 2^{-/-}$ yields exactly the same non-segregated phenotype as complete activity blockade (Rossi et al. 2001, Muir-Robinson et al. 2002), strongly supporting a segregation mechanism based on correlated activity.

In conclusion, it has become more and more apparent over the last decades that cooperation between molecular factors and activity-dependent mechanism seems to be a common rule for the formation of neuronal networks, while the relative importance of the different cues might vary for different developmental processes.

1.3. Ocular dominance plasticity in mouse visual cortex

During the last phases in neural system maturation, neuronal activity, especially evoked by sensory experience, becomes a major factor in shaping and refining neuronal circuits. While earlier stages of sensory processing quickly lose the ability to be modified by sensory experience in postnatal development, in order to guarantee reliable transmission of information, the mammalian cortex maintains experience-dependent plasticity throughout life, enabling learning and adaptation to the surrounding environment. Ever since in the 1960s Torsten Wiesel and David Hubel discovered that the binocular representation in primary visual cortex is particularly susceptible to changes in visual experience, ocular dominance (OD) served as an important model system for exploring the cellular and molecular

1. Introduction

mechanisms underlying the plasticity of cortical circuits. Their groundbreaking studies in young kittens demonstrated fast and strong adaptive changes of neuronal circuits in response to the imbalanced binocular input caused by transient lid closure of one eye (referred to as monocular deprivation, MD), leading to a shift in the preference of cortical neurons for the eye that remained open (Wiesel and Hubel 1963). This shift in OD is associated with degraded vision through the deprived eye after reopening (Muir and Mitchell 1973).

Although the phenomenology of OD shifts has been described in detail in several species (Dräger 1978, Hubel et al. 1977), the underlying cellular and molecular mechanisms are still largely unresolved and merit further study. In this context, the mouse, which shows OD shifts that are comparable to those of higher mammals (Fig. 1.3, Dräger 1978, Gordon and Stryker 1996), has emerged as a valuable experimental model due to its amenability to genetic manipulation. Since a major part of this thesis is concerned with the mechanisms of OD plasticity, below I will summarise the relevant findings on OD plasticity obtained over the last few years, especially focusing on underlying mechanisms and the recent discovery of plasticity in the visual cortex of adult mice.

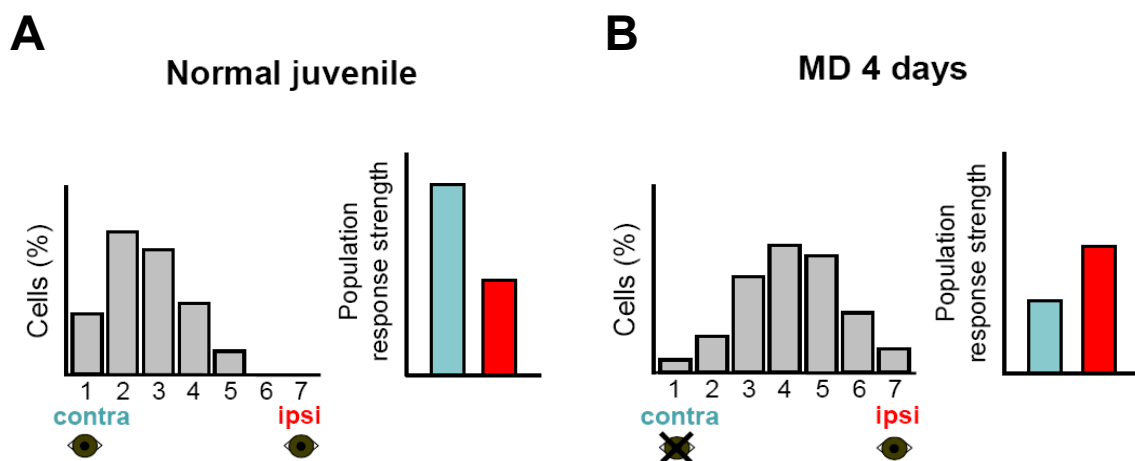


Figure 1.3. Schematic depicting OD plasticity in juvenile mice. Four days of MD in juvenile mice (around P28) lead to strong changes in binocular cortical responses. The ocular dominance of neurons, which normally show a strong preference for the contralateral eye (A), shifts towards the non-deprived, ipsilateral eye (B). This shift is mainly due to weakening of deprived eye responses (right panels). Ocular dominance classes from 1-7 indicate relative responsiveness of neurons to contra- and ipsilateral eye stimulation (1 or 7, cells only respond to the contralateral or ipsilateral eye, respectively; 4, equal response to both eyes).

Ocular dominance plasticity in juvenile animals

In the primary visual cortex of higher mammals, strong OD shifts following eye closure have only been reported during a limited postnatal period, the so called critical period (Hubel and Wiesel 1970). Although recent studies revealed pronounced plasticity in mouse visual cortex throughout life (see below), the binocular representation still seems to be more sensitive to experiential changes early in life (Gordon and Stryker 1996). In general, the early sensitive period is not a fixed developmental phase but rather is influenced by external cues – its onset can be accelerated or delayed, as demonstrated by overexpressing brain-derived neurotrophic factor (BDNF) or rearing animals in the dark, respectively (Huang et al. 1999, Mower 1991). These manipulations affect the maturation of inhibitory circuits in the visual cortex (Huang et al. 1999, Chen et al. 2001), which appear to be the key determinant for initiating the critical period: A certain level of local inhibition seems to be the crucial trigger, as mice deficient of the minor GABA synthesizing enzyme GAD65, which display a relatively mild phenotype of weaker GABA release upon stimulation, do not exhibit OD shifts after short-term MD (Hensch et al. 1998). Enhancing inhibitory transmission pharmacologically at any time restores normal OD plasticity in GAD65 knock-out mice, and is also able to precociously trigger critical period onset in normal mice (Hensch et al. 1998, Fagiolini and Hensch 2000). Specifically, OD plasticity may only become possible when the mature balance of excitation and inhibition in cortical networks arises through the activity of fast-spiking basket cells providing input onto pyramidal neuron synapses that contain the $\alpha 1$ subunit of the GABA_A receptor (Fagiolini et al. 2004).

Mechanisms of OD plasticity

Whereas a mature inhibitory network is important for enabling OD plasticity, the majority of studies addressing the mechanisms of OD plasticity have concentrated on changes at excitatory synapses. Early, long-favoured theories postulated that inputs from the eyes concurrently compete for postsynaptic space and resources from target neurons, such as neurotrophic factors (Guillery 1972, Bonhoeffer 1996). However, as yet no evidence has been provided for such a direct competition in the binocular cortex. In fact, in rodents, modifications in the monocular zone of the visual cortex (where no competition can occur) have been demonstrated after contralateral MD, resembling those taking place in the binocular

region (Heynen et al. 2003, Pham et al. 1999). Hence, in the last decade, the focus of discussion shifted towards alternative, homosynaptic mechanisms of OD plasticity, whereby inputs from the two eyes are affected independently by MD (Bear 2003). In support of this idea, eye closure in young animals causes *first* a weakening of deprived eye connections and *only later* a strengthening of inputs from the eye that remained open (Fig. 1.3, Mioche and Singer 1989, Frenkel and Bear 2004, Antonini and Stryker 1993).

Many recent studies have tried to gain insight into the cellular and molecular mechanisms underlying the strengthening and weakening of inputs from the eyes by relating them to those involved in long term potentiation (LTP) and depression (LTD) at central synapses. Although the electrical induction of synaptic plasticity in vitro cannot be directly compared to the complex experience-dependent changes of neuronal circuits in an intact animal, such studies are nonetheless helpful in exposing the molecular pathways potentially contributing to plasticity in vivo. Indeed, the very early phase of MD-induced plasticity in the visual cortex resembles NMDA receptor-dependent LTD or at least employs similar mechanisms (Heynen et al. 2003). Likewise, the signalling pathway through specific isoforms of cAMP-dependent protein kinase (PKA), has been shown to be required for OD plasticity as well as different forms of synaptic plasticity in the visual cortex in vitro (Fischer et al. 2004, Rao et al. 2004). In contrast, synaptic depression mediated by metabotropic glutamate receptor type 2 (mGluR2) does not seem to play a role (Renger et al. 2002).

Some recent data in mice are at odds with the view that homosynaptic LTD at excitatory synapses is the sole mediator of OD shifts during the first days of deprivation. Alpha calcium calmodulin kinase II (alpha-CaMKII) activity, which is mainly associated with synaptic LTP in vitro, plays a role in short-term OD plasticity (Taha et al. 2002). Furthermore, OD plasticity is blocked after overexpression of the protein phosphatase calcineurin (Yang et al. 2005), which is known to be important for synaptic LTD (Torii et al. 1995). Enhanced activity of this enzyme is not expected to inhibit the weakening of deprived eye inputs, especially since visual cortex LTD appears normal in calcineurin overexpressing mice (Yang et al. 2005). In addition, further downstream in the potential signalling pathways, the activation of kinases and transcriptional regulators, such as erk and CREB, respectively, and changes in gene expression have been implicated in OD shifts (Di Cristo et al. 2001, Mower et al. 2002, Krahe et al. 2005). Together, these results indicate that OD plasticity is not mediated by a single, straightforward

signalling cascade, but rather involves several interacting processes that may act differentially on different cell types.

It is also well established that the shift in functional connectivity is followed by substantial reorganisation of thalamocortical axon arbors (Antonini and Stryker 1993). In the mouse, however, notable axonal remodelling takes several weeks of deprivation (Antonini et al. 1999). This finding is perhaps not surprising considering that axons subserving the left and the right eye are strongly intermingled in this species and provide input to many cells in the binocular visual cortex, and therefore reorganisation during the early phase of MD is only expected to occur on a local scale. Indeed, OD plasticity correlates with much more rapid structural changes in mouse visual cortex at the level of dendritic spines, which bear the majority of excitatory synapses in the brain. Two days of MD increased the motility of spines, hinting at a destabilization of functional connections (Oray et al. 2004). Four days of MD, which induce saturating OD shifts in juvenile mice (Gordon and Stryker 1996), led to significant spine loss on apical dendrites of layer 2/3 pyramidal neurons (Mataga et al. 2004), consistent with the initial, strong reduction of cortical responsiveness to deprived eye stimulation. Formation of new connections from open eye inputs may occur only after longer deprivation periods (Mataga et al. 2004), consistent with the subsequent strengthening of the representation of the open eye.

Tissue plasminogen activator (tPA) may provide an important link between the early stages of synaptic plasticity and the structural changes following MD, since in tPA knockout mice neither functional OD shifts nor structural changes occur after MD (Mataga et al. 2002, Mataga et al. 2004, Oray et al. 2004). This secreted protease presumably enables or promotes synapse destabilization and spine pruning by cleavage of cell adhesion molecules and other extracellular matrix proteins (Shiosaka and Yoshida 2000). Alternatively, tPA might also act indirectly, for instance via activation of BDNF (Pang et al. 2004), a molecule associated with synaptic plasticity *in vitro* and OD shifts *in vivo* (Huberman and McAllister 2002).

Interestingly, spine loss was not observed in the monocular portion of mouse visual cortex after short-term MD (Mataga et al. 2004), even though brief deprivation induces LTD-like changes in this region (Heynen et al. 2003). Since LTD is known to be associated with spine pruning (Nägerl et al. 2004, Zhou et al. 2004), these findings necessitate a more complex

explanation of how MD affects individual neurons. It is conceivable that intrinsic, compensatory mechanisms prevent severe changes in the innervation of monocular neurons. A flexible modification threshold, as outlined in the Bienenstock-Cooper-Munro (BCM) model (Bienenstock et al. 1982, Bear 1995), could regulate the strength and direction of plasticity at individual synapses, depending on the overall strength of activation of the neuron. The higher firing rates of binocular neurons, which also receive non-deprived eye inputs, would thereby promote synaptic depression of the weak, deprived-eye inputs, whereas in neurons only receiving inputs from the deprived eye, the low post-synaptic activity would inhibit further weakening of synaptic transmission. This idea of an indirect interaction of eye inputs according to the BCM theory is supported by the finding that complete silencing of one eye by TTX injections seems to prevent weakening of deprived-eye inputs, but accelerates strengthening of open-eye inputs in visual cortex (Rittenhouse et al. 1999, Frenkel and Bear 2004).

While the cellular and molecular mechanisms of OD plasticity have recently attracted much attention and debate, a more basic question remains unexplored, namely which features of the altered sensory input initiate the synaptic modifications. Do the changes induced by MD simply arise from the weaker drive at deprived eye synapses or are OD shifts instead mediated by changes in the temporal structure of the inputs? The precise millisecond timing of pre- and postsynaptic activity can determine the direction of synaptic plasticity in vitro (Bi and Poo 1998, Markram et al. 1997). Such spike timing dependent plasticity (STDP) also leads to changes in response properties of neurons in the visual cortex in vivo (Schuett et al. 2001, Froemke and Dan 2002). In the somatosensory cortex, the timing of stimulation-evoked spiking is altered strongly after whisker deprivation (Celikel et al. 2004). It will therefore be important to investigate whether in the visual cortex MD also alters the relative timing of arrival of inputs from the eyes and whether STDP shifts OD. This could explain why the maturation of the inhibitory circuitry is important for OD plasticity, enabling more precise timing of postsynaptic activity by fast inhibition (Fagiolini et al. 2004).

While it is commonly believed that it is the level or pattern of activity reaching the cortex which determines the extent and direction of cortical plasticity, recent data points to another potential mechanism (Mandolesi et al. 2005): MD was found to decrease the levels of BDNF in the deprived retina, and replenishing retinal BDNF by exogenous application

counteracted the MD effect in the cortex. Moreover, it was also shown that BDNF is transported from the retina to the LGN. These results suggest that there might be an additional signal which informs the cortex of an altered sensory input, namely the anterograde transport of molecular factors.

OD plasticity in adult visual cortex

In contrast to the classic notion of a critical period for experience-dependent plasticity (Hubel and Wiesel 1970), several studies have recently reported that OD shifts in mice can also be induced in adulthood (Sawtell et al. 2003, Lickey et al. 2004, Tagawa et al. 2005). Strong OD plasticity was demonstrated after MD in adult mice with visually evoked potentials under different anaesthetic regimes and, importantly, also in awake animals (Sawtell et al. 2003, Lickey et al. 2004). A study using the activity reporter gene *Arc* to assess functional eye representation in mouse visual cortex additionally showed MD effects prior to as well as after the traditional critical period (Tagawa et al. 2005). Given these results, the concept of a strict critical period for OD plasticity seems, at least in the mouse, not to hold true. Nevertheless, the binocular cortical representation is still more sensitive in juvenile mice, as in adults OD shifts require longer MD durations and are generally somewhat smaller (Sawtell et al. 2003, Lickey et al. 2004).

Previous studies failing to detect adult plasticity used barbiturate anaesthesia (Fagiolini and Hensch 2000), which seems to specifically mask the OD shift in adult mice (Pham et al. 2004). Interestingly, the differential effect of barbiturates in juvenile and adult mice suggests that mechanisms of OD plasticity may change with age, which is also apparent from other studies. Whereas in juvenile mice both an initial weakening of deprived eye responses and subsequent strengthening of open eye responses contribute to the shift in OD (Frenkel and Bear 2004), in adults the MD effect is mostly due to NMDA receptor-dependent strengthening of open-eye inputs, when testing the hemisphere contralateral to the deprived eye (Sawtell et al. 2003). The absence of the fast loss of input from the contralateral eye after deprivation probably explains why short periods of MD (≤ 3 days) are insufficient to induce OD shifts at older ages, since strengthening of the open-eye representation is delayed and takes longer to develop even in juvenile animals (Frenkel and Bear 2004). In general, however, depression of inputs is still possible in adult visual cortex. The innately weaker, ipsilateral eye representation undergoes

further weakening after ipsilateral eye closure in adult mice (Tagawa et al. 2005), and therefore seems to remain particularly susceptible to altered experience in adulthood.

It remains unknown whether substantial structural rearrangements that accompany functional OD shifts in juvenile animals also occur in the mature cortex during MD. Morphological plasticity of synaptic structures is associated with functional reorganisation after retinal lesions in visual cortex of adult cats (Darian-Smith and Gilbert 1994). Moreover, in adult mice, formation and pruning of synapses still occur in visual cortex (Holtmaat et al. 2005), and in the somatosensory cortex spine turnover is enhanced by sensory deprivation (Trachtenberg et al. 2002). The spine loss apparent in the juvenile visual cortex after four days of contralateral eye MD was not observed in adult animals (Mataga et al. 2004), consistent with the absence of significant weakening of deprived-eye inputs in the contralateral hemisphere at older ages (Sawtell et al. 2003). Interestingly, however, there was a weak trend for spine gain, which may correspond to the strengthening of non-deprived eye inputs (Mataga et al. 2004). Since in adult visual cortex longer deprivation periods are necessary for saturating OD shifts, it is plausible that longer periods of MD (>6 days) would yield significant synaptic remodelling. Because structural plasticity is thought to become more limited in scope as the brain matures (Grutzendler et al. 2002, Holtmaat et al. 2005, Pizzorusso et al. 2002), it is possible that OD plasticity in adulthood relies more on other mechanisms – including changes in inhibitory circuitry, as implicated by the masking of adult OD shifts by barbiturates, which mainly agonise inhibitory transmission. For instance, the potentiation of the non-deprived, ipsilateral eye responses may actually be caused by a depression of eye-specific inhibitory activity. In fact, *in vitro*, the potentiation of field potentials in adult visual cortex has been shown to be entirely due to LTD at inhibitory synapses (Yoshimura et al. 2003). The application of barbiturates might therefore enhance inhibitory transmission and thereby occlude the ‘disinhibition’ of the non-deprived eye inputs.

The potential for large-scale plasticity in adult primary visual cortex is restricted in most mammals, and even in the mouse it does not match the extent of plasticity found in juvenile animals. Rearing animals in the dark has long been known to enable strong plasticity in the visual cortex of older animals by retarding the maturation of cortical circuits (Cynader and Mitchell 1980). Recently, it has also been demonstrated that visual deprivation in adult rats re-established a more immature cortical state, leading to enhanced OD plasticity (He et al. 2006).

However, the influence of this sensory deprivation paradigm is short-lasting, since brief periods of vision restore a mature, less plastic status quo in cortical circuits (Philpot et al. 2003). Three recent studies identified factors that restrict plasticity in the mature visual cortex. Pharmacological degradation of the ECM by cleaving glycosaminoglycan chains reactivated OD plasticity in adult rats (Pizzorusso et al. 2002, Pizzorusso et al. 2006). Genetic deletion of the Nogo receptor, which mediates myelin-associated inhibition of neurite outgrowth after nerve injury, equally enhanced adult plasticity (McGee et al. 2005). The maturation of ECM and myelin-associated molecules therefore presumably adversely affects OD plasticity by inhibiting the remodelling of synaptic structures.

Recovery from MD

Another way of exploring visual cortex plasticity is to study the effect of re-establishing binocular vision after MD. In models of OD plasticity based solely on competition, recovery from MD is not expected to occur when the deprived eye is simply re-opened. But in fact full recovery of binocular responses after a period of binocular vision has been shown in different species (Mitchell et al. 1977, Kind et al. 2002, Liao et al. 2004). One might assume that recovery from MD is simply a reversal of the initial MD effect, but recent studies suggest otherwise. The induction of OD shifts and their recovery seem to be mediated by fundamentally differential processes, as recovery from MD does not require CREB activation or protein synthesis (Liao et al. 2002, Krahe et al. 2005). Moreover, in ferrets, the recovery of deprived eye responses has been demonstrated to occur within hours, thus much faster than the initial OD shift, and it is not restricted to the critical period for MD effects (Liao et al. 2004, Krahe et al. 2005). No substantial recovery occurs after early-onset, long-term MD (Prusky and Douglas 2003, Liao et al. 2004). This is not surprising, since depriving one eye of salient input early in postnatal development is very likely to prevent regular formation of thalamocortical connections and integration of deprived eye inputs into the cortical network, thus permanently disrupting visual processing through this eye.

Open questions

Ocular dominance plasticity in visual cortex has long served as a useful model for examining how cortical circuits are shaped by experience. Altered activity at deprived eye synapses initiates a sequence of cellular and molecular events such that the cortex becomes more

responsive to the eye that remained open. While progress has been made in identifying some of the underlying physiological and biochemical processes, many important questions remain unanswered. In particular, the differential factors that mediate and influence cortical plasticity in juvenile and adult animals require further investigation. A fast screening method is therefore essential, which ideally should be capable of measuring absolute changes in population responses to stimulation of each eye. Optical imaging of intrinsic signals is a method which can do exactly that. At present it is also largely unresolved how the local circuitry within the cortex is affected by MD. Are there differential effects depending on input type, cell class or cortical layer? Monitoring network activity at the single cell level by means of *in vivo* 2-photon calcium imaging (Ohki et al. 2005) is very well suited to solve some of these important questions.

Exploring the MD-induced shifts in cortical responsiveness might also give more general insights into how the brain learns and makes use of previous experiences. In this context it is important to investigate the long-term consequences of the cortical adaptations following MD. In the barn owl auditory localization system it was found that prior experience of altered sensory input in juvenile animals enhances similar types of plasticity in adulthood (Knudsen 1998). It is tempting to speculate that this represents a general concept for learning, which might also hold true in the visual cortex. If so, one might expect that the experience of MD could alter the capacity for plasticity, making the cortex more susceptible to a similar experience later in life.

This thesis aims at answering some of these questions by applying modern imaging techniques to the mouse visual cortex (Chapter 3 and 4).

1.4. Summary of aims

It is by now well established that molecular cues and neuronal activity work hand in hand to set up a functional nervous system. Neuronal spiking becomes especially important during later phases of development, but even before sensory experience starts to evoke neuronal activity, intrinsically generated spiking patterns contribute to shaping neuronal networks. The work presented in this thesis aims to explore the role of neuronal activity in the formation and plasticity of neuronal circuits at different developmental stages, using the visual system of the mouse as a model system. The employed methods were chosen to assess functional organization and plasticity at different levels, from single cell to population responses.

In **Chapter 2** I will investigate to what degree the formation of topographic maps is influenced by neuronal activity. As described above, it is generally assumed that neuronal connections and maps are refined by activity-dependent mechanisms. Applying optical imaging of intrinsic signals to obtain functional retinotopic maps in mouse superior colliculus, I will examine the role of patterned retinal activity in the refinement of functional connectivity as well as for setting up the overall retinotopic organization.

In **Chapter 3** I will employ intrinsic signal imaging as well as extracellular recordings to assess experience-dependent plasticity in binocular visual cortex of juvenile and adult mice. In particular, I will describe experiments investigating the processes underlying the strong changes in cortical circuitry following MD and the long-term consequences of such a transiently altered experience on cortical circuits at different ages.

In **Chapter 4** I will explore the functional fine-scale architecture of mouse visual cortex and OD plasticity using in vivo 2-photon calcium imaging. By studying MD-induced changes in cortical networks at the single-cell level I hope to learn more about the plasticity rules governing experience-dependent circuit changes.

2. Altered map of visual space in the superior colliculus of mice lacking early retinal waves

2.1. Abstract

During the development of the mammalian retinocollicular projection, a coarse retinotopic map is set up by the graded distribution of axon guidance molecules. Subsequent refinement of the initially diffuse projection has been shown to depend on the spatially correlated firing of retinal ganglion cells. In this scheme, the abolition of patterned retinal activity is not expected to influence overall retinotopic organization, but this has not been investigated. We used optical imaging of intrinsic signals to visualize the complete retinotopic map in the superior colliculus (SC) of mice lacking early retinal waves, caused by the deletion of the $\beta 2$ subunit of the nicotinic acetylcholine receptor. As expected from previous anatomical studies in the SC of $\beta 2^{-/-}$ mice, regions activated by individual visual stimuli were much larger and had less sharp borders than those in wild-type mice. Importantly, however, we also found systematic distortions of the entire retinotopic map: the map of visual space was expanded anteriorly and compressed posteriorly. Thus, patterned neuronal activity in the early retina has a substantial influence on the coarse retinotopic organization of the SC.

2.2. Introduction

The principles of retinotopic map formation in the midbrain have been studied extensively over the past decades (Bonhoeffer and Huf 1982, Sperry 1963, Cline and Constantine-Paton 1989). However, a comprehensive understanding of the mechanisms that specify the coarse retinotopic layout of the retinocollicular projection is still lacking. Whereas the initial preference of retinal ganglion cell (RGC) axons for topographically appropriate positions is mediated by axon guidance molecules (Cheng et al. 1995, Drescher et al. 1995, Feldheim et al. 2000, Frisen et al. 1998, Hindges et al. 2002), the precise topography develops during the first postnatal week by large-scale retraction of inappropriately-targeted axonal branches and selective arborisation within the target region (McLaughlin et al. 2003b, Simon and O'Leary 1992). As discussed in greater detail in Chapter 1 (Section 1.2.), this remodelling is thought to be regulated by waves of activity which sweep across the immature retina and correlate the firing of neighbouring RGCs (Bansal et al. 2000, Galli and Maffei 1988, Meister et al. 1991, Wong et al. 1995), thereby stabilizing their connections to common target neurons (Changeux and Danchin 1976, Butts 2002, Willshaw and von der Malsburg 1976, Wong 1999).

Because retinal waves are initially mediated by cholinergic (nicotinic) synaptic transmission during the first postnatal week (Bansal et al. 2000, Feller 2002, Wong et al. 2000, Zhou and Zhao 2000), mice deficient for the $\beta 2$ -subunit of the nicotinic acetylcholine receptor ($\beta 2$ -/- mice; (Picciotto et al. 1995, Xu et al. 1999) lack early retinal waves while maintaining decorrelated spontaneous activity (McLaughlin et al. 2003b). Retinofugal projections in $\beta 2$ -/- mice are indeed broader than in control animals (Grubb et al. 2003), arguing strongly for correlated retinal activity being instrumental in refinement of RGC axon arborisations in target structures. Moreover, electrical recordings from LGN neurons in $\beta 2$ -/- mice revealed disrupted fine-scale mapping (Grubb et al. 2003), indicating that imprecise projections bear functional consequences. Although these results made a clear case for patterned activity in the regional refinement of retinofugal projections, they did not demonstrate whether the disruption of retinal waves influences the coarse layout of the retinotopic map. If the retinotopic preference of RGC axons is predominantly specified by molecular cues, it is expected that the abolition of retinal waves during the remodelling period would result in an expansion of RGC axon arborisations without a significant perturbation of gross retinotopy.

To understand how the lack of retinal waves affects the overall retinotopic organization in target areas requires the complete visualization of the retinotopic map, which was not possible in previous studies. We used optical imaging of intrinsic signals (Grinvald et al. 1986, Bonhoeffer and Grinvald 1996, Schuett et al. 2002, Kalatsky and Stryker 2003) to obtain functional retinotopic maps from the surface of the entire SC. We show that visual stimuli activate much larger regions of the SC in $\beta 2^{-/-}$ mice than in control animals, and that, surprisingly, coarse retinotopy is systematically altered. Our results suggest that patterned retinal activity is more influential than previously thought in establishing retinotopic maps.

2.3. Material and Methods

Surgery

Experiments were performed on 15 wild-type (wt) and 13 $\beta 2^{-/-}$ mice (3-5 months old, (Picciotto et al. 1995) that were back-crossed at least 10 times to the C57BL/6 strain. All surgical and experimental procedures were in accordance with the guidelines of the local government. Mice were chamber-anaesthetized with 2-2.5% halothane in a 1/1 mixture of N_2O/O_2 , then intubated (1.5 mm polythene tubing) and ventilated with 1.5-2% halothane in the same gaseous mixture. After affixing the ear bars, the scalp was resected, and a 3×4 mm craniotomy was carried out over the posterior part of the left hemisphere. The left SC was exposed by careful aspiration of the overlying cortex, covered over with 2% agarose in saline, and sealed with a coverslip (Fig. 2.1A). The skull was glued to a head bar, and the ear bars were removed to allow unobstructed vision.

Intrinsic signal imaging and visual stimulation

Details of the imaging equipment and visual stimulation were described previously (Schuett et al. 2002). The SC was illuminated with 707 nm light and images (600 ms in duration) were captured with a cooled slow-scan CCD camera (ORA 2001, Optical Imaging, Germantown, NY), focused 200-300 μm below the SC surface. During each 9-second stimulation trial, 4 blank frames were acquired before the 11 frames during which visual stimuli were presented. A monitor (Mitsubishi Pro 2020) was placed 13.5 cm from the right eye, at a 45° angle to the long body axis, covering the visual field between 0° to 108° in azimuth and -10° to 62° in

elevation. Stimuli were rectangular square-wave drifting gratings (0.04 cycles/degree; 2 cycles/s) that changed their orientation every 0.6s, presented randomly at different positions in the visual field. Overall retinotopy was mapped with 24 abutting 18° stimuli (6×4 grid design), spanning 108° in azimuth and 72° in elevation. For comparing the spread of SC responses in wt and $\beta 2^{-/-}$ mice, stimuli of five different sizes (side length 12°, 15°, 20°, 24.5°, 30°) were each shown at 3 fixed, adjacent positions (15° centre spacing) within the central region of the right visual hemifield.

Image analysis

Single position maps were computed by clipping (1.5%) and high-pass filtering blank-corrected image averages of 12-30 stimulus repetitions (see Schuett et al. 2002 for details). For each single condition map the patch area was determined as the area of all pixels with values \geq 50% of the maximum response. The 50% response region was defined by plotting a contour line for 50% of the maximum response in Gaussian-smoothed single position maps. The overlap between adjacent patches was calculated according to the following formula: $O = (N_o) / (N_1 + N_2 - N_o)$, where N_o is the number of shared pixels by both patches, and N_1 and N_2 are the number of pixels for the two patches which had values \geq 50% of the maximum response. Patch semi-profiles are normalized responses as a function of distance from the centre of the patch, obtained by radial averaging of pixel values from the patch centre. Colour-coded 'best position maps' were calculated from single position maps that were additionally clipped (3%), Gaussian-smoothed (kernel width = 99 μ m) and thresholded at >1 SD of the mean blank image value. The colour of each pixel indicates the stimulus that elicited the strongest response in that pixel, whereas colour saturation indicates the inverse magnitude of that response. Maps obtained from different animals were averaged after alignment by translation and rotation, such that the patches evoked by the middle 2 rows of stimuli (of the 6×4 grid) were matched best. Patch centres are the centre coordinates of 2D Gaussians fitted to patches in single position maps. The magnification factor was calculated by dividing the Euclidean distance between patch centre coordinates by the difference of visual field angle (18°). Patch orientation was defined as the angle, relative to the image axes, of the major axis of the 2D Gaussian fits of individual patches, whereas patch elongation was the ratio of the major to minor axes of those fits.

2.4. Results

2.4.1. Imaging intrinsic signals in the SC

Previous intrinsic imaging studies in rodents have been carried out in structures that lie on the surface of the brain and are thus immediately amenable to optical techniques (Masino et al. 1993, Rubin and Katz 1999, Schuett et al. 2002). We have adapted this technique to obtain functional maps also from a deeper structure in the brain - the SC of the midbrain. After aspiration of the overlying cortex, it was possible to image intrinsic signals from the SC surface (Fig. 2.1A), evoked by visual stimulation with small patches of drifting gratings at different positions in the contralateral visual field, spanning 108° in azimuth and 72° in elevation (Fig. 2.1B,C), thus allowing us to acquire maps of functional retinotopy.

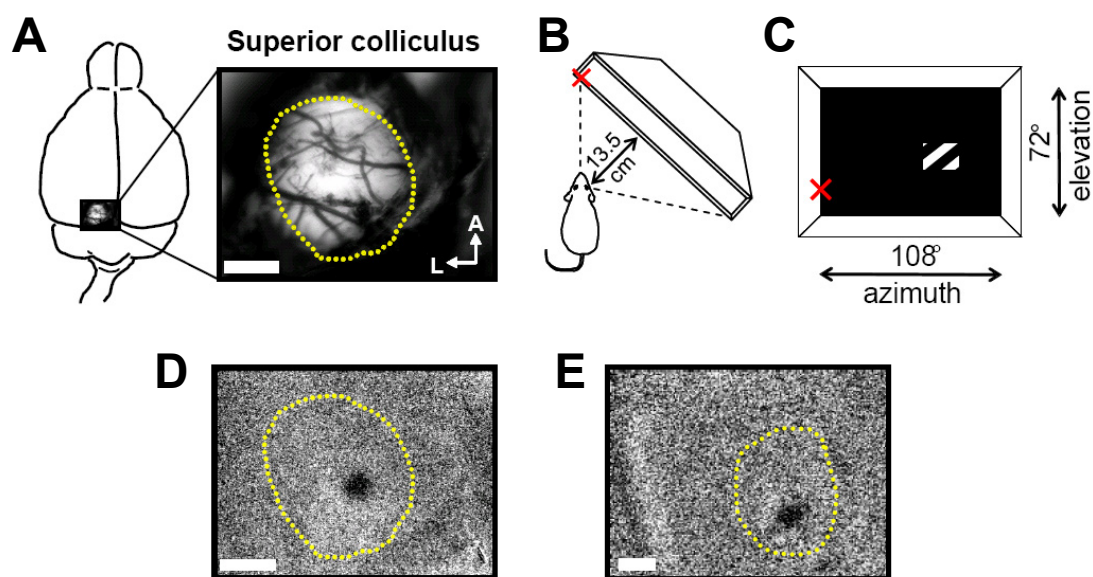


Figure 2.1: Intrinsic imaging of visual responses in superior colliculus. (A) Dorsal view of mouse brain depicting the location of the imaged area (left) that shows the surface of the left SC (right), exposed by aspirating the overlying cortex. The dotted line represents a rough outline of the SC. (B) Position of the stimulus monitor relative to the mouse, angled at 45° from the long body axis. (C) Schematic of monitor screen spanning $\sim 108^\circ \times 72^\circ$ (azimuth \times elevation) in visual space. The stimuli were square-shaped, black/white drifting gratings presented at different locations in the visual field. The red cross marks the vertical meridian and the position of the eye in elevation. (D) A single position map of the contralateral SC showing a spatially restricted response (dark patch) evoked by the presentation of a $20^\circ \times 20^\circ$ stimulus (average map from 12 stimulus presentations). (E) A single position map of a different animal from a single, 600 ms frame. Scale bars, 0.5 mm.

The activity map in Figure 2.1D shows SC activation (dark patch), obtained by presenting a $20^\circ \times 20^\circ$ stimulus (Fig. 2.1C) twelve times at the same position in the visual field and averaging the resulting reflectance changes of the SC surface. This ‘single position’ map demonstrates that the responses in the SC to individual stimuli are spatially very restricted. Intrinsic signals in the SC were also highly robust, as we could obtain maps of high signal-to-noise, without averaging, from a single, 600 ms frame (Fig. 2.1E).

2.4.2. Stimulus mapping reveals broader activations in the SC of $\beta 2^{-/-}$ mice

In order to assay functionally how the lack of early retinal waves, mediated by the nicotinic acetylcholine receptor (nAChR), during retinotopic map refinement affects the precision of topographic mapping we compared visually-evoked responses in the SC of adult wild-type (wt) and $\beta 2^{-/-}$ mice. For each group of animals, functional maps were obtained in response to stimuli of five different sizes presented at the same position in the visual field. An example from a wt SC is shown in Figure 2.2A. Increasing stimulus size, which activates increasingly larger regions of the retina, resulted in an enlargement of the activated SC area. Note that the borders of patches remained sharp irrespective of stimulus size. Maps from $\beta 2^{-/-}$ animals were similar in that they showed a stimulus size-dependent expansion of SC activation (Fig. 2.2B). The relationship between stimulus size and activated SC area (number of pixels in the patch whose values were $\geq 50\%$ of the maximum reflectance change) was largely linear in both wt and $\beta 2^{-/-}$ animals (Fig. 2.2C). However, for any given stimulus size, patch area was significantly larger in $\beta 2^{-/-}$ mice (Fig. 2.2B,C; ANOVA, $p < 10^{-5}$). Moreover, unlike in wt mice, the patches in $\beta 2^{-/-}$ animals had a blurry appearance (Fig. 2.2B), with a significantly shallower decline of response strength from the patch centre to its periphery (Fig. 2.2D; ANOVA, $p < 10^{-5}$). These results are in keeping with anatomical studies showing expanded termination zones of retinal axons in the SC of $\beta 2^{-/-}$ mice (McLaughlin et al. 2003b, Chandrasekaran et al. 2005).

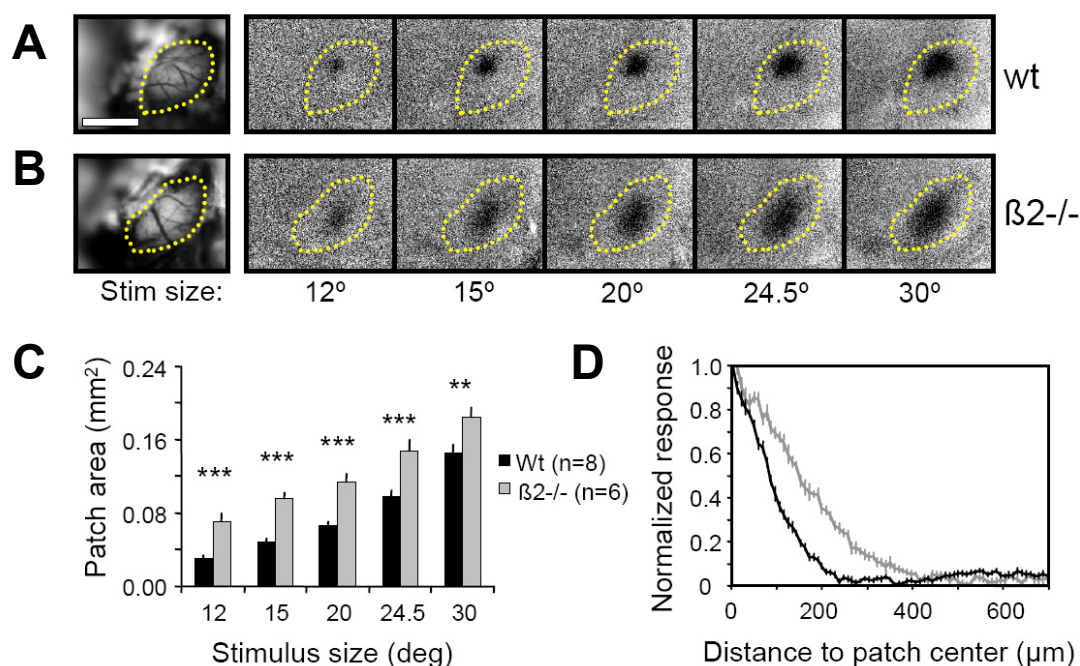


Figure 2.2. Stimulus representations in the SC of $\beta 2^{-/-}$ mice are broader than in wt animals. (A,B) Single position maps obtained with five stimulus sizes (side length: 12°, 15°, 20°, 24.5°, 30°) presented at the same position in visual space from a wt (A) and $\beta 2^{-/-}$ (B) animal. The patch area increases with stimulus size, but responses in $\beta 2^{-/-}$ animals are larger and blurrier for a given stimulus size. The dotted line outlines the border of SC, which in these experiments was not exposed fully. Scale bar: 1mm. (C) Quantification of SC response area. Mean patch area values for each of the 5 stimulus sizes from wt and $\beta 2^{-/-}$ animals. ***, $p < 0.001$, **, $p < 0.01$, t-test. (D) Mean, normalized semi-profiles of patches evoked by 12° stimuli in wt (black) and $\beta 2^{-/-}$ (gray) animals. Note that in $\beta 2^{-/-}$ mice there is a shallower decline of response with distance from patch centre and that patch width is broader for all values below the peak response. Error bars represent SEM.

Given the expanded representation of stimuli in the SC of $\beta 2^{-/-}$ mice, the same position in the SC should be activated by a larger region of visual field than in wt animals. We confirmed this by measuring the extent of overlap between representations of neighbouring stimuli. Stimuli presented at three adjacent positions (Fig. 2.3A, stimulus centre spacing: 15°) activated neighbouring regions in the SC (Fig. 2.3B-E). Keeping the centre positions constant but increasing the size of stimuli resulted in more overlap between neighbouring stimuli (Fig. 2.3A) and, as predicted, between their representations in the SC (Fig. 2.3B-E). The area of SC jointly activated by neighbouring stimuli was indeed consistently larger in $\beta 2^{-/-}$ mice (Fig. 2.3F, ANOVA, $p < 0.001$).

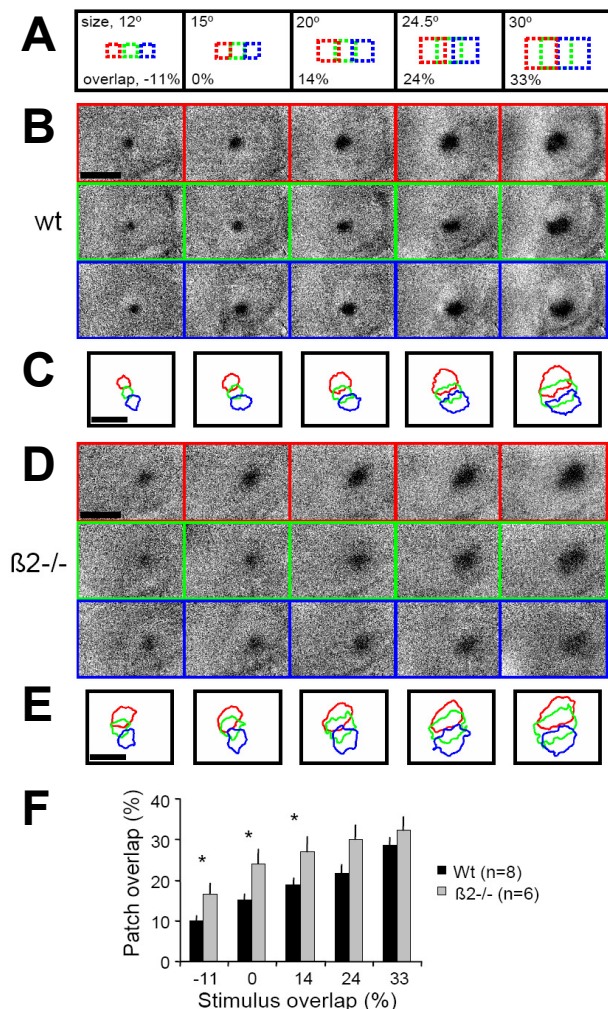


Figure 2.3. Responses to neighbouring stimuli overlap more in $\beta 2^{-/-}$ than in wt SC. (A) Stimulus configuration for the analysis of patch overlap. As stimulus size increases, the centre positions of the three stimuli remain fixed, resulting in more overlap between adjacent stimuli. Stimulus side length and overlap are indicated. (B,D) Single position maps in response to stimuli depicted in A, for a wt (B) and a $\beta 2^{-/-}$ (D) animal. (C,E) Coloured contours circumscribe the area responding stronger than 50% of response maximum of maps shown in B,D. The contour colours correspond to stimuli shown in A. Note that the responses to adjacent stimuli in $\beta 2^{-/-}$ animals overlap more than in wt mice regardless of stimulus size. Scale bars, 1mm. (F) Quantification of SC patch overlap in wt and $\beta 2^{-/-}$ animals. Patch area values for each of the 5 stimulus sizes averaged across wt and $\beta 2^{-/-}$ animals. The spread of activity in the SC was invariably larger in $\beta 2^{-/-}$ than in wt mice. The patches overlapped significantly more in $\beta 2^{-/-}$ mice. Error bars represent SEM. *, $p < 0.05$, t-test.

One possible concern is that the larger patch sizes in $\beta 2^{-/-}$ mice may arise as a consequence of increased eye movements, since it has been reported that nicotinic transmission in the monkey SC influences saccades (Watanabe et al. 2005). However, we could not detect any noticeable eye movements in anesthetized mice of either genotype. This was further confirmed by measuring the drifts of patch centres across different data acquisition blocks, and these did not differ between wt and $\beta 2^{-/-}$ mice ($p = 0.56$, t-test).

2.4.3. Mapping functional retinotopy in the SC

The representation of visual space in the mouse SC spans approximately 130° in azimuth and 90° in elevation (Dräger and Hubel 1976). In our case, the retinotopic organization of the SC was revealed by imaging intrinsic responses to adjacent $18^\circ \times 18^\circ$ stimuli that partitioned the

visual field into a 6×4 grid (Fig. 2.4B), totalling $108^\circ \times 72^\circ$. This design ensured that each stimulus could be fully seen by the mouse and drive SC responses in its entirety.

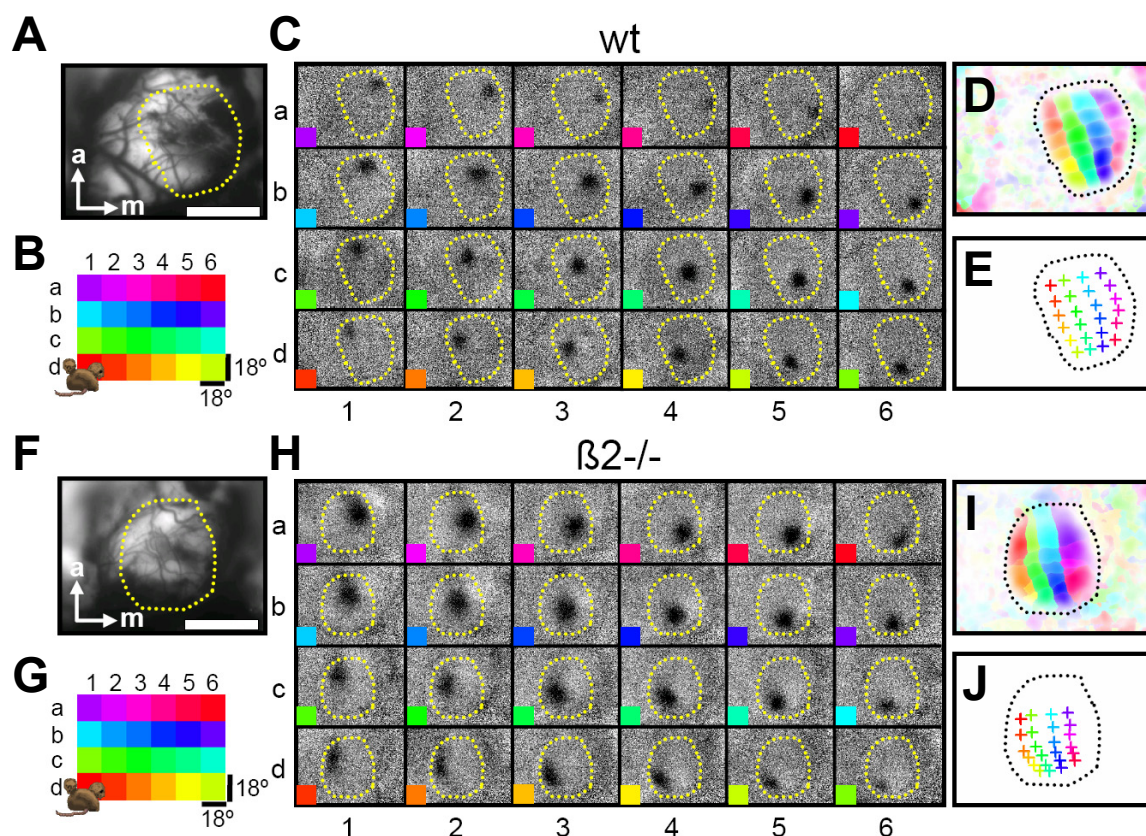


Figure 2.4. Mapping retinotopy in SC of wt and $\beta 2^{-/-}$ mice. (A,F) Imaged area. The dotted line represents a rough outline of the SC. Scale bars, 1 mm. (B,G) Layout of stimuli used for mapping SC responses. Colour denotes stimulus position. (C,H) Individual activity maps showing responses (dark patches) to 24 stimulus positions as indicated by coloured squares. Note that neighbouring stimuli activate adjacent positions in the SC. (D,I) Colour-coded maps of overall retinotopic organization in SC. For each pixel, colour denotes the stimulus position that elicited the greatest response in that part of the SC, whereas colour saturation equals the minimum intensity of all single position maps. (E,J) Spatial arrangement of patch centres (crosses), which are the centre coordinates of 2D Gaussians fitted to patches in single position maps. Note larger patches in the $\beta 2^{-/-}$ mouse, as well as a pronounced compression of visual azimuth in the posterior SC.

Each stimulus elicited a patch of activity that was adjacent to that evoked by a neighbouring stimulus (see Fig. 2.4C, for an example from a wt animal). To illustrate the organization of the entire retinotopic map, we used a colour code: each pixel in the map was assigned a colour of the stimulus position (Fig. 2.4B) that had evoked the largest response at that position in the SC (Fig. 2.4D). Shifting the stimulus position from nasal to lateral visual field resulted in a

posterior shift of SC activation. Similarly, increasing stimulus elevation activates more medial portions of the SC. To reveal the orderly progression of visual space across the SC surface, we constructed a map with discrete positions, by plotting the centre coordinates of 2-D Gaussians fitted to patches in single-position maps (Fig. 2.4E). Retinotopic maps from other wt animals ($n = 5$) were very similar.

2.4.4. Gross retinotopic organization is altered in the SC of $\beta 2^{-/-}$ mice

Having demonstrated that we can reliably map functional retinotopy from the surface of almost the entire SC, we measured responses in $\beta 2^{-/-}$ mice to assess the effect of the elimination of retinal waves on the gross retinotopic organization (Fig. 2.4F-J). It is evident that a rough topographic order was preserved, despite larger patch sizes. However, in contrast to wt mice, the patches in the anterior SC were much more elongated along the antero-posterior (A-P) axis (compare, for instance, panels a1-d1 in Fig. 2.4C,H), resulting in a shift of their centres towards more posterior positions and a compression of the retinotopic map in the posterior half of the SC (Fig. 2.4J).

For clearer visualization and to further explore these differences in retinotopic organization, we generated maps of retinotopy from averaged single-position maps within each animal group (Fig. 2.5A,B). Averaging across animals (wt: $n = 5$, $\beta 2^{-/-}$: $n = 5$) was possible because the variability between retinotopic maps from different animals was very small, as indicated by the length of error bars (standard deviation) in plots of patch centre coordinates (Fig. 2.5C,D).

The overall retinotopic organization was quantified by the magnification factor (MF), a scaling factor that relates visual field angle to distance in the SC. The MF was calculated from averaged Euclidian distances between centres of patches evoked by stimuli separated by 18° either in azimuth or elevation. In both wt and $\beta 2^{-/-}$ mice, the MFs were predominantly larger for stimuli separated in elevation (mediolateral axis of SC) compared to those separated in azimuth (Fig. 2.5F,G), and there was a slight but significant drop in MF along the A-P SC axis (Fig. 2.5F; ANOVA, $p < 10^{-5}$).

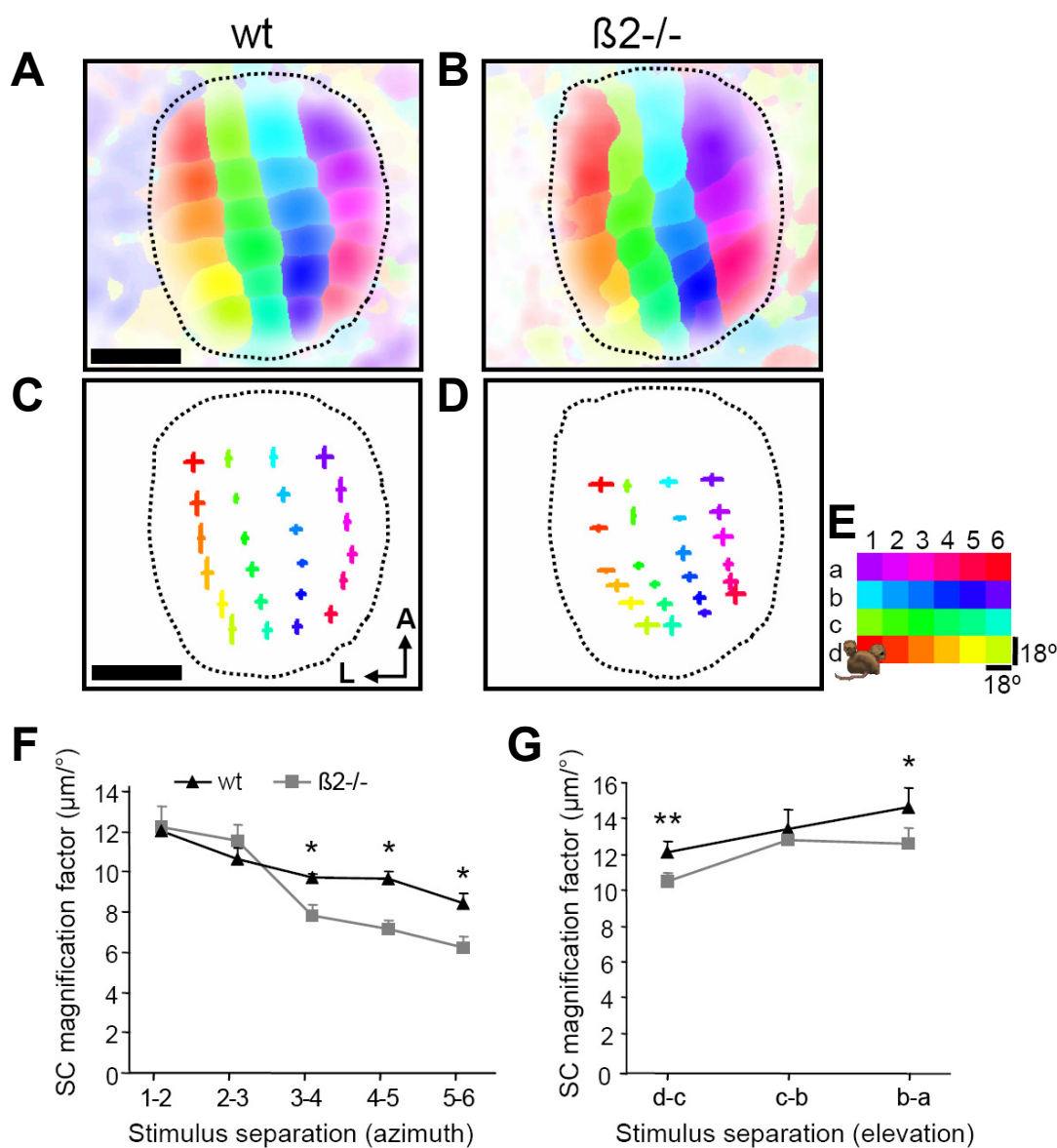


Figure 2.5. Overall retinotopic organization is altered in the SC of $\beta 2^{-/-}$ animals. (A,B) Averaged retinotopic maps from 5 wt (A) and 5 $\beta 2^{-/-}$ (B) mice. (C,D) Centres of patches from maps in A and B. The lengths of crossing lines are the standard deviations of patch centre coordinates in vertical and horizontal directions. Note the small variations within each experimental group as well as the compression of stimulus representation in the posterior part of the SC in $\beta 2^{-/-}$ animals as compared to wt animals. Colour denotes stimulus position, as shown in E. Scale bar, 0.5 mm. (F,G) Quantification of SC magnification factors (MFs). Plots show MFs calculated from mean distances between centres of patches evoked by stimuli separated in azimuth (F, averaged across elevation) or in elevation (G, averaged across azimuth) from wt (black) and $\beta 2^{-/-}$ (gray) mice. The abscissa indicates stimulus separation (always $\Delta 18^\circ$) at different visual field positions, as indexed in E. Error bars are SEM. **, $p < 0.01$, *, $p < 0.05$, t-test.

However, whereas the MFs varied smoothly across the SC surface in wt mice (Fig. 2.5C,F,G, black symbols), the retinotopic map from $\beta 2^{-/-}$ mice showed a pronounced compression of visual azimuth in the posterior part of the SC (Fig. 2.5D,F, gray symbols). This compression was specific for the representations of the temporal visual field (average MF for azimuths $> 36^\circ$, wt: 9.26 ± 0.22 , $\beta 2^{-/-}$: $7.07 \pm 0.27 \mu\text{m}/^\circ$, mean \pm SEM., $p < 10^{-5}$, t-test), as there was no difference in the MFs from the nasal visual field in the anterior SC between wt and $\beta 2^{-/-}$ mice (average MF for azimuths $< 36^\circ$, wt: 11.34 ± 0.28 , $\beta 2^{-/-}$: $11.87 \pm 0.41 \mu\text{m}/^\circ$, $p = 0.29$, t-test). There was additionally a slight but significant compression in the representation of elevation at the medial and lateral parts of the SC in $\beta 2^{-/-}$ mice (Fig. 2.5D,G; wt versus $\beta 2^{-/-}$ MF, lateral: $p < 0.01$, medial: $p < 0.05$, t-test). This is most likely a consequence of the anisotropy of spatial organization of projections innervating the SC borders in $\beta 2^{-/-}$ mice: whereas the retinocollicular axons projecting diffusely to the central regions of the SC can extend in all directions, those targeted to the edges can arborise ectopically only towards the middle. Consequently, the ‘centres of mass’ of patches from the medial and lateral SC borders, evoked by uppermost and lowermost stimuli, respectively, will necessarily be shifted centrally, and, as a result, the values of MFs in those regions of the SC are smaller (Fig. 2.5G).

The asymmetry in ectopic arborisations of projections targeted to SC periphery can, however, not explain the compression in the representation of azimuth along the A-P axis, because 1) there was no difference in MFs at the anterior edge of the SC between wt and $\beta 2^{-/-}$ mice, and 2) the compression extended far into the SC, well away from its posterior edge. In principle, changes in magnification factor values could have arisen if the overall area or shape of SC was different between $\beta 2^{-/-}$ and wt mice. However, we found no difference in the total activated area (wt: 1.57 ± 0.17 , $\beta 2^{-/-}$: $1.55 \pm 0.15 \text{ mm}^2$, $n = 5$ per group, $p = 0.76$, t-test) or aspect ratio (wt: 1.13 ± 0.04 , $\beta 2^{-/-}$: 1.15 ± 0.07 , $n = 5$ per group, $p = 0.63$, t-test) of SC between the two groups of animals.

2.4.5. Size, elongation and orientation of response patches vary systematically along the SC

Which parameters of the retinotopic map in $\beta 2^{-/-}$ mice can account for the selective compression in the representation of visual azimuth in the posterior SC? Contour plots of response patches from averaged single-position maps reveal large differences in functional

topography of retinocollicular mapping between wt and $\beta 2^{-/-}$ mice (Fig. 2.6A,B). These include changes in patch size, overlap and shape. In both wt and $\beta 2^{-/-}$ mice, patch areas were largest in the anterior SC, and decreased toward its posterior end (Fig. 2.6D). Patch sizes from the $\beta 2^{-/-}$ mice were invariably larger than in the wt mice (Fig. 2.6D), but without a significant change in the relative size difference along the A-P axis of the SC (Fig. 2.6F, black symbols). Patch area per se is therefore unlikely to account for the differences in the azimuthal MF. We therefore analyzed the shapes of the patches in both groups of mice by determining their elongation and orientation (Fig. 2.6E). In this plot, the length of each line represents patch elongation, defined as the aspect ratio of the major and minor axes of the 2-D Gaussians fitted to each response patch. The elongation values were largest in the anterolateral region of the SC in both wt and $\beta 2^{-/-}$ mice. In $\beta 2^{-/-}$ mice, however, patches were significantly more stretched out along the A-P axis (Fig. 2.6E; mean patch aspect ratio, wt: 1.27 ± 0.02 , $\beta 2^{-/-}$: 1.51 ± 0.05 , $p < 10^{-3}$, t-test). Moreover, the differences in elongation between wt and $\beta 2^{-/-}$ mice varied across the SC, being most prominent in its anterior part and rather small in the posterior part (Fig. 2.6F, gray symbols). The degree of patch elongation along the A-P axis of the SC correlated positively with MF across azimuth in $\beta 2^{-/-}$ mice, whereas no such trend was apparent in the wt animals (Fig. 2.6G). Thus, the more stretched out the patch, the greater the inter-patch distance along the A-P axis in the SC of $\beta 2^{-/-}$ animals. These data suggest that the compression in the representation of visual azimuth in posterior SC may arise because of an increased posterior expansion of retinocollicular projections in the anterior SC.

A previous study suggested that the projection from the ipsilateral eye is more exuberant in the SC of $\beta 2^{-/-}$ than in wt mice (Rossi et al. 2001). This raises the possibility that the posterior shift of patch centres in the anterior SC of $\beta 2^{-/-}$ mice (Fig. 2.5D) could arise from an increased ipsilateral projection into this region. We therefore measured SC responses through either eye in response to stimulation of frontal visual space, but failed to detect any ipsilaterally-evoked activity in both wt ($n = 2$) and $\beta 2^{-/-}$ ($n = 2$) mice (data not shown). This implies that the alterations in the topography of the contralateral eye projection take place without significant competitive influences from the ipsilateral projection.

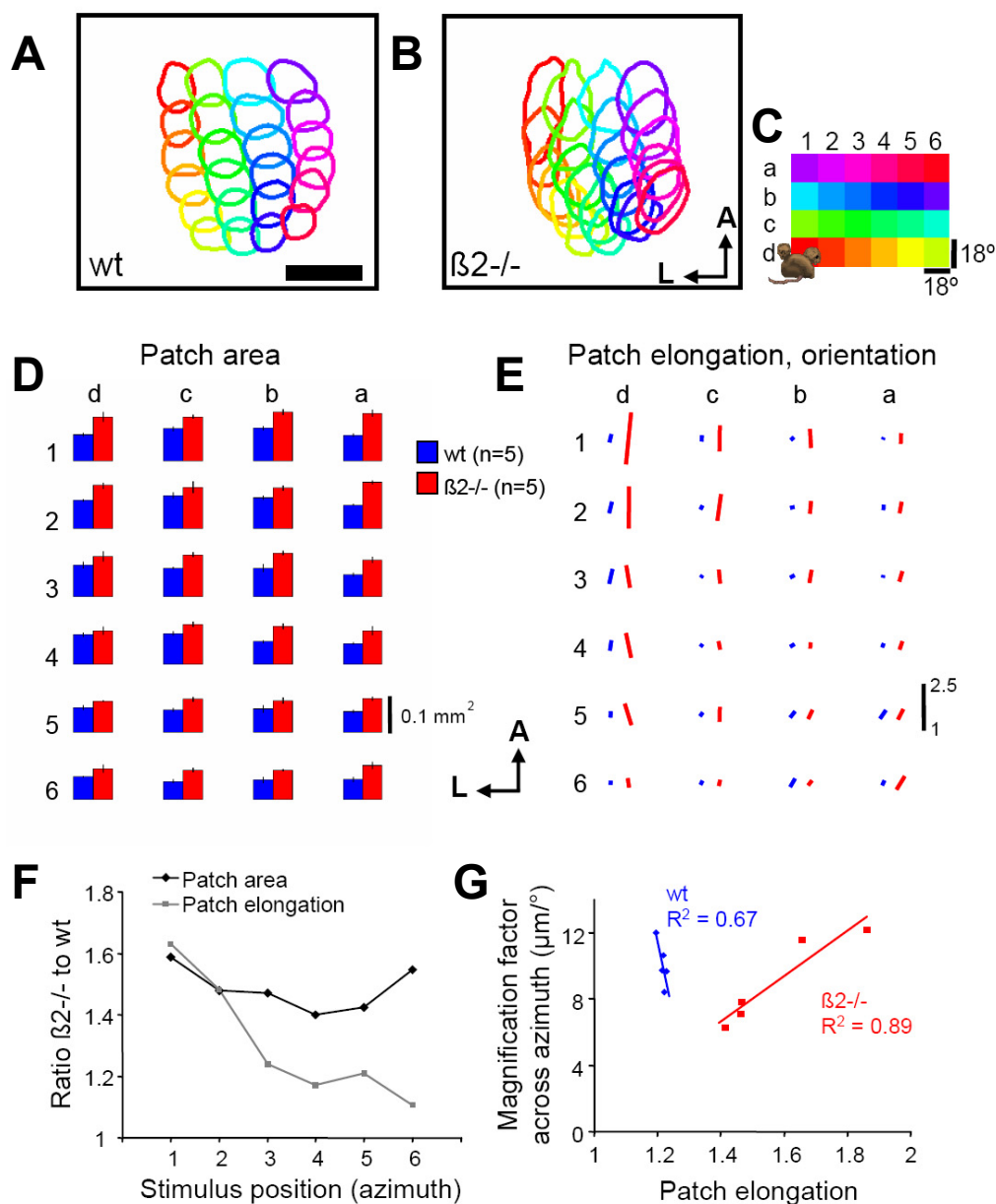


Figure 2.6. More elongated response patches in the SC of $\beta 2^{-/-}$ mice. (A,B) Coloured contours of averaged retinotopic maps (from Fig. 5A,B) circumscribe patch area that is $\geq 65\%$ of response maximum. (D) Area of SC activated by stimulation at different positions. The values represent average patch areas corresponding to $\geq 50\%$ of response maximum from wt (blue) and $\beta 2^{-/-}$ (red) mice. Stimulus position corresponds to indices in C. Error bars are SEM. (E) Patch aspect ratio and orientation for each stimulus position, as indexed in C. The line length is the aspect ratio of the major and minor axes of the 2-D gaussians fitted to each patch (i.e. a value of 1 indicates a round patch). (F) Ratios ($\beta 2^{-/-}$: wt) of mean area (black) and elongation (gray) values from patches evoked by stimuli separated in azimuth (as indexed in C), and averaged across elevation. Note here that, relative to wt mice, the patches from $\beta 2^{-/-}$ mice are much longer in the anterior SC than more posteriorly. (G) MF values of visual azimuth (from Fig. 5F) plotted against patch elongation for wt (blue) and $\beta 2^{-/-}$ (red) mice from the equivalent positions in the SC. There was a positive correlation between MF and patch length ($R^2 = 0.89$) in the $\beta 2^{-/-}$ animals while there was no such correlation for wt animals.

2.5. Discussion

We used intrinsic imaging to map functionally the overall retinotopic organization of the SC in mice that lack early retinal waves. In contrast to wt mice, the representations of individual stimuli in $\beta 2^{-/-}$ mice were overall larger and more elongated along the A-P axis, and there was a marked compression of visual azimuth representations in the posterior half of the SC. This compression can be explained by the anisotropy in the shape and orientation of individual stimulus representations across the A-P axis of the SC. Our results indicate that spontaneous activity in the immature retina is not only required for the local refinement of the retinotopic map, but also for shaping its gross organization.

2.5.1. Mapping intrinsic signals in the SC

Optical imaging offers several advantages over conventional methods used for mapping the topography of retinocollicular projections. Whereas injections of anterograde anatomical tracers can at best resolve projections from very few retinal sites of set size and microelectrode recordings are prone to sampling errors, optical imaging can be reliably used to map precisely the topography of visually-evoked responses from almost the entire surface of the SC. The fact that we could resolve patches as small as $\sim 100 \mu\text{m}$ in diameter (e.g. Fig. 2.2A) demonstrates not only the precision of retinocollicular projections, but also the mapping accuracy of this method. Optical imaging is therefore ideally suited to detect both local and global changes in functional topography, which makes it a useful tool for screening mice deficient in genes important for establishment of retinotopic maps in the SC.

2.5.2. Local topography is functionally less refined in $\beta 2^{-/-}$ mice

Precise topography in the SC develops during the first postnatal week by large-scale remodelling of RGC axonal arbors (McLaughlin et al. 2003b, Simon and O'Leary 1992), and is thought to be regulated by retinal waves that correlate the firing of neighbouring RGCs (Bansal et al. 2000, Galli and Maffei 1988, Meister et al. 1991, Wong et al. 1995). In line with this idea, the regional topography of retinofugal projections is disrupted but not abolished in mice lacking early retinal waves, suggesting that correlated activity patterns in the retina are

important primarily for retinotopic map refinement (Grubb et al. 2003, McLaughlin et al. 2003b).

In this study, we provide the functional correlate of these anatomical changes, by showing that a given region of the retina drives activity over a greater area of SC in $\beta 2^{-/-}$ mice than in wt animals. Based on intrinsic imaging alone, one cannot distinguish whether the unrefined retinocollicular projection is accompanied by an enlargement of receptive field sizes, or a large scatter of positional preferences of neurons within a given region of the SC. Recent evidence indicates that receptive field structure and size is indeed altered in $\beta 2^{-/-}$ mice (Chandrasekaran et al. 2005).

There is a possibility that the disruption in remodelling of the retinocollicular projection in $\beta 2^{-/-}$ mice arises from the lack of cholinergic signalling in the developing SC, especially as acetylcholine is known to be a potent modulator of synaptic transmission and plasticity (Dani 2001). Specifically, nAChRs are expressed throughout the developing rodent brain (Naeff et al. 1992, Tribollet et al. 2004), and $\beta 2$ -containing nAChRs are expressed in the adult mouse SC (Marks et al. 2002). However, the developmental effects of the loss of cholinergic signalling in the SC should be minimal, as nAChR blockade with dihydro- β -erythroidine in the rat SC during the first postnatal week does not disrupt the topography of the retinocollicular projection (Simon et al. 1992). Moreover, partial topographic refinement was still observed during the first two postnatal weeks in the $\beta 2^{-/-}$ SC (McLaughlin et al. 2003b), suggesting that the capacity for developmental plasticity was maintained. We therefore consider it unlikely that the imprecise topography in $\beta 2^{-/-}$ mice is caused by impaired plasticity in the SC.

2.5.3. Coarse retinotopy is altered in $\beta 2^{-/-}$ mice

In wt animals, the visual field was mapped uniformly across the SC surface. Although neighbouring stimuli still mapped to neighbouring positions in the SC of $\beta 2^{-/-}$ mice, the retinotopic map exhibited a posterior shift of nasal visual space and a marked compression of visual azimuth in the posterior SC.

The gross abnormalities in the retinotopic organization can be attributed to the disruptions in the precision of local topography, which were more pronounced along the A-P axis. Stimulus representations in the SC of $\beta 2^{-/-}$ mice were spatially most exuberant anteriorly. Moreover,

the elongated representations were oriented predominantly along the A-P axis, and there was more overlap between them along the A-P than along the M-L axis. This phenotype is a likely consequence of the way retinal axons grow into the SC at around the time of birth (McLaughlin et al. 2003b, Simon and O'Leary 1992). First, there is a bias in the anatomical order of the ingrowing optic tract fibres which seem to be initially more ordered along the M-L than in the A-P axis of the SC (McLaughlin et al. 2003b, Simon and O'Leary 1992, Simon and O'Leary 1991). The lack of retinal waves in $\beta 2^{-/-}$ mice during the first postnatal week, which prevents refinement, may accentuate the differences in the initial mapping precision between the two SC axes. Second, during the remodelling period, the overall degree of retraction that eliminates inappropriately-targeted arborisations appears to be greater for projections from the temporal retina, which innervate the anterior SC, as overshooting axons and their branches have to be withdrawn from a far larger area than for those from the nasal retina (Simon and O'Leary 1992). In effect, the lack of correlated activity patterns in the retina, which mediate the retraction of ectopic arborisations, may result in a relatively greater elongation of stimulus representations in the anterior SC than of those more posteriorly.

Our explanation, then, of why the retinotopic map is compressed posteriorly in $\beta 2^{-/-}$ mice is based on the following reasoning. Due to the lack of retinal waves during the first postnatal week, the temporal RGC axons targeted to the anterior SC preferentially maintain their ectopic branches more posteriorly, where these can compete for post-synaptic neurons with axons projecting from more nasal portions of the retina. This results in the posterior shift of the 'centre of mass' of stimulus representations from the anterior SC. In contrast, at the posterior end of the SC, the projections from the nasal retina are not nearly as large or elongated, and do not invade, and therefore cannot compete for, post-synaptic target space more anteriorly. The net result is both a shift in the representation of nasal visual space more posteriorly and a compression in the representation of visual azimuth in the remaining, posterior part of the SC in $\beta 2^{-/-}$ mice. Therefore, the deficit in the local topographic refinement that arises from the lack of early correlated activity in the retina, in combination with the orientated ingrowth of RGC axons, could lead to general changes in the retinotopic map layout.

2.5.4. General implications for activity-dependent map formation

Previous studies using TTX or genetic manipulations to block retinal ganglion cell firing also showed that neuronal activity alters retinotectal mapping (Gnuegge et al. 2001, Thompson and Holt 1989). However, these studies could not distinguish between a permissive role, whereby neuronal activity merely permits axons to respond to molecular cues, or an instructive one, whereby the spatio-temporal pattern of neuronal activity determines topographic order, most likely by elimination of inappropriately connected axons (Ruthazer et al. 2003). Since the $\beta 2^{-/-}$ mice differ from wt animals only in the spatio-temporal pattern of retinal ganglion cell firing, without a significant reduction in overall activity levels, our data in conjunction with the anatomical data in the SC of $\beta 2^{-/-}$ mice (McLaughlin et al. 2003b), show that neuronal activity has an instructive function in retinotopic mapping.

Whereas the results from this and previous studies have demonstrated that patterned activity in the retina is essential for regional refinement of topography in retinal targets (McLaughlin et al. 2003b, Grubb et al. 2003), our results also stress the requirement of correlated retinal activity in shaping the gross retinotopic map structure in the SC. The marked distortion of both fine-scale (this study, Grubb et al. 2003) and coarse (this study) retinotopy along the nasotemporal axis in targets of retinal projections in $\beta 2^{-/-}$ mice indicates that early retinal waves have a greater role than previously thought in the specification of retinotopic order, at least along one visual axis.

The importance of patterned retinal activity has also been demonstrated for the segregation of RGC axons into eye-specific domains in the LGN (Rossi et al. 2001, Stellwagen and Shatz 2002, Torborg et al. 2005, but see Huberman et al. 2003), suggesting that similar activity-dependent mechanisms may guide the formation of both eye-specific connections and precise topographic maps during early postnatal development. Thus, at several stages of the mammalian nervous system, the specific pattern of neuronal activity is instructive in shaping the structure of functional maps.

3. Prior experience enhances plasticity in adult visual cortex

3.1. Abstract

The brain has a remarkable capacity to adapt to alterations in its sensory environment, which is normally much more pronounced in juvenile animals. Here we show that in adult cerebral cortex the ability to adapt to changes can be improved profoundly if the animal had already experienced a similar change in its sensory environment earlier in life. Using the standard model for sensory plasticity in mouse visual cortex – ocular dominance (OD) plasticity – we found that a transient shift in OD induced by monocular deprivation (MD) earlier in life renders the adult visual cortex highly susceptible to subsequent MD many weeks later. Irrespective of whether the first MD was experienced during the traditional critical period or in adulthood, OD shifts induced by a second MD were faster, more persistent and specific to repeated deprivation of the same eye. The capacity for plasticity in the mammalian cortex can therefore be conditioned by past experience.

3.2. Introduction

Exposure to an altered sensory environment, a new sensorimotor task, or a foreign language earlier in life makes for easier learning the same information at a later time (Knudsen 2002, McGonigle and Flook 1978, Krakauer et al. 2005, Kuhl 2004). The initial experience thus seems to leave a trace in the brain, which facilitates subsequent behavioural adaptation. Strong evidence for a neural correlate of facilitated learning comes from the sound localization system of the barn owl, where adaptation to altered sensory cues early in life leads to lasting structural changes that strongly enhance the ability to adapt to similar manipulations during adulthood (Knudsen 1998, DeBello et al. 2001, Linkenhoker et al. 2005). In contrast, a physiological basis for this phenomenon has not been demonstrated in the mammalian brain.

A favoured model to study mammalian cortical plasticity is monocular deprivation (MD), as it reveals strong changes in cortical circuitry and visual behaviour in response to altered sensory input (Wiesel and Hubel 1963, Muir and Mitchell 1973, Shatz and Stryker 1978). The experience of imbalanced binocular input after closure of one eye causes a shift in the ocular dominance (OD) in visual cortex, such that neurons reduce their responsiveness to stimuli delivered to the deprived eye while the open eye increases its influence on cortical cells. When the deprived eye is later allowed to regain vision, binocular responses in the visual cortex have the capacity to recover (Mitchell et al. 1977, Kind et al. 2002, Liao et al. 2004). Although MD has been employed to induce cortical plasticity in a large number of studies over the last 40 years, the cellular and molecular mechanisms underlying the strong shifts in cortical eye representation still remain largely unresolved (see Chapter 1, Section 1.2). In the past decade, the mouse model has become very popular for the study of OD plasticity, since it allows the application of transgenic and knockout techniques. Even though the mouse visual cortex has a more simple organization, which lacks the prominent OD columns found in cats and primates (LeVay et al. 1978, Dräger 1975), OD plasticity in this species is well comparable to higher mammals (Dräger 1978, Gordon and Stryker 1996).

Most of our knowledge about MD effects in mice is based on recordings with extracellular microelectrodes. However, this method is quite time-consuming, prone to sampling errors, and it does not easily allow for repeated measurements to monitor changes in eye

representation over time. We therefore established the use of optical imaging of intrinsic signals as a fast and reliable method to assess OD of neuronal populations in mouse visual cortex and to explore MD-induced changes at different ages. We further employed optical imaging of intrinsic signals to investigate the effect of a transient OD shift in mouse visual cortex on subsequent cortical plasticity later in life.

3.3. Material and Methods

Eyelid suture

All experiments were carried out in compliance with the appropriate government authorities (Regierung von Oberbayern). In mixed-background mice (C57BL/6 x SV/129J), one eyelid was sutured shut either during the critical period (between postnatal day, P, 23 and 28) or in adult mice (P60–200) under anaesthesia induced by a mixture of Fentanyl (0.05 mg/kg), Midazolam (5.0 mg/kg) and Medetomidin (0.5 mg/kg). During surgery, the eye was kept moist with drops of saline. After cleaning the surrounding area, all hair close to the eye was removed with fine scissors. For MD durations longer than three days, lid margins were trimmed prior to suturing. The skin was then carefully separated from the subjacent layer of tissue and a very small amount of ophthalmic cream (Isoptomax) was applied to the eye. The lid was sutured shut with two to three mattress stitches using 6-0 silk (Ethicon). The best results regarding potential reopening of the suture and minimal eye damage were obtained by placing large and very loose stitches that held the margins together but did not squeeze the tissue. Before awaking the mouse from anaesthesia with a mixture of antagonists (Naloxon 1.2 mg/kg, Flumazenil 0.5 mg/kg, Atipamezol 2.5 mg/kg), it was injected subcutaneously with about 1 mg Chloramphenicol (from a 100mg/ml solution in saline) and about 0.1 mg/kg Buprenorphin (from a 0.1 mg/ml solution in saline). For most animals, this injection was repeated the following day. Deprivation lasted between 3 and 10 days, with a maximum variation of ± 2 hours for a 3 day MD. Eye reopening was carried out under the same anaesthetic or under halothane anaesthesia (see below) prior to an imaging experiment. Animals with signs of corneal injuries after eye reopening or at any later time point were excluded from further experiments.

Optical Imaging of intrinsic signals

Neuronal response strength to stimulation of either eye in the binocular region of the visual cortex was determined by optical imaging of intrinsic signals. Mice were initially chamber-anesthetized with 2–2.5% halothane in a 1:1 mixture of N₂O:O₂ for about 20 minutes (roughly 8 minutes with 2% halothane, then 2.5%). When the breathing rate had decreased significantly, the animals were suspended supine by their incisors on an inclined platform and intubated with a small polyethylene tubing (~2.5 cm long) attached to a cut cannula (juvenile mice up to P35: tubing of inner diameter 0.58 mm, wall thickness 0.20 mm; adult mice: inner diameter 0.86, wall thickness 0.20 mm). For subsequent ventilation the N₂O:O₂ ratio was reduced to 45:55 and the halothane concentration (initially set to about 2%) was gradually decreased further to 1.7 – 1.8% until the beginning of data acquisition. About 25 µl of a 1:1 diluted saline/glucose solution (Sterofundin, Braun) was given subcutaneously. This injection was repeated once during the course of the experiment. In mice that had undergone MD the eye was now reopened. After inserting the ear bars loosely, the scalp was resected, and a removable bar was attached frontally to the skull with glass beads and tissue glue (Histoacryl, Braun). The bone over the visual cortex was then covered with 2.5% agarose in saline and sealed with a coverslip (10 mm diameter). Throughout surgery, the eyes were protected with cream (Isoptomax), which was removed except for a thin film prior to imaging. Heartbeat and temperature of the animal were monitored continuously.

For optical imaging of intrinsic signals the cortex was evenly illuminated with monochromatic light of 707 nm from two sides. Image frames (600 ms) were taken with a cooled, slow-scan CCD camera (12 bit, 384 x 288 pixel, ORA 2001, Optical Imaging Inc.) focused to about 300 µm below the skull surface (at 546 nm illumination). In each trial, three blank frames were acquired, followed by 12 frames, during which visual stimuli were presented. Trials were separated by 4 s. In animals undergoing chronic experiments the scalp was re-sutured at the end of the experiment (5-0 silk, Ethicon) and the mice were recovered under ventilation with pure O₂. Prior to extubation, doxapram was applied subcutaneously (20 µl from a 20mg/ml solution, Dopram, Albrecht, Germany) to stimulate spontaneous breathing. Chloramphenicol and Buprenorphin were administered as well (see above).

Visual stimulation and data analysis

Visual stimuli consisted of rectangular, square-wave drifting gratings (side length 16° , centre-spacing 14° , 0.04 cycles/ $^\circ$, 2 cycles/s) projected with a video beamer on a plastic screen in front of the animal at 20-25 cm distance. The orientation of the grating changed randomly during each trial every 0.6 s. Computer-controlled shutters allowed independent stimulation of either eye. At the beginning of each experiment the visual field representation for the ipsilateral eye was briefly mapped, in order to determine the exact location and extent of the binocular cortex. Next, a 2×2 stimulus grid was positioned such that the two left stimuli evoked responses in the centre of the binocular region. For quantification (see below), we only used the averaged responses to the two left stimuli, thereby ruling out any contribution from the monocular portion of the visual cortex.

Single response maps were computed by clipping (1.5%) and high-pass filtering blank-corrected image averages of 15–30 stimulus repetitions. Each single-condition map was thresholded (image background mean + 0.8 std) to define a region containing the most responsive pixels. After subtracting the mean background value from an artefact-free non-responsive area, pixel values (reflectance change) within the region above threshold were summed to yield an integrated measure of response strength and responsive area size. Response strength values obtained from the two left stimuli, which evoked maximal responses to stimulation of the ipsilateral eye, were averaged for each eye. Colour-coded 'best position' maps were calculated from a minimum intensity projection of single position maps that were additionally clipped and gaussian-smoothed. Each pixel was then assigned the colour corresponding to the stimulus that elicited the strongest response at this pixel. The quantification of absolute response strength for each eye was limited to animals that were imaged only once, as repeated exposure of the skull changed its transparency, such that the apparent signal strength in subsequent imaging sessions was lower. In acute experiments, however, absolute response strength varied only little for mice of a given age. The ratio of contralateral to ipsilateral eye response strength (contra/ipsi ratio) was calculated as a measure for ocular dominance. All statistical comparisons were made by using the Mann–Whitney U Test.

In vivo electrophysiology

Multi-unit activity was recorded using silicon multi-channel electrodes (NeuroNexus Technologies) under the same anaesthetic regime as for optical imaging. Data acquisition and stimulus generation were controlled using BrainWare and the Pentusa multi-channel processor (Tucker-Davis Technologies). Electrode penetrations (9–32 per animal) were targeted to the binocular visual cortex, as defined functionally by prior optical imaging. Flashed white squares (2×100 ms) were presented to each eye randomly interleaved at different visual field positions (15 repetitions/stimulus). All recording sites were carried out at 100–800 μm depth from the cortical surface. Sites were at least 100 μm apart, within the depth of and across penetrations. Responses calculated from averaged spike counts over the peri-stimulus response period (corrected by subtracting the mean spontaneous activity immediately preceding stimulus onset), for stimuli eliciting the strongest response in each eye, were used to compute the ratio of contralateral to ipsilateral eye responses (contra/ipsi ratio). The median contra/ipsi ratio value from each animal was used to obtain group averages.

3.4. Results

3.4.1. Imaging of mouse binocular visual cortex

We used optical imaging of intrinsic signals to map the representation of the two eyes in the binocular region of mouse visual cortex (Grinvald et al. 1986, Schuett et al. 2002, Kalatsky and Stryker 2003). Small visual stimuli presented at different positions in front of the mouse evoked small patches of activity in retinotopically corresponding regions in the visual cortex (Fig. 3.1B,C): Nasal stimulus positions elicited responses in the lateral part of the visual cortex and more peripheral stimulus positions resulted in a more medial activation of the cortex. Similarly, stimuli in the upper visual field were represented caudally, and stimulation of the lower visual field activated more rostral portions of the visual cortex. The overall spatial organization of the binocular region was revealed by colour-coded retinotopic maps (Fig. 3.1D,E), obtained by combining responses from individual stimuli presented to the two eyes independently, and assigning to each pixel the colour of the stimulus position eliciting the strongest response at this location in the visual cortex.

The weaker and spatially more restricted responses of the ipsilateral eye defined the extent of the binocular region (Fig. 3.1E), which receives corresponding input from both eyes. In agreement with previous studies (Dräger 1975, Wagor et al. 1980, Gordon and Stryker 1996), we found the binocular region to be largest in the caudal visual cortex, representing the upper visual field. There the area seen by both eyes spanned more than 40° in azimuth, compared to about 30° in the lower visual field (Fig. 3.1E). To quantify the strength of each eye's representation, we limited the analysis to responses from the centre of the binocular visual cortex (Fig. 3.2A,B, see methods for details).

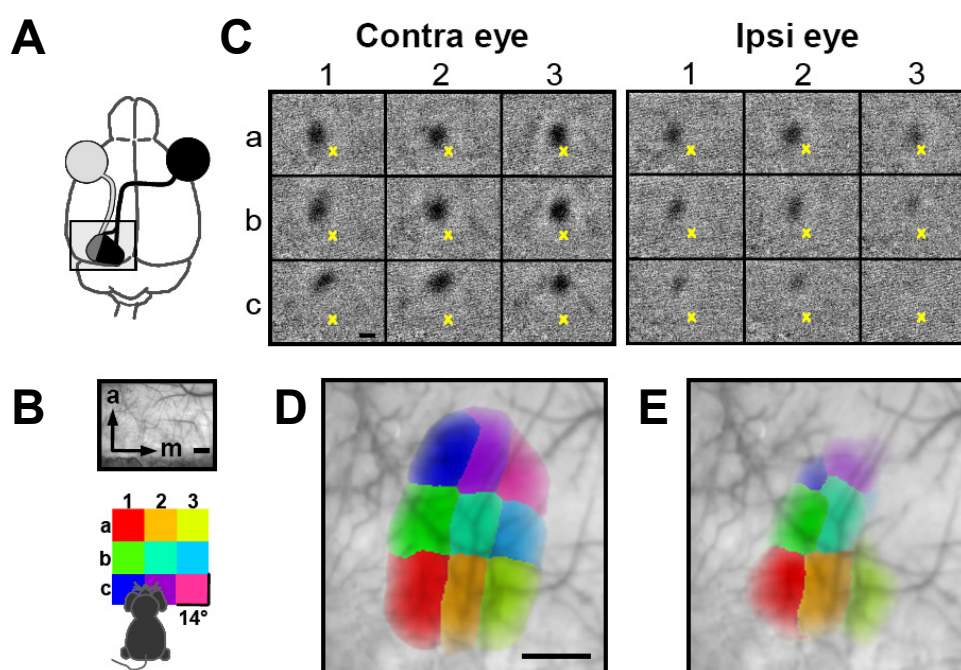


Figure 3.1. Retinotopic mapping of mouse binocular visual cortex using optical imaging of intrinsic signals. **(A)** Schematic of mouse brain, depicting the imaged area (black rectangle), which contains an outline of the primary visual cortex with the binocular zone (dark grey) located laterally. **(B)** Top, cortical blood vessel pattern as imaged through the skull. Bottom, arrangement of grating stimuli used to map the central visual field. Color denotes stimulus position. **(C)** Individual activity maps displaying responses to the 3×3 stimulus grid depicted in **B** are presented separately to the two eyes. The coordinates of the yellow cross are fixed in each map. **(D,E)** Color-coded maps of the combined responses to contralateral (**D**) and ipsilateral (**E**) eye stimulation superimposed on the cortical blood-vessel pattern, revealing the extent of the binocular zone. Color indicates stimulus position eliciting the strongest response at each pixel. Scale bars: 0.5 mm.

3.4.2. Determining OD shifts with intrinsic optical imaging

In normal juvenile mice (postnatal day, P, 29–39), activity patches evoked by the stimulation of the contralateral eye in the central binocular region were consistently darker and/or larger than those of the ipsilateral eye (Fig. 3.2B). Deprivation of the contralateral eye at around the peak of the critical period (P28) strongly shifted OD (contra/ipsi ratio) towards the ipsilateral eye (Fig. 3.2C,E, F, $p < 0.001$, Mann–Whitney U test).

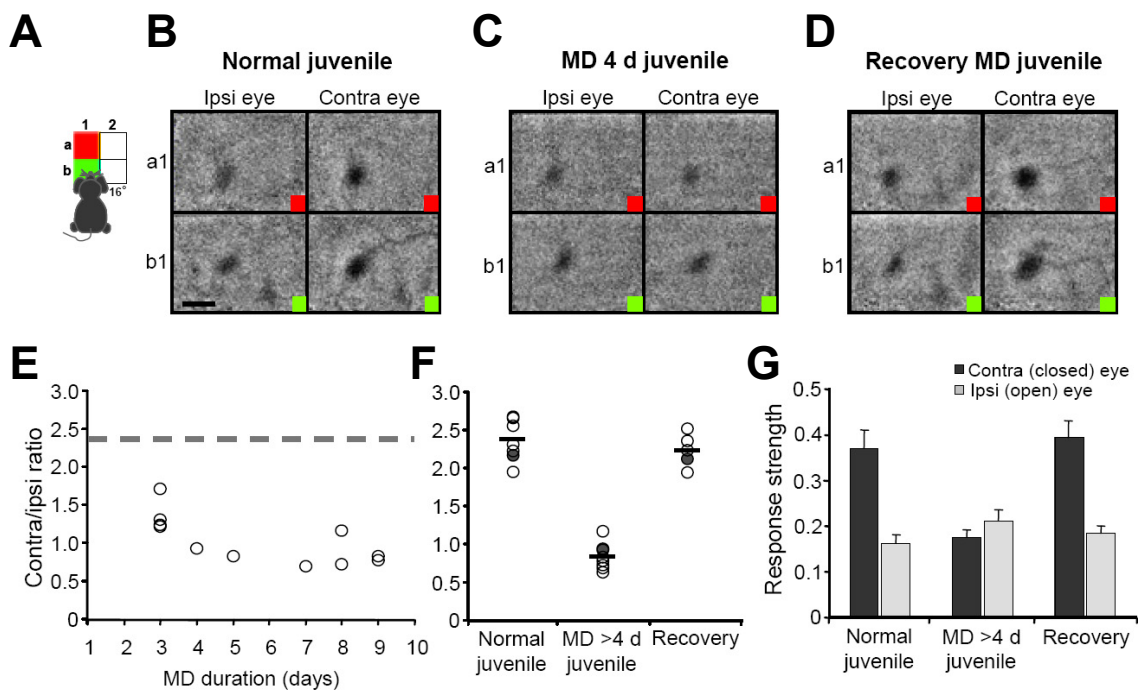


Figure 3.2. MD induces strong OD plasticity during the critical period. (A) Schematic of stimulus arrangement. (B,C,D) Ipsilateral (left) and contralateral (right) eye responses from the central region of the binocular visual cortex to stimuli shown in A from a normal P35 mouse (B), following MD (P26–P30) of the contralateral eye (C), and 46 days after a 4-day MD (D). Scale bar, 1 mm. (E) OD shifts after MD shown as ratio of contralateral to ipsilateral eye responses (contra/ipsi ratio) from individual animals (circles) plotted against MD duration. Dashed line shows average from non-deprived controls. (F) Contra/ipsi ratio values for normal juvenile mice (mean \pm SEM: 2.40 ± 0.10 ; $n = 8$), after 4–10 days of MD (0.84 ± 0.06 ; $n = 8$), and 4–7 weeks after a 4–5-day MD (2.24 ± 0.10 ; $n = 5$). Horizontal lines indicate mean group values. Filled symbols show data points from the experiments shown in B,C and D. (G) Response strength of each eye (see methods) that contributed to the shift in the contra/ipsi ratio (shown in F) after contralateral eye closure and re-opening. Error bars indicate SEM.

Whereas a deprivation period of three days already led to a considerable reduction in the contra/ipsi ratio, four to five days of MD were necessary to induce a saturating effect (Fig. 3.2E). Longer periods of MD did not yield stronger shifts in OD. On average, the OD shift in juvenile mice was primarily caused by a reduction of deprived eye responses, with only a weak, non-significant increase of the non-deprived eye response (Fig. 3.2G, deprived eye: $p < 0.001$; non-deprived eye: $p = 0.1$). Sample sizes for the different MD durations were not large enough to allow a reliable description of the time course of response strength changes, as has been described by other studies (Frenkel and Bear 2004).

Allowing the initially-closed eye to regain vision (after 4–5 days of MD) completely restored normal OD (Fig. 3.2D,F,G, $p > 0.1$, in comparison to normal adult mice), demonstrating that binocular responses in mouse visual cortex are able to recover fully from short-term MD during the critical period.

3.4.3. Critical period MD facilitates OD plasticity in adults

Having thus established that a transient change in sensory input does not permanently change binocular responses, we went on to test whether the induction of MD would nevertheless have long-term consequences on cortical circuitry, thereby changing the capacity for plasticity in adult cortex. Following a recovery period of four to nine weeks from the first, saturating MD (4–5 days) in the critical period, the now adult mice (P60–P100) experienced a second, short term MD (three days) of the same, contralateral eye (Fig. 3.3A). The second MD indeed led to a robust OD shift towards the non-deprived eye (Fig. 3.3C,D,E, $p < 0.001$). In contrast, three days of MD in ‘naïve’ adult mice (P70–P160) without prior MD experience did not significantly alter OD (Fig. 3.3B,D, $p = 0.34$). The difference in the contra/ipsi ratio values between mice with or without prior MD was highly significant ($p < 0.001$). The MD effect was independent of age in both groups, and it was not affected by the duration of the interval between MD episodes (for all groups: $p > 0.6$, $R^2 < 0.06$). In mice previously deprived during the critical period, a partial weakening of the closed eye without substantial strengthening of the open eye ($p = 0.052$ and $p = 0.18$, respectively; in comparison to response strengths of litter-mate controls after recovery) produced the robust shift in ocular dominance induced by the second MD (Fig. 3.3E).

3. Prior experience enhances plasticity

These results demonstrate that the induction of ocular dominance plasticity during the critical period causes a lasting change in visual cortex, which substantially enhances the effectiveness of a second MD many weeks later. Importantly, during the intervening period, there was no apparent functional hint of this change, as the cortex had fully recovered from the first MD (Fig. 3.2, 3.3).

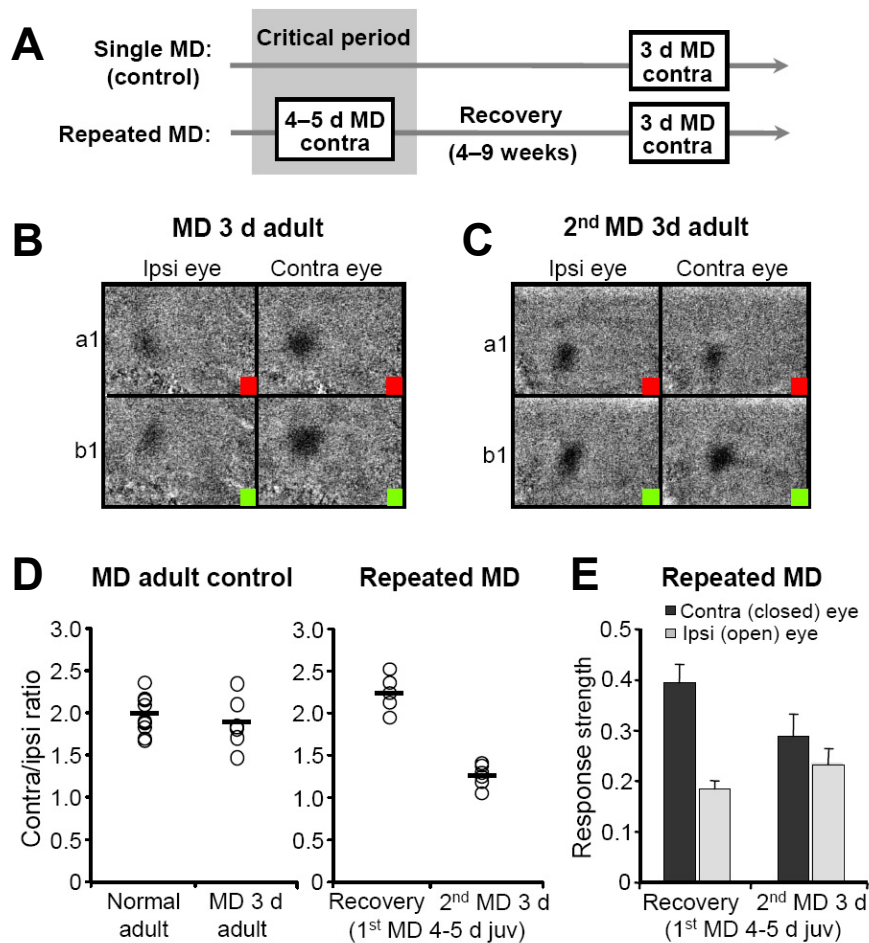


Figure 3.3. MD during the critical period facilitates OD plasticity in adult mice. (A) Experimental timelines for the assessment of the effect of repeated MD in the contralateral eye. (B,C) Ipsilateral (left) and contralateral (right) eye responses after 3 days of contralateral MD from a normal adult mouse (B), and from a mouse that had been undergone prior MD (4 days) during the critical period (C). Stimulus arrangement as in Fig. 2A. (D) Contra/ipsi ratio values from individual animals (circles) for the different conditions: Three days of MD in adult mice were insufficient to induce plasticity in naïve animals (1.89 ± 0.12 ; $n = 6$; normal adult mice: 2.01 ± 0.07 ; $n = 12$), but led to a strong OD shift in mice with prior 4–5 day MD in the critical period (1.26 ± 0.05 ; $n = 7$; recovery from critical period MD: 2.24 ± 0.10 ; $n = 5$). Horizontal lines indicate mean group values. (E) Changes in eye response strength that contributed to the shift in the contra/ipsi ratios after repeated contralateral MD. Error bars indicate SEM.

3.4.4. Adult MD experience facilitates subsequent OD plasticity

Recent studies reported that OD plasticity in mouse visual cortex is not limited to a critical period, but can be induced later in life, too (Sawtell et al. 2003, Lickey et al. 2004, Tagawa et al. 2005). In keeping with a previous report (Sawtell et al. 2003), we found that three days of contralateral MD in normal adult mice were insufficient to induce a change in OD (Fig. 3.3B,D). However, 6–7 days of MD resulted in a clear OD shift in mice up to 200 days old (Figs. 3.4A,B and 3.7B,C, $p < 0.001$), which was independent of age (Fig. 3.4C, $R^2 = 0.12$, $p = 0.24$).

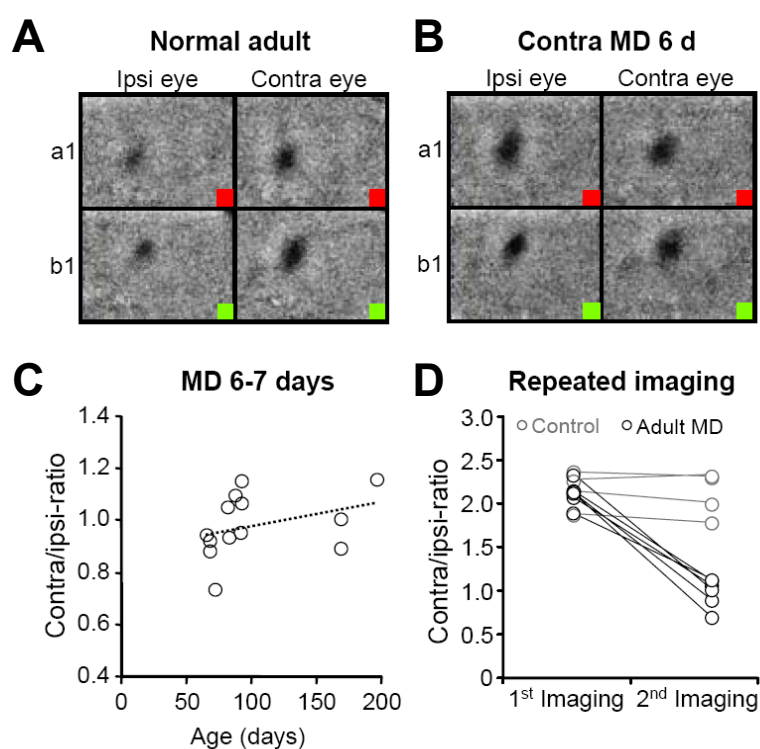


Figure 3.4. OD plasticity in adult visual cortex. (A,B) Ipsi- and contralateral eye responses in the same mouse before (A, P80, contra/ipsi ratio=2.21) and after 6 days of MD (B, P92, contra/ipsi ratio=1.09). Stimulus arrangement as in Fig. 2a. (C) Ratio of contra- to ipsi-lateral eye response strength after 6-7 days of MD in normal adult mice plotted against age shows no significant correlation. $R^2 = 0.12$, $p = 0.24$. (D) Contra/ipsi ratio values from repeated experiments (inter-imaging period 1-3 weeks) in adult control animals (grey) and in deprived adult animals before and after 6 days of MD in the contralateral eye (black).

In contrast to juvenile mice, OD shifts in adults were mediated mainly by an increase in the response strength of the non-deprived, ipsilateral eye, without a significant weakening of deprived eye inputs (Fig. 3.4A, B, deprived eye: $p = 0.1$; non-deprived eye: $p < 0.001$; see also Fig. 3.7C). As intrinsic signal imaging was performed through the intact skull, repeated experiments in the same animal permitted the measurements of eye-specific responses over

3. Prior experience enhances plasticity

time. In control animals the contra/ipsi ratio was very stable over repeated imaging sessions, whereas 6-7 days of MD led to strong shifts in OD (Fig. 3.4D), fully matching the data from animals imaged only once (Fig. 3.7B).

To further corroborate the results on adult plasticity obtained with intrinsic signal imaging, we measured multi-unit spiking activity by targeted extracellular recordings in the binocular visual cortex. Whereas in normal animals most neurons responded more vigorously to contralateral than to ipsilateral eye stimulation (Fig. 3.5A,C,D), equivalent responses were observed for both eyes after six days of MD (Fig. 3.5B,C,D, $p < 0.001$, see methods for details). Notably, contra/ipsi ratio values obtained from the supra-threshold responses in normal and deprived mice (Fig. 3.5C,D) closely matched the population response data measured by intrinsic signals (Fig. 3.4D, 7B). However, spike rates were too variable between different animals to reveal the absolute changes in eye response strength underlying the OD shifts (data not shown).

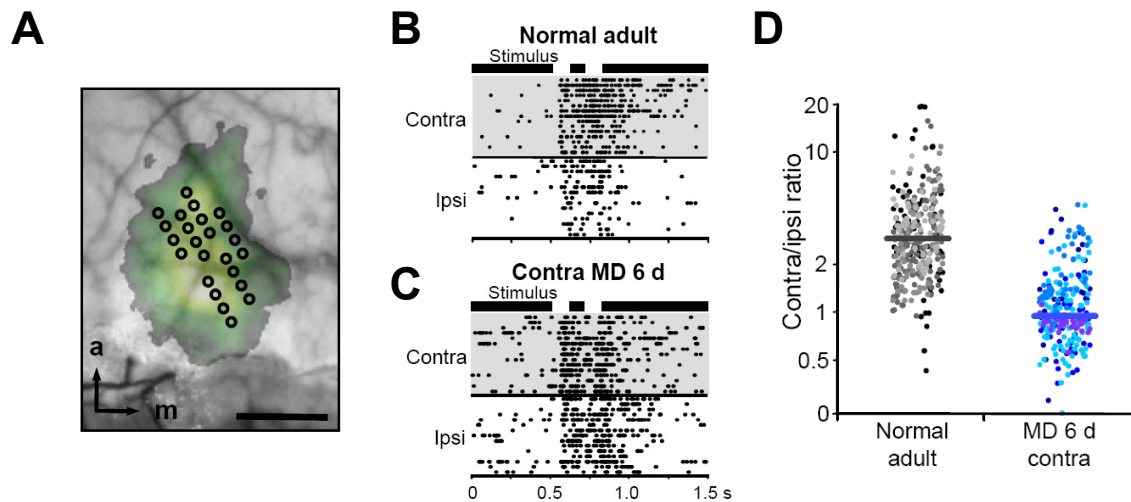


Figure 3.5. Assessment of adult OD plasticity using microelectrode recordings. (A) Functional map of the binocular region (green), used for targeting electrode penetrations (circles). Scale bar: 0.5 mm (B,C) Raster plots from two recording sites showing responses to 15 repetitions of the same stimulus through each eye from a normal adult (B, P91, contra/ipsi ratio = 3.51) and a 6-day MD animal (C, P73, contra/ipsi ratio = 1.32). Stimulus timing is indicated above plots. (D) Distribution of contra/ipsi ratio values from all recording sites of adult control (2.99 ± 0.28 , mean \pm SEM, 324 recording sites, 4 mice) and deprived (1.05 ± 0.12 , 260 recording sites, 5 mice) animals, showing strong OD shifts in response to MD. Each color represents a different animal. Horizontal lines indicate mean group values.

As after MD induction in juvenile animals, complete recovery of ocular dominance was revealed by optical imaging in adult mice as soon as eight days after the end of 6-7 days of deprivation (Fig. 3.7B,D, $p = 0.93$, in comparison to the contra/ipsi ratio of normal adult mice). However, even though contra/ipsi ratios were already similar to normal mice at this time, cortical responses to each eye were initially stronger than in non-deprived animals ($p < 0.05$), and only gradually returned to normal levels over the subsequent two weeks (Fig. 3.6).

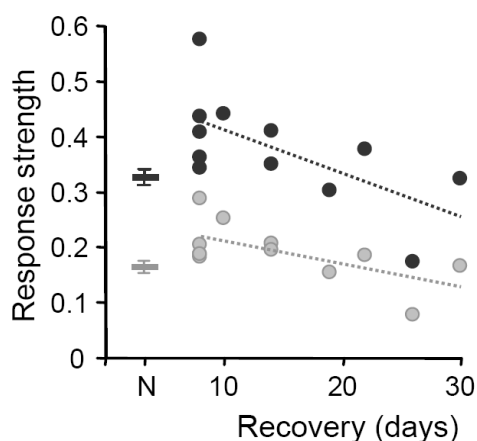


Figure 3.6. Response magnitudes for the contralateral (dark grey) and the ipsilateral (light grey) eye, plotted against the duration of binocular vision after MD, and for normal adult animals (N, mean \pm SEM). For both eyes, response strength decreases with length of recovery (contra: $R^2 = 0.41$, $p = 0.02$; ipsi: $R^2 = 0.40$, $p = 0.03$).

Having demonstrated robust plasticity and recovery in adult animals, we investigated whether the effect of prior MD on subsequent plasticity is also observed if the first MD was experienced in adulthood (Fig. 3.7A). Indeed, if a second MD was induced three to six weeks after the first deprivation in adult mice, three days of eye-closure were sufficient to strongly shift OD towards the open eye, in contrast to “naïve” adult mice (Fig. 3.7B, $p < 0.001$). The magnitude of this shift was independent of the duration of the recovery period, and it was mediated primarily by the potentiation of non-deprived eye inputs (Fig. 3.7C, deprived eye: $p = 0.37$; non-deprived eye: $p = 0.001$), akin to the changes observed after a single MD in normal adult animals (Fig. 3.7C). In order to strengthen these findings, we again imaged a subset of adult mice repeatedly, thus allowing us to measure the effects of repeated MD in individual animals over time (Fig. 3.7B). The OD shifts observed in these mice were indistinguishable from those obtained in animals imaged only once. Taken together, these results indicate that a ‘priming’ MD in adults had the same facilitatory effect on subsequent OD plasticity as a ‘priming’ MD in the critical period.

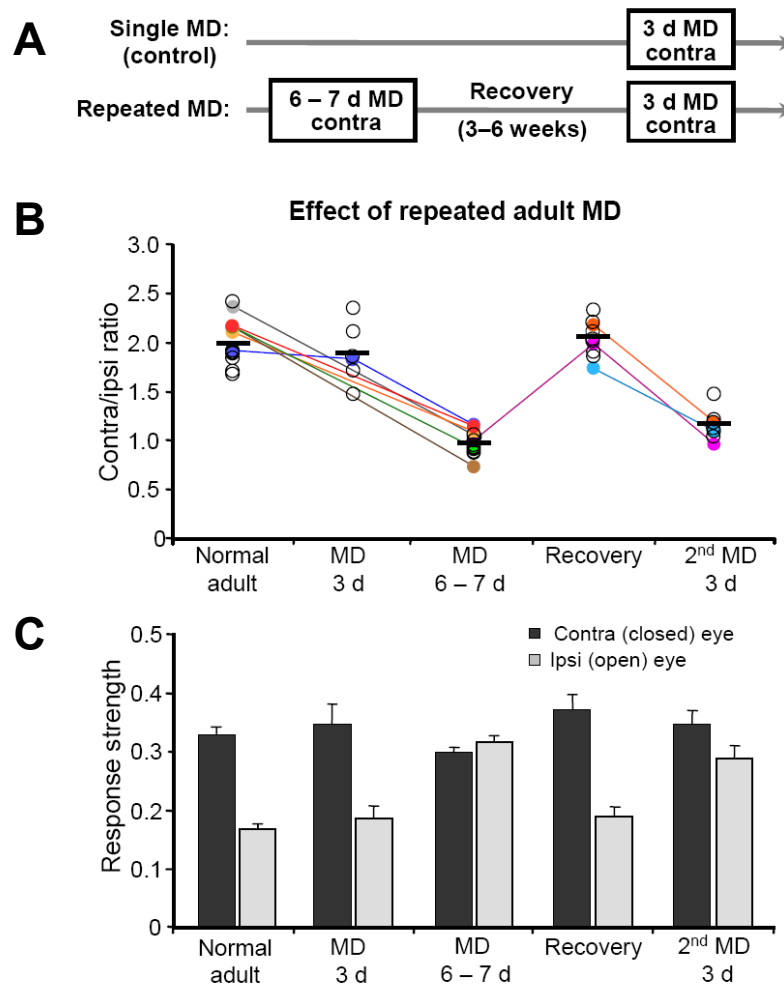


Figure 3.7. Prior MD in adult mice facilitates subsequent OD plasticity. (A) Experimental timelines for the assessment of the effect of repeated adult MD in the contralateral eye. (B) Strong OD shifts after 6–7 days of MD in adult mice (contra/ipsi ratio = 0.98 ± 0.03 ; mean \pm SEM; $n = 13$) recover completely with restored binocular vision (2.00 ± 0.05 , $n = 11$; imaged 8–30 days after eye re-opening). Re-closure of the eye results in strong OD shifts even after 3 days (1.16 ± 0.06 ; $n = 8$), unlike in naïve mice (1.89 ± 0.12 ; $n = 6$). Horizontal lines indicate mean group values. Coloured symbols denote data from mice imaged repeatedly. (C) Average changes in responses strength of each eye underlying the shifts in OD shown in B after closure, re-opening and re-closure of the contralateral eye in adulthood. Error bars indicate SEM.

Another way of investigating the nature of the enhancing effect of prior deprivation is to measure the persistence of the OD shift in response to the second MD. Following a single, seven day MD in adults, eight days of binocular vision were sufficient to restore normal contra/ipsi ratio values (Fig. 3.8B). In contrast, after a second, seven day MD, the recovery was dramatically prolonged, and a strong OD shift was still apparent eight days after the end

of deprivation (Fig. 3.8B,C, $p = 0.016$, in comparison to 8 days of recovery from the first MD). Remarkably, these OD shifts persisted for longer than those from a single fourteen day MD episode (Fig. 3.8B,C, $p = 0.029$), indicating that it is not the total duration but rather the recurrent experience of deprivation which enhances cortical plasticity. Thus, an episode of MD not only accelerates the subsequent shifts of the cortical representations of the two eyes into another state, but this shift also becomes more persistent with repeated epochs of deprivation.

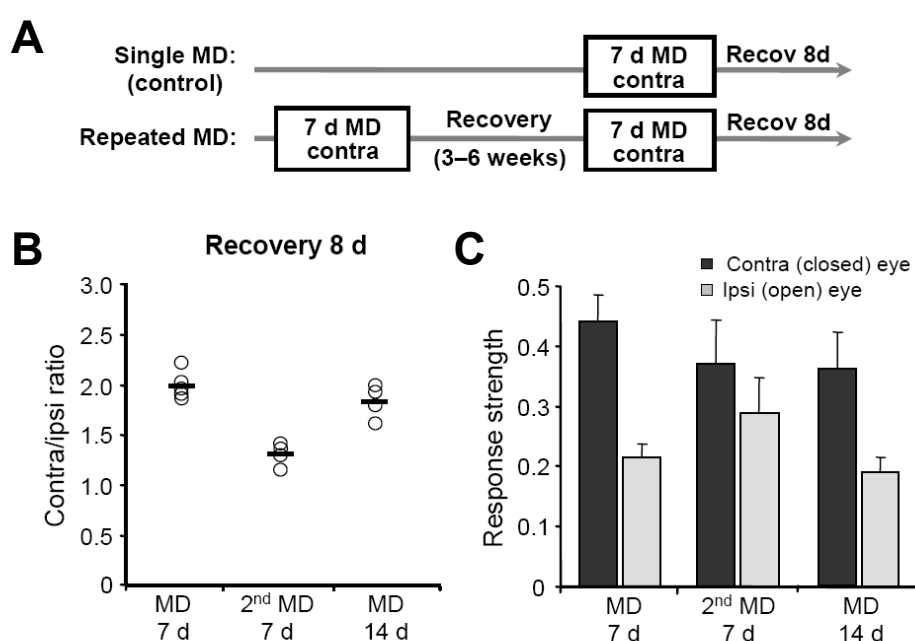


Figure 3.8. More persistent OD changes after prior MD. (A) Experimental timelines for the assessment of recovery from repeated adult MD in the contralateral eye. (B) Contra/ipsi ratio values (left) and after 8 days of recovery from a single 7 day MD (2.02 ± 0.08 , $n = 5$), repeated MD (7 days–recovery–7 days; 1.31 ± 0.05 , $n = 4$), and a single 14 day MD (1.84 ± 0.08 , $n = 4$) in adult mice. The OD shifts were more persistent in animals with recurrent MD experience. (C) Average eye response magnitudes for the conditions shown in B. Error bars indicate SEM.

3.4.5. The facilitatory effect of prior MD is eye specific

In principle, two types of mechanisms could account for the facilitation of OD plasticity described above. Prior MD experience could lead either to a general increase of cortical plasticity or to specific changes in the circuits or synapses affected by the initial deprivation.

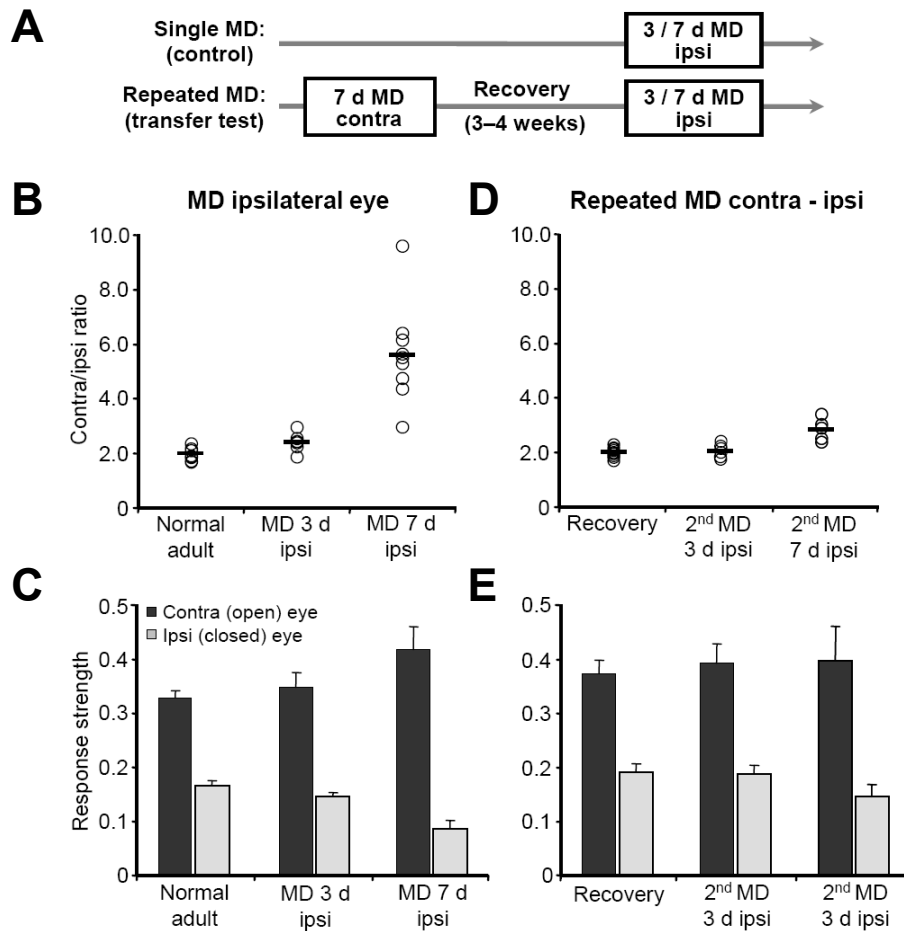


Figure 3.9. Facilitatory effect of repeated MD is eye specific. (A) Experimental timelines for successive MD of opposite eyes. (B) In naïve adult mice, contra/ipsi ratio values increased marginally after 3 days of MD (2.41 ± 0.15 , $n = 6$) and strongly after 7 days of MD (5.63 ± 0.60 , $n = 9$) of the ipsilateral eye. (C) Response strength of each eye for the same conditions as in B. (D) Previous 7-day MD of the contralateral eye and subsequent recovery (2.00 ± 0.05 , $n = 11$) did not accelerate plasticity in response to a 3-day ipsilateral eye closure (2.11 ± 0.10 , $n = 6$). In contrast, the prior deprivation impaired OD plasticity induced by a 7-d ipsilateral MD (2.83 ± 0.18 , $n = 5$). Individual animals are depicted by open circles, horizontal lines indicate mean values. (E) Response strength of each eye for the same conditions as in D. Error bars denote SEM.

One way to distinguish between these possibilities is to test whether the facilitation of OD plasticity transfers from one eye to the other (Fig. 3.9A). Three days of ipsilateral eye MD, which led to only a small OD shift in naïve mice (Fig. 3.9B,C, $p = 0.024$, in comparison to normal adult mice), did not result in a stronger shift in animals that had experienced deprivation of the other (contralateral) eye three to four weeks earlier (Fig. 3.9D,E, $p > 0.4$, in

comparison to both naïve 3d ipsilateral eye MD and litter-mate controls after recovery from contralateral eye MD). In normal adult mice, however, seven days of ipsilateral eye MD strongly altered OD in favour of the contralateral eye (Fig. 3.9B, $p < 0.001$), predominantly through a depression of ipsilateral eye responses (Fig. 3.9C, deprived eye: $p = 0.002$; non-deprived, contralateral eye: $p = 0.12$), indicating that the adult visual cortex is also susceptible to deprivation of the ipsilateral eye.

This result demonstrates that OD plasticity cannot be augmented by previous deprivation of the opposite eye, but that the facilitatory effect of prior experience is specific to deprivation of the same eye. Surprisingly, prior closure of the opposite eye even impaired OD plasticity, as was revealed by longer deprivation of the ipsilateral eye (Fig 3.9D,E): The shift of contra/ipsi ratio values after seven days of ipsilateral MD was dramatically reduced if the animal had undergone MD in the contralateral eye three to four weeks earlier ($p < 0.01$).

3.5. Discussion

Our results show that one episode of MD paved the way for a second one, in that the effects of the second MD appeared faster and lasted longer. This facilitation of plasticity occurred irrespective of whether the first MD was induced during the critical period or in adulthood, but it was only observed if the same eye was deprived during both episodes. Thus, a specific trace is left in visual cortex, which maintains a memory of its deprivation history. This trace is not apparent in the intervening period of several weeks, but rather requires a second MD to be disclosed.

3.5.1. Intrinsic signal imaging of OD plasticity

In this study we demonstrated that intrinsic signal imaging can be used to report reliably the strength of the representation of both eyes in the binocular region of mouse visual cortex. We used this method to show that closure of one eye led to robust OD shifts both during a critical period early in life and in adulthood. Our results on OD plasticity during the critical period are consistent with the previous literature (Gordon and Stryker 1996, Sawtell et al. 2003, Fagiolini and Hensch 2000). However, there have been contrasting reports regarding the susceptibility of adult mice to MD: studies using visually-evoked potentials and immediate

early gene expression revealed substantial capacity for OD plasticity (Sawtell et al. 2003, Lickey et al. 2004, Tagawa et al. 2005), which was not apparent in the measurements of single-unit activity under barbiturate-anaesthesia (Gordon and Stryker 1996, Fagiolini and Hensch 2000, McGee et al. 2005). The discrepancy between these studies could have arisen either from a difference in the sensitivity of the techniques or from different anaesthetic conditions (Pham et al. 2004). We therefore supplemented our intrinsic imaging data with extracellular recordings to show that strong adult OD plasticity (after 6 days of MD) can be indeed measured at the level of supra-threshold activity of neurons in visual cortex under halothane anaesthesia. Moreover, the close correspondence of OD values between our multi-unit and intrinsic signal recordings indicates that optical imaging faithfully reports the spiking activity of neuronal populations.

3.5.2. Strength of eye representation after juvenile and adult MD

Recent studies have demonstrated that OD plasticity in the mouse visual cortex can be studied in terms of its component parts: potentiation versus depression of inputs from the two eyes (Frenkel and Bear 2004, Sawtell et al. 2003). We showed that in juvenile mice MD of the contralateral eye primarily led to the weakening of deprived eye responses, while in adults it selectively strengthened non-deprived, ipsilateral eye responses. The mechanisms underlying OD plasticity may therefore change with age, as suggested previously (Sawtell et al. 2003, Pham et al. 2004). However, we could also show that deprivation of the ipsilateral eye in adults strongly reduced responses to that eye, indicating that the depression of inputs is still possible in adult visual cortex, contrary to a previous finding (Sawtell et al. 2003). The fact that strong bidirectional modification of the ipsilateral responses accompany MD in adults (depending on which eye was deprived), without significant changes of contralateral eye responses, indicates that the representation of the weak eye in the mature visual cortex is particularly susceptible to an imbalance of binocular input. These results are in agreement with a recent study assessing expression of the immediate early gene *Arc* (Tagawa et al. 2005).

A period of binocular vision after MD restored normal binocularity in the visual cortex of both juvenile and adult mice. Interestingly, this recovery appeared to be mediated by a combination of at least two different processes. Whereas contra/ipsi ratios were found to be at a normal level already eight days after reopening of the deprived eye in adult mice, the

absolute cortical responsiveness needed a longer time period to recover fully. This suggests that different types of plasticity with diverging time courses of recovery might act on cortical cells after MD. The higher magnitude of cortical responses to both eyes apparent eight days after eye re-opening could for instance originate from long-lasting homeostatic mechanisms that scale up neuronal responses during deprivation. This interpretation is also supported by the calcium imaging data presented in Chapter 4, Section 4.4.2.

However, regardless of the nature of the underlying changes, our results demonstrate that the mammalian cortex can adapt reversibly to an imbalance of sensory inputs throughout life. The mouse model of OD plasticity therefore provides an excellent opportunity to assess the influence of recurrent sensory experience on the capacity of the cortex for change.

3.5.3. Facilitation of adult OD plasticity by prior MD experience

In naïve adult mice, three days of contralateral eye MD were not sufficient to induce measurable OD plasticity. However, the same duration of MD resulted in a marked shift of OD in mice that had experienced MD of the same eye up to two months earlier. Although adult plasticity was accelerated irrespective of whether the first deprivation occurred during the critical period or in adulthood, the mechanisms underlying this facilitation may differ depending on the age of the priming MD. In mice that had been initially deprived during the critical period, there was a trend for a weakening of the closed eye without a notable strengthening of the open eye, which contributed to the strong shift in OD induced by the second episode of MD in adulthood (Fig. 3.3). However, these changes in input strength of the two eyes induced by a second MD did not resemble those accompanying OD plasticity in naïve adult mice. Rather, they partially recapitulated the effects seen in young animals. In contrast, when both MD episodes were induced in adulthood, the changes of response strength were akin: after the second deprivation – just like after the first – the representation of the deprived eye stayed strong and the open eye increased its influence. Taken together, these results indicate that the mechanisms underlying enhanced OD plasticity in adult mouse visual cortex may depend on the deprivation history.

Not only was the shift of cortical OD accelerated by prior experience, it also persisted for much longer after the restoration of binocular vision. At first glance this might appear

counterintuitive. If recovery from MD is simply a reversal of the initial MD effect and follows the same mechanisms, should OD not also shift back faster? Previous studies have indicated that shift and recovery of binocularity after MD are mediated by different mechanisms. Unlike MD induced plasticity, recovery does not require CREB activation (Liao et al. 2002) or protein synthesis, can occur much more rapidly (Krahe et al. 2005). Most importantly, enhancing CREB activity in adult mice seems to result in longer lasting OD shifts (Pham et al. 2004). These studies are in good agreement with our finding that enhanced plasticity might lead to more persistent MD effects.

3.5.4. Specific trace in the visual cortex

The enhancement of plasticity was apparent only after repeated deprivation of the same eye, since deprivation of the other eye three to four weeks later did not lead to a facilitated OD shift. In contrast, depriving the opposite eye earlier in life even impaired OD plasticity. These findings indicate that prior deprivation does not increase cortical plasticity in general to any input, as has been observed after dark rearing (Cynader and Mitchell 1980) or after pharmacological manipulations (Pizzorusso et al. 2002). Instead, they argue for very specific changes in cortical circuitry, which support the facilitation of OD shifts only in the same direction as experienced earlier in life, and interfere with inverse modifications that would give rise to OD shifts in the opposite direction.

What is the nature of these changes? Prior MD experience could establish a trace in the form of lasting biochemical and/or structural changes, which are (re)activated upon the second MD. For instance, activity-dependent changes in visual cortex associated with the initial MD episode could lead to altered postsynaptic density composition of pre-existing synapses, or the generation of new synapses that would become silent during the recovery, which would subsequently facilitate future circuit adaptations. The view that structural changes might form the basis for the facilitation of OD plasticity is supported by closely related observations in the barn owl's auditory localization system (Knudsen 1998). Here, the capacity for plasticity of auditory midbrain neurons in response to a prism-induced visual field displacement is extended into adulthood if the owls had a similar prism experience as juveniles. The shifts of auditory space fields in adult owls is explained by the formation of new axonal connections during initial prism-rearing (DeBello et al. 2001), which are physically maintained but

functionally disabled after the removal of the prisms and the shifting back of auditory space fields (Linkenhoker et al. 2005). In mouse visual cortex, too, MD can result in anatomical changes, which have been observed at the presynaptic (Antonini et al. 1999) as well as the postsynaptic level (Mataga et al. 2004, Oray et al. 2004). It is therefore tempting to speculate that these structural changes might outlast the first MD, facilitating the OD shift during a second episode of MD.

3.5.5. General implications

Changes in cortical circuitry following MD affect vision. The imbalance of binocular inputs early in postnatal life leads to the development of poor visual acuity (Muir and Mitchell 1973, Prusky and Douglas 2003). In contrast, in adult amblyopic humans and normal mice, occlusion of one eye can lead to the improvement of spatial vision (Levi 2005, Douglas et al., Soc. Neurosci. Abstracts, No. 866.15, 2004). Notably, these behavioural findings are in close keeping with the loss of deprived-eye function and the gain of non-deprived-eye function in the contralateral visual cortex of the mouse after juvenile and adult MD, respectively. The MD paradigm in mice, therefore, provides a useful general model for studying the mechanisms underlying plasticity of cortical circuits (Hensch 2005, Hübener 2003) and related behaviours (Prusky and Douglas 2003). We used this model to show that the repetition of altered sensory experience leads to a faster adaptation of neural circuits in visual cortex. Moreover, we demonstrated that cortical changes after repeated experience are more persistent, and that the conditioning effect of experience is not restricted to a period early in life but that it also occurs in adulthood. Since facilitation of adult plasticity by prior experience has been demonstrated also in the barn owl midbrain (Knudsen 1998), it seems likely that this is a general characteristic of plasticity in the CNS. It remains to be seen whether the phenomenon reported here also explains the more general observation that learning of specific tasks or abilities and the retention of this knowledge are improved by previous learning experiences of the same kind.

4. Monocular deprivation induces bidirectional scaling of eye-specific responses in primary visual cortex

4.1. Abstract

Ocular dominance (OD) plasticity in visual cortex has long served as a useful model for examining how cortical synapses are shaped by experience. Following a brief period of eyelid closure (monocular deprivation, MD), neurons in binocular cortex shift their relative responsiveness to stimulation of the two eyes. However, it is largely unclear how the magnitude of eye-specific responses in individual neurons is altered by MD, and how this relates to changes of other functional properties like orientation selectivity. To address this, we combined two-photon microscopy with bulk loading of a calcium-indicator dye, which enabled us to measure the activity of hundreds of neurons within the binocular region of mouse visual cortex. We found that the response strength evoked by stimulation of one eye was inversely related to that of the other as a function of OD, such that the summed response remained roughly constant, irrespective of the neuron's OD. This was true in normal as well as in monocularly deprived animals. The shifts in OD observed after 4-7 days of MD were caused by a scaling down of deprived eye responses and a scaling up of non-deprived responses across almost the entire range of response values. Monocular neurons responding to the deprived eye, however, were an exception, as they selectively increased their responsiveness. These results indicate that both competitive and homeostatic mechanisms operate together to regulate the strength of neuronal responses during MD, depending on the relative contributions of eye-specific inputs a neuron receives. Finally, we found that while the reduction of deprived-eye responses was not associated with a significant loss of orientation selectivity, the gain of input for the non-deprived eye under some conditions led to degraded response specificity.

4.2. Introduction

Two general mechanisms of plasticity have been proposed to govern long-lasting activity-dependent modifications of neural circuits. First, changing the pattern of input activity can rapidly adjust the strength of individual inputs, resulting in either long-term potentiation (LTP) or depression (LTD) of synaptic transmission (Hebbian or correlation-based plasticity). Second, chronically altering the level of neuronal activity can be compensated for on longer timescales by global changes in responsiveness or plasticity of a given cell (homeostatic plasticity). How these general forms of plasticity contribute to experience-dependent modifications of functional properties of individual neurons in vivo is at present unclear.

Ocular dominance (OD) plasticity in visual cortex has long served as a useful model for examining how cortical synapses are shaped by experience. As shown in Chapter 3, following a brief period of eyelid closure (monocular deprivation, MD), neurons in binocular cortex shift their relative responsiveness to stimulation of the two eyes (Wiesel and Hubel 1963, Gordon and Stryker 1996). The coexistence of correlation-based and homeostatic plasticity during OD shifts has been difficult to demonstrate because MD at the same time reduces the overall amount and changes the balance of activity between the eyes. Current thinking favours the explanation that OD shifts are largely driven by Hebbian mechanisms (Bear and Rittenhouse 1999), which lead to a depression of deprived eye responses and an enhancement of non-deprived eye responses. Direct experimental support for this idea was provided by a recent study in mice, which demonstrated that MD induces an overall loss of deprived eye responsiveness and a delayed increase of non-deprived eye responsiveness (Frenkel and Bear 2004). This study using population measurements of neuronal activity provided no evidence for homeostatic changes, because the reduction of cortical activity by binocular deprivation did not alter the strength of visually-evoked responses. Recently, however, visual deprivation has been shown to lead to compensatory changes in neurons residing in the monocular cortex (where no competition occurs) by increasing the amplitude of excitatory synaptic currents (Desai et al. 2002). It is not known if such compensatory changes also occur in the binocular cortex during OD plasticity. If correlation-based and homeostatic mechanisms operate in parallel during OD shifts, their relative contributions may depend on the proportions of eye-specific inputs each cell receives. However, addressing this question requires the measurement

of the absolute magnitude of eye-specific responses at the level of individual cells, which was not carried out in previous studies (Frenkel and Bear 2004, Mioche and Singer 1989). Moreover, the two forms of plasticity predict different outcomes for how MD affects the absolute strength of eye-specific responses: correlation-based plasticity, which may primarily affect neurons receiving substantial input from both eyes, is expected to lead to a reduction of deprived-eye responses. In contrast, homeostatic compensation may lead to an increase of deprived eye responses in monocular cells, which are immune to competition from the non-deprived eye.

Investigating how MD changes other functional properties of neurons in the binocular cortex might give additional hints at the mechanisms of OD plasticity. Early, long-term MD has been shown to reduce the proportion of orientation selective neurons responding to the deprived eye (Shatz and Stryker 1978, Sherman and Spear 1982), presumably by interfering with the development of orientation tuning. However, it is unclear how MD affects neurons with mature orientation selectivity at a later phase in development (Crair et al. 1997, Beaver et al. 2002). Is the loss of deprived-eye responsiveness accompanied by a reduction of orientation tuning? How is orientation selectivity affected by a competitive situation, as a cell loses synapses from the deprived eye and gains additional ones from the non-deprived eye? Addressing these questions will provide further insights into how computation of functional attributes of cortical neurons is altered by experience.

In this study, we investigated the mechanisms of OD plasticity by exploring in greater detail how the responsiveness and functional properties of neurons are changed after MD. We combined two-photon microscopy with bulk loading of cortical tissue with a calcium-indicator dye (Stosiek et al. 2003, Ohki et al. 2005) which enabled us to image the activity of hundreds of neurons within the binocular region of mouse visual cortex. This approach offered great advantages over conventional methods for quantifying and mapping visually-evoked neuronal responses, since it allowed for simultaneous monitoring of activity from dozens to hundreds of cells with known spatial distribution at single-cell resolution.

4.3. Material and Methods

Animal preparation and lid suture

All experimental procedures were carried out in compliance with institutional guidelines and the local government. C57Bl/6 mice (postnatal day (P) 20-35) were anesthetized with a mixture of Fentanyl (0.05 mg/kg), Midazolam (5.0 mg/kg) and Medetomidin (0.5 mg/kg). Anaesthesia was maintained by re-injecting half of the initial dose approximately every hour, supplemented by a low concentration of halothane (0.2-0.5%) in a 1:1 mixture of N₂O:O₂, delivered via a small nose cone. Cream (Isoptomax) was applied to the eyes to prevent dehydration during surgery. The skull was exposed, cleaned and attached to a metal plate with dental cement to immobilize the head. A small craniotomy (~ 2mm) was carried out above the binocular visual cortex as determined by stereotaxic coordinates. The exposed cortical surface was kept moist with cortex buffer (125 mM NaCl, 5 mM KCl, 10 mM glucose, 10 mM Hepes, 2 mM MgSO₄, 2 mM CaCl₂, pH 7.4). After dye injection (see below) the cortex was sealed with agarose in cortex buffer (~ 2%) and a coverslip.

Monocular deprivation was induced by suturing shut one eye-lid four to eight days before the imaging experiment using the same injectable anaesthesia as described above. Lid margins were trimmed and the eye lid was closed shut with two mattress stitches (see Chapter 3.3.). Eye-reopening was carried out prior to imaging, directly after the dye injection.

Dye loading and two-photon imaging

Bulk loading of cortical neurons (Stosiek et al. 2003) was performed with the calcium-sensitive dye Oregon Green 488 BAPTA-1 AM (OGB1-AM, Molecular Probes). The dye was dissolved in 4µl DMSO containing 20% Pluronic, and further diluted (1/10) in dye buffer (150 mM NaCl, 2.5 mM KCl, 10 mM Hepes, pH 7.4) to yield a final concentration of 1 mM. The solution was pressure-injected into the cortex at a depth of 200 to 300 µm with a micropipette (3-5 MΩ, 8-12 psi, 2-3 min). This resulted in a stained area of about 250 - 400 µm diameter. In most animals, dye was injected at two or three positions to ensure labelling within the binocular region.

Activity of cortical neurons was monitored by imaging fluorescence changes with a custom-built microscope and a mode-locked Ti:sapphire laser (Mai Tai, Spectra-Physics) at 830 nm through a 40x water immersion objective (0.8 NA, Olympus). Scanning and image acquisition was controlled by Fluoview software (Olympus). The average power delivered to the brain was < 50 mW.

Visual stimulation and data acquisition

At the beginning of each experiment the appropriate retinotopic position was confirmed using small grating stimuli at eight to twelve neighbouring positions. Neuronal responses to stimulation of the two eyes were assessed using two rectangular-shaped grating stimuli (25° azimuth, 50° elevation, 0.03 cycles/ $^\circ$, 2 cycles/s) presented on a monitor in the central visual field of the animal every 11 s for 4 s. Computer-controlled shutters allowed independent stimulation of either eye during each recording sequence. Orientation selectivity was determined by presentation of whole-field gratings drifting in eight directions (0.04 cycles/ $^\circ$, 2 cycles/s). In each stimulus condition, the grating remained stationary for 4.9 s, before moving for 4 s. In most experiments, images (512×512 pixels) were acquired at 1.1 s per frame. Maps containing no or unevenly distributed responses to ipsilateral eye stimulation, indicating an imaging position outside or at the border of the binocular visual cortex, were excluded from further analysis.

Data analysis

Image sequences were aligned for tangential drift and analysed with custom programmes written in ImageJ (NIH) and Matlab (Mathworks). Cell outlines were detected using a semi-automated algorithm based morphological measurements of cell's intensity, size and shape, and subsequently confirmed by visual inspection. All pixels within a cell's outline were averaged to give a single time course ($\Delta F/F$). Neuronal response strength was calculated from the average of 8 to 15 stimulus repetitions, as the average $\Delta F/F$ of the three, 1.1 s frames immediately following stimulus onset, typically centred around the stimulus-evoked response maximum. The baseline was computed as the mean $\Delta F/F$ of the three frames immediately preceding stimulus onset. Cells were considered responsive if the response to any of the stimuli was significantly different from the baseline (ANOVA at $p < 0.01$). The ocular

dominance (OD) score represents the ratio of the contralateral eye response to the summed response of both eyes. An OD score of 0 or 1 indicates exclusive dominance by the ipsilateral or contralateral eye, respectively. Orientation preference was calculated by vector averaging the responses to four different orientations (responses to both directions for each orientation were pooled). Orientation selectivity index (OSI) was calculated as $(1 - \text{average response to non-preferred orientation} / \text{preferred orientation})$. Cells with OSI values of < 0.3 were taken as non-selective for orientation. Cell-based OD maps were computed by colour-coding each cell with the hue corresponding its OD score. In cell-based orientation maps, the hue corresponds to the cell's preferred orientation, whereas the lightness codes for the magnitude of its response ($\Delta F/F$). For pixel-based maps, binned images (256 x 256 pixels) were averaged across stimulus repetitions. The time course of each pixel was then processed to extract OD or OSI values, as described above for cell-based analysis.

Differences between cumulative distributions were assessed using the Kolmogorov-Smirnov test (K-S test). Differences across independent groups of animals or neurons were tested with Kruskal-Wallis ANOVA and Wilcoxon ranksum tests. For statistical analysis of the spatial distribution of cells with different ocular dominance (OD) scores, we computed a cumulative function, $L(t)$, which describes the mean number of cells (of the same OD score) that are within a given distance, t , of a cell's centre, corrected by the cell density. To test whether OD is randomly distributed, we used the Monte Carlo analysis from Diggle (1986). We computed the L function for the real map and each of the 99 random simulations (where OD is randomly assigned for each cell). If the rank of the U score (sum of variance) for the real map was 5 or less out of 100, we rejected the null hypothesis of a random OD distribution at 5% significance level.

4.4. Results

4.4.1. Mapping ocular dominance with in vivo calcium imaging

We investigated how OD is represented in the binocular visual cortex (Fig. 4.1A) at the resolution of individual cells and the surrounding neuropil by means of two-photon calcium imaging. The cortical tissue was bulk-loaded with the AM ester form of the calcium indicator dye Oregon Green Bapta-1 (OGB-1 AM; Fig. 4.1B) (Stosiek et al. 2003, Ohki et al. 2005), resulting in a stained region of approximately 300 μm diameter. Drifting grating stimuli ($25^\circ \times 50^\circ$, Fig. 4.1C), presented independently to the two eyes, evoked fluorescence changes ($\Delta F/F$) in neuronal cell bodies and their surround (Fig. 4.1D,E). The response to each eye was used to calculate the OD score (contralateral eye response, divided by the summed responses to either eye) for each pixel or cell (Fig. 4.1F, see methods). This enabled us to construct maps of eye preference which reveal the OD of every cell in the imaging region. Neurons in the binocular visual cortex of normal mice displayed a range of OD scores, including those driven predominantly by the ipsilateral or the contralateral eye (Fig. 4.1D). The majority of cells was driven by both eyes, but there was an overall dominance of the contralateral eye, consistent with previous studies (see also Chapter 3, Dräger 1975, Gordon and Stryker 1996).

Methods used in earlier mapping studies have not been able to provide conclusive evidence for or against the existence of OD columns in the mouse visual cortex (Dräger 1974, Metin et al. 1988, Schuett et al. 2002). Obtaining OD maps at multiple depths below the cortical surface (down to $\sim 420 \mu\text{m}$, equivalent to superficial layer 5) allowed us to investigate both how OD varies with cortical layer and whether cells with similar OD scores form clusters (Fig. 4.2). We found that proportions of neurons with different OD did not vary systematically with depth. This is perhaps not surprising considering that, in the mouse, axons of LGN afferents are not confined to layer 4, but also ramify within superficial layers (Antonini et al. 1999). However, in some animals we did find evidence for spatial clustering of OD in the tangential plane. This became particularly apparent when cells from different optical sections were collapsed into the same image (Fig. 4.2A,B, see also Fig. 4.3A). Statistical analysis (see Methods) revealed significant clustering of OD in four out of five tested animals. Thus, while

there was some tendency for a clustered organisation of OD, mouse visual cortex clearly lacks distinct OD columns.

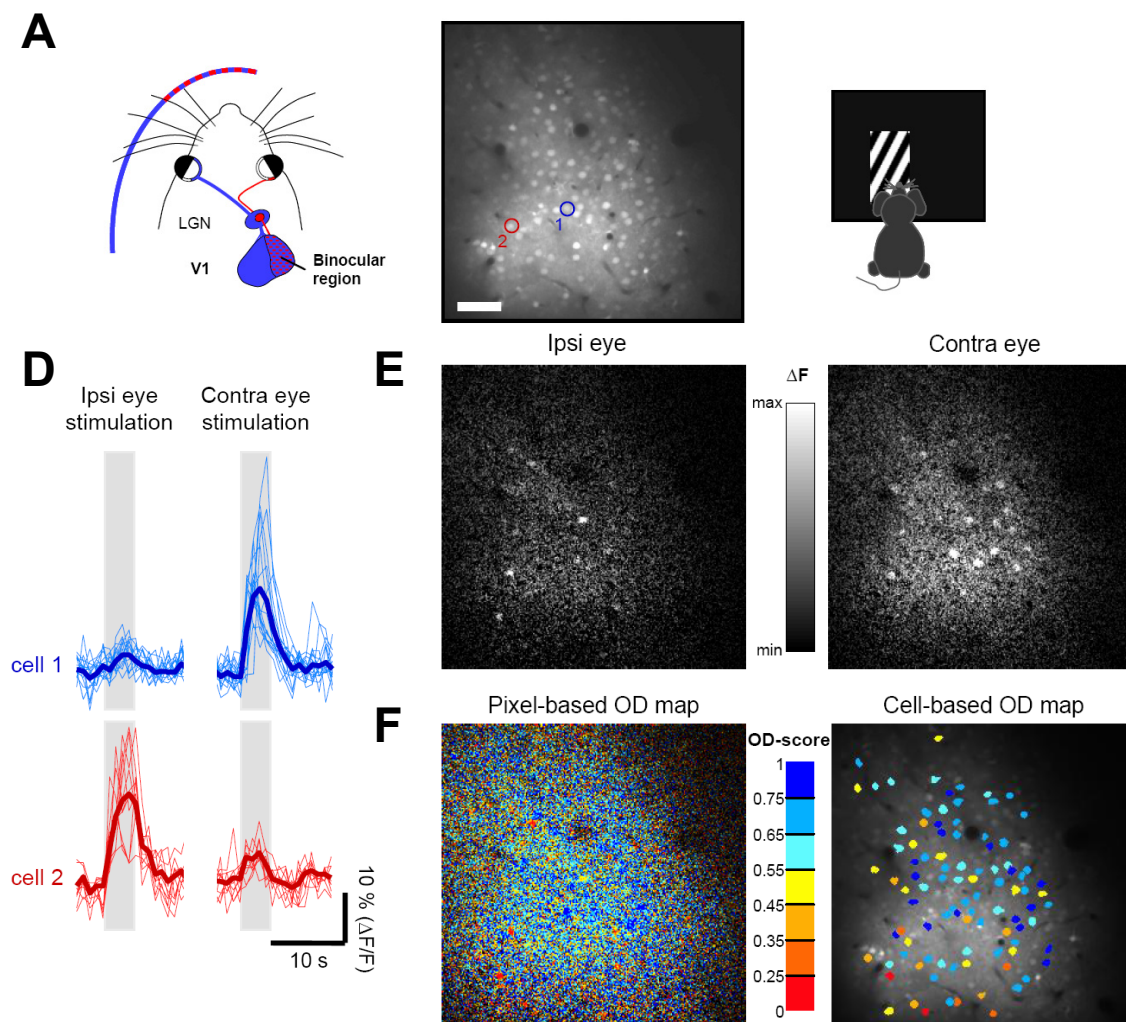


Figure 4.1. In vivo two-photon calcium imaging of ocular dominance in binocular mouse visual cortex. (A) Schematic of the mouse visual system. (B) In vivo image from OGB1-AM loaded cells (average of 400 frames) 230 μm below the brain surface in the binocular visual cortex of a normal mouse. Scale bar, 50 μm . (C) Schematic showing the position of a visual stimulus ($25^\circ \times 50^\circ$) presented to each eye separately, used to evoke eye-specific responses in the binocular visual cortex. (D) Visually evoked calcium transients from two neurons depicted in B. The thin traces show individual responses to stimulation of each eye, thick traces are average responses to 10 presentations. Stimulation periods are indicated by grey bars. (E) Single-condition maps of $\Delta F/F$ for responses to the contralateral (left panel) and ipsilateral (right panel) eye. (F) Pixel-based (left) and cell-based (right) OD maps, colour coded by the OD score (see methods), as indicated in the legend. OD score of 1 or 0 denotes exclusive response to contra- or ipsilateral eye stimulation, respectively, a value of 0.5 indicates equal response to both eyes.

Importantly, the absence of clear OD columns in the mouse does not narrow the overall range of OD scores, since neurons with very distinct eye preferences were frequently located in close proximity. Thus, despite the lack of large-scale grouping of neurons with similar OD preferences, the input preference of individual neurons is nonetheless highly specific.

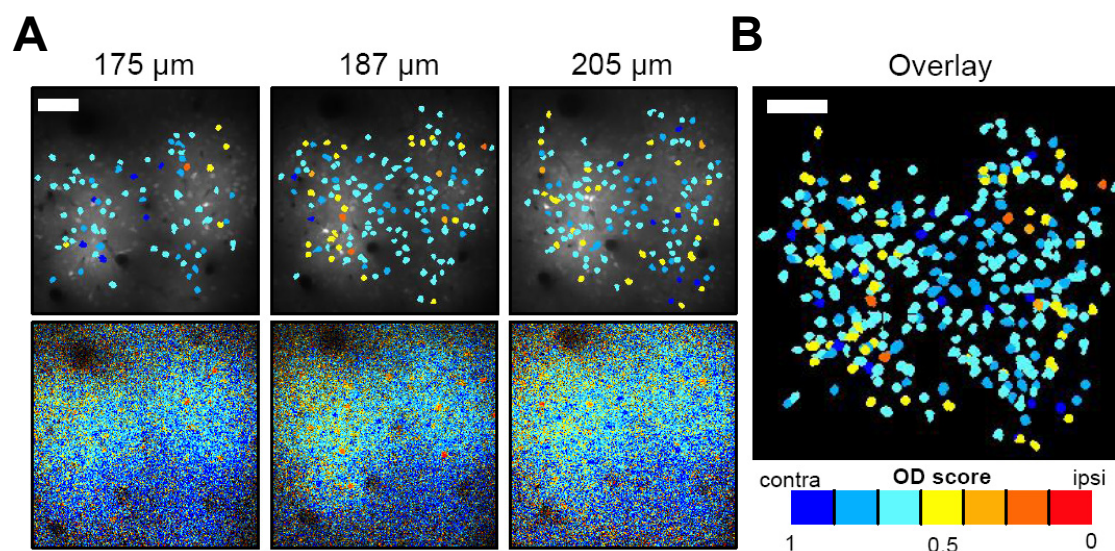


Figure 4.2. Determining ocular dominance at different depths in the visual cortex. (A) Cell-based (top) and pixel-based (bottom) OD maps at three cortical depths in layer 2/3 from a normal mouse. (B) Overlay of the three cell-based maps shown in A demonstrates clustering of cells with mixed or ipsilateral eye inputs. Scale bars, 50 μm .

4.4.2. Bidirectional changes of eye-specific responses induced by MD

We next explored how a period of MD in juvenile mice changed the OD of individual cells in visual cortex. Four to seven days of MD induced a strong shift in the OD scores (Fig. 4.3) in favour of the non-deprived eye, concurrent with previous studies (Gordon and Stryker 1996). Deprivation of the contralateral eye shifted OD towards the ipsilateral eye, such that most neurons responded equally to both eyes (Fig. 4.3, middle panels). Ipsilateral eye closure expectedly caused a shift in the opposite direction, resulting in a large majority of neurons that strongly preferred the non-deprived, contralateral eye (Fig. 4.3, right panels). These results demonstrate that two-photon calcium imaging can reliably report OD shifts in mouse visual cortex.

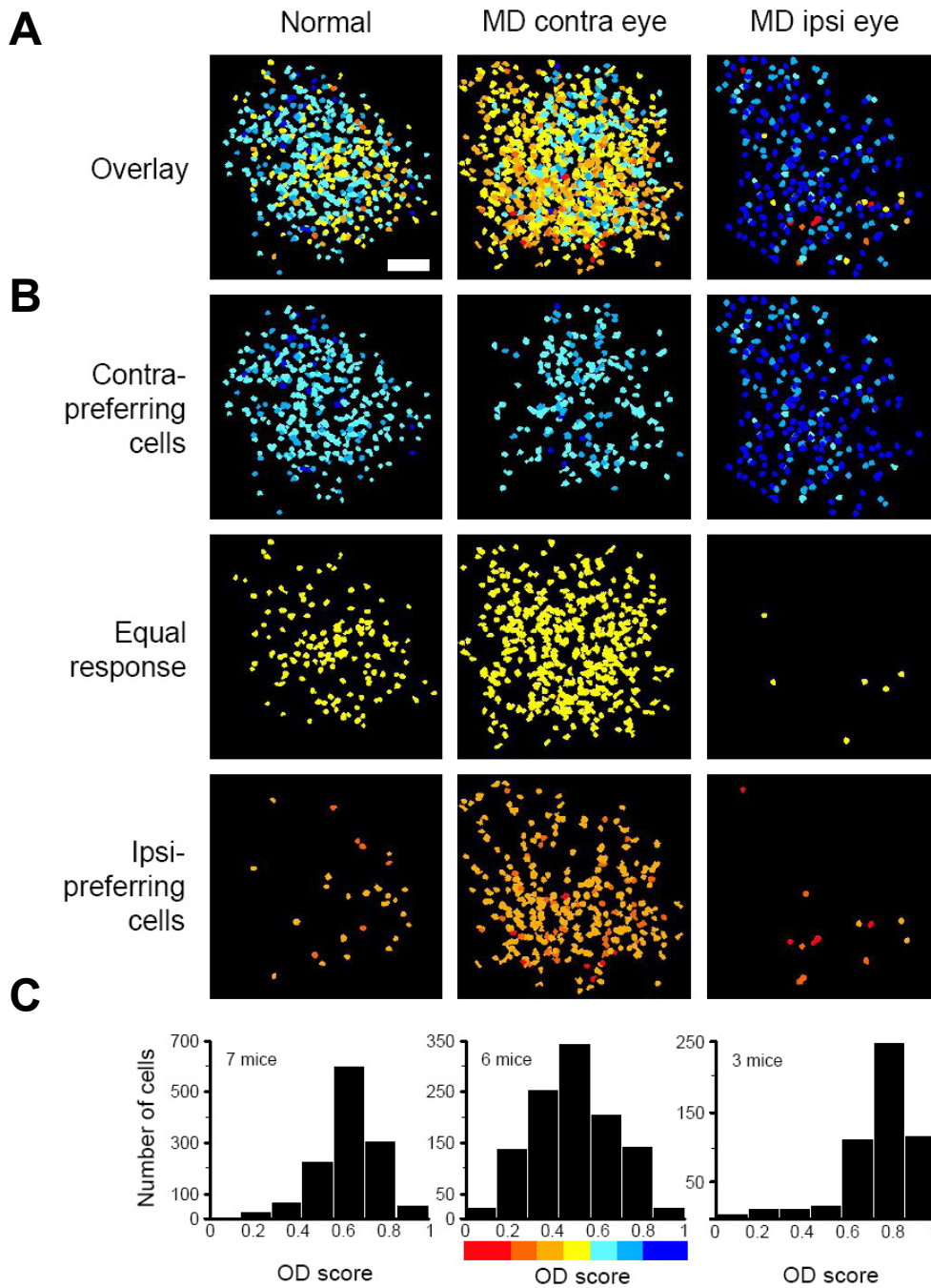


Figure 4.3. Monocular deprivation induced shifts in ocular dominance. (A) Overlay of cell-based OD maps at different depths for a normal mouse (left, P 31, 4 depths, 190 – 290 μm), after a 5-day contralateral MD (centre, P 32, 6 depths, 195 – 410 μm) and after a 5-day ipsilateral MD (right, P32, 2 depths, 200 and 225 μm). Scale bar, 50 μm . (B) Maps from A, with cells split into three groups, depending on OD; top: OD score 0.55-1, centre: 0.45-0.55, bottom: 0-0.45. (C) Distribution of OD scores for all mice under the different conditions.

As shown in Chapter 3, assessing OD plasticity with intrinsic signal imaging had enabled us to measure changes in the absolute response magnitudes for both eyes. This has also been achieved in recent MD-studies recording visually evoked potentials (VEPs), which demonstrated the contribution of both depression of deprived eye responses as well as potentiation of non-deprived eye responses to the MD-effect (Frenkel and Bear 2004). Both intrinsic signal imaging as well as VEP recordings, however, can only measure the integrated activity of large populations of neurons.

Calcium imaging allows us to study OD plasticity in much greater detail by exploring absolute responsiveness at the level of individual cells. Cumulative histograms of response strength for all neurons demonstrate that MD shifted response amplitudes to either smaller or larger values depending on which eye was deprived (Fig 4.4A,B, k-s test, $p < 10^{-10}$ for all cases). Irrespective of which eye was closed, non-deprived eye responses were elevated across the whole population of neurons while deprived-eye responses were mostly scaled toward lower values.

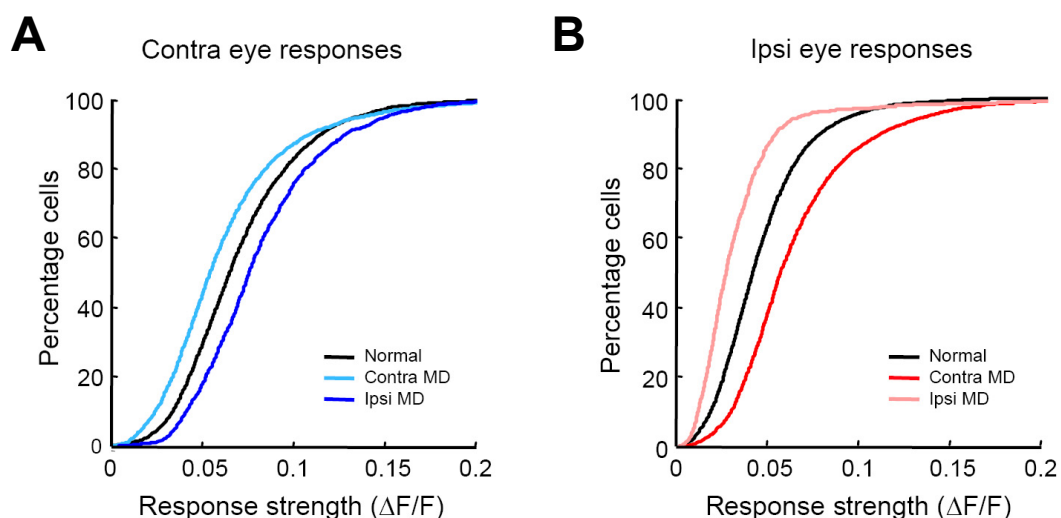


Figure 4.4. Cumulative distribution of response magnitudes for both eyes. Cumulative histograms of response magnitudes to contralateral (A) and ipsilateral eye (B) stimulation, for all cells of normal and deprived mice. Note strong changes in neuronal response strength for both eyes caused by MD.

Pixel-based maps of OD reveal the relative distribution of eye-specific responses in both single neurons as well as their surrounding neuropil (Fig. 4.1F and 4.5). In normal animals the

average OD score of the neuropil was similar to the median OD score of all the neurons for that map (Fig. 4.5A, upper panels, $p > 0.2$). Similarly, after MD of either eye, both the neuropil and most cells shifted their preference in favour of the non-deprived eye (Fig. 4.5A, middle and lower panels). In all cases, however, we found that the OD of individual cells could deviate dramatically from the immediate surround (Fig. 4.5B), indicating that neurons derive their tuning in a highly selective manner.

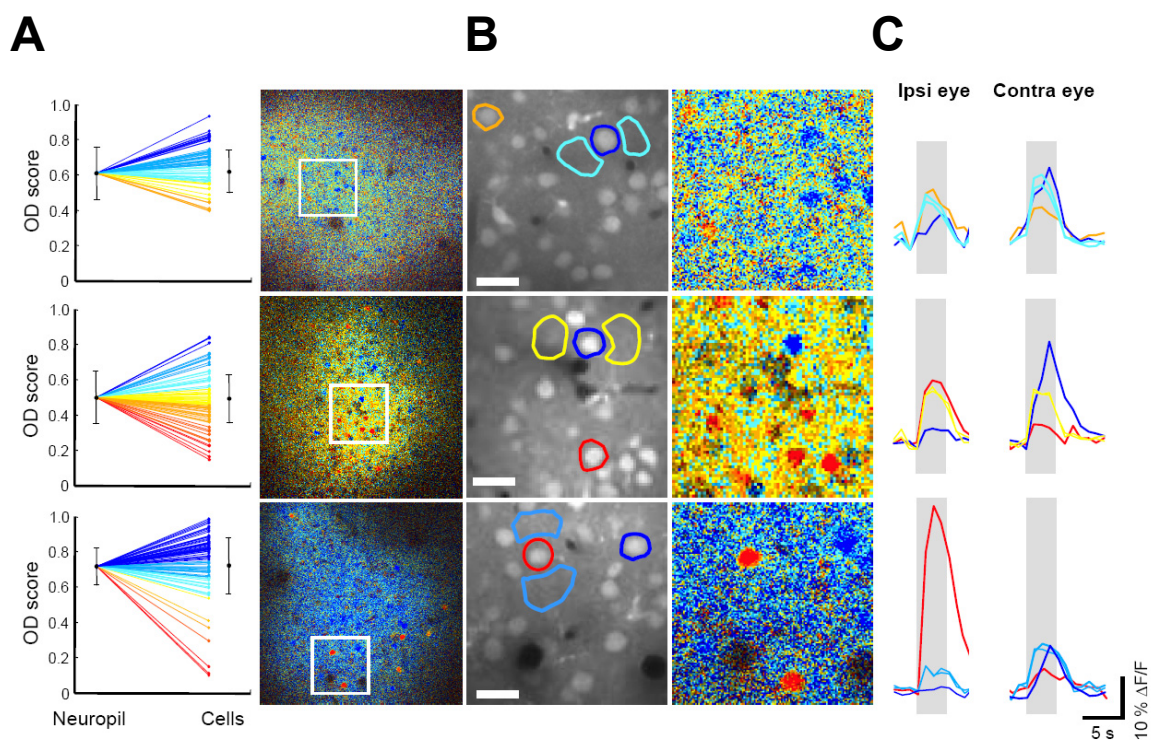


Figure 4.5. Comparison of OD in individual neurons and the surrounding neuropil of normal and deprived mice. OD distribution and eye-specific responses from example maps, obtained in cortical layer 2/3 of a normal mouse (top panels), a contralaterally deprived (6 d, middle panels) and an ipsilaterally deprived animal (4 d, bottom panels). **(A)** Mean OD values of cells and neuropil, and OD score distribution of cells (left panels), as obtained from the pixel-based maps shown to the right. Error bars indicate standard deviation. **(B)** Enlarged regions from the three maps shown in **A**, demonstrating cells with highly deviating response preferences in close proximity. Corresponding images of the staining pattern (left panels) and pixel-based OD maps (right panels) from the region depicted in **A** are shown. Scale bar, 20 μm . **(C)** Averaged responses (10 repetitions) to ipsi- and contralateral stimulation for cells and neuropil regions depicted in **B**. Note that neurons strongly dominated by the deprived eye show enlarged responses. Colour-coding of OD is identical to Figures 4.1, 4.2 and 4.3.

A strong deviation in OD of some cells from the surrounding neurons and neuropil was particularly apparent in deprived animals (Fig.4.5B, middle and lower panels). Those cells belonged to a minority of cortical neurons which apparently did not shift their OD towards the non-deprived eye during MD, but showed strong preference for or exclusive responses to the deprived eye. Comparing response magnitudes of those cells to neighbouring neurons and neuropil (Fig. 4.5C) revealed that they did not exhibit weakened responses to the deprived eye. Rather, these monocular neurons subserving the deprived eye showed elevated responses to deprived eye stimulation in comparison to other cells and the neuropil (Fig 4.5C).

These data prompted us to explore in greater detail how MD changes the relationship between absolute magnitude of neuronal response at the level of individual neurons. In normal animals, with increasing monocular stimulation of the dominant eye, absolute responses evoked by monocular stimulation of the dominant eye increased, while those to the non-dominant eye decreased (i.e. as OD scores approach 0 or 1 for ipsilateral or contralateral eye responses, respectively, Fig.4.6A). This relationship was also clearly apparent after deprivation of either the contra- or the ipsilateral eye, as the overall distribution of OD values shifted toward the non-deprived eye. Thus, on an absolute scale, the response strength of one eye was inversely related to the response strength of the other eye as a function of OD, such that the summed responses of a neuron remained roughly constant irrespective of its OD score. After MD, however, this relationship was not obeyed by neurons dominated by the deprived eye (OD score > 0.6 or < 0.4 for contralateral or ipsilateral eye, respectively). The responses of these neurons were significantly larger after MD than in normal mice (Wilcoxon ranksum test: contralateral eye, $p < 10^{-4}$, ipsilateral eye, $p < 0.01$), while the average response magnitude of neurons within the remaining OD classes did not change substantially (Fig. 4.6B).

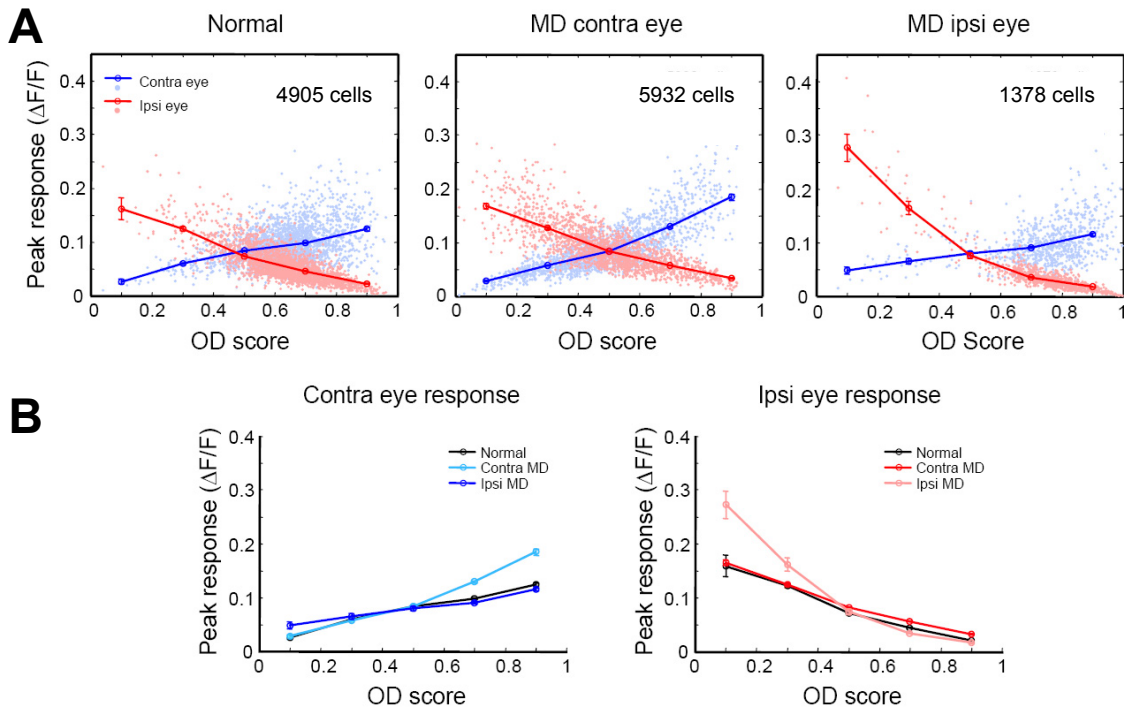


Figure 4.6. Relationship of response magnitude and OD before and after MD.

(A) Response magnitude to ipsi- (red dots) and contralateral (blue dots) stimulation for each cell, plotted against its OD-score for normal and deprived mice. Thick lines show mean responses for five equally divided OD-classes. (B) Mean response magnitudes from the three conditions shown in A, plotted for each eye separately. Note enhanced responses of neurons dominated by the deprived eye after MD. Error bars indicate SEM.

This increased responsiveness of neurons predominantly or exclusively responding to the deprived eye could have already been surmised from the cumulative response strength histograms in Figure 4.4. While deprived-eye responses were reduced for almost the whole population of cells, the highest responses (which are predominantly from monocular neurons as is apparent from Figure 4.6) were increased. And indeed, separating the responses of the deprived eye by OD score revealed that neurons dominated by deprived eye selectively scaled up their responses, while the responses of the remainder were scaled down (Fig. 4.7A,B, k-s test, $p < 10^{-4}$ for all cases). Together, these data suggest that MD has distinct effects on different types of cortical neurons. In neurons driven by both eyes, deprived-eye inputs seem to lose influence in competition with those from the open eye. In contrast, in cells with little or no input from the open eye, deprived eye responses were not weakened, but instead were scaled up, possibly by homeostatic mechanisms.

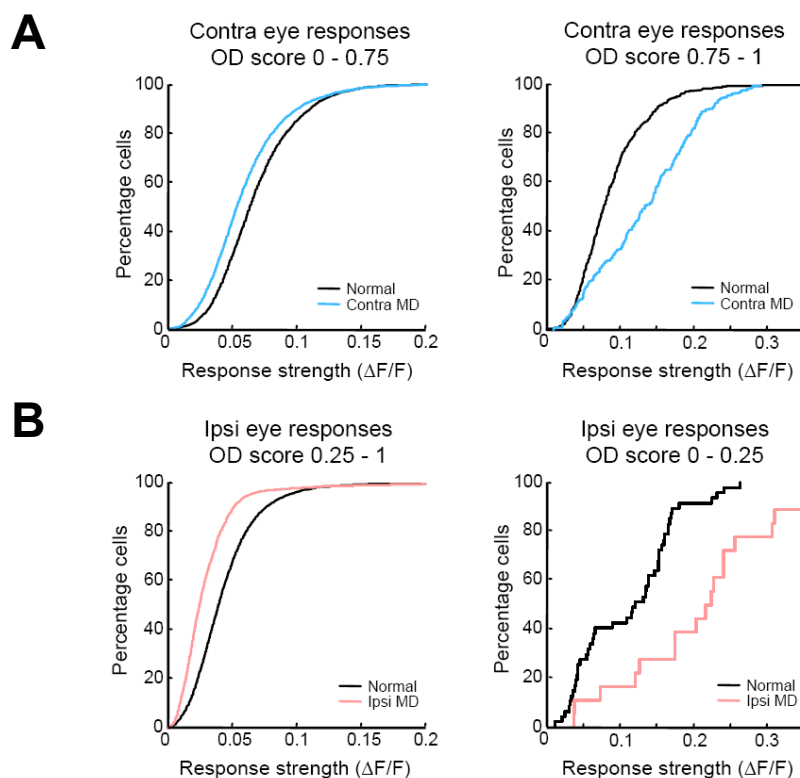


Figure 4.7. Bimodal scaling of deprived eye responses. (A,B) Cumulative histograms of response magnitude for deprived-eye responses after contralateral (A) and ipsilateral (B) MD in comparison to normal eye-specific responses. Cells are split in two groups according to their OD values. Neurons strongly dominated or exclusively driven by the deprived eye (right panels) and the remaining cells (left panels) show scaling in opposite directions.

4.4.3. Orientation selectivity in mouse visual cortex after MD

It is unclear how shifts in OD affect other functional properties of cortical neurons. To investigate if MD changes orientation selectivity in the binocular cortex, we measured the responses to drifting gratings of eight different directions presented to each eye independently (Fig. 4.8A,B). This allowed us to quantify orientation selectivity (orientation selectivity index, OSI, see methods) and OD for each cell and generate fine-scale maps of orientation preference in normal and monocularly deprived mice (Fig. 4.8C,D). In general, cells preferring different orientations were scattered across the binocular region, without any obvious clustered organization. The majority of responsive neurons (61%) showed considerable orientation selectivity ($OSI > 0.3$).

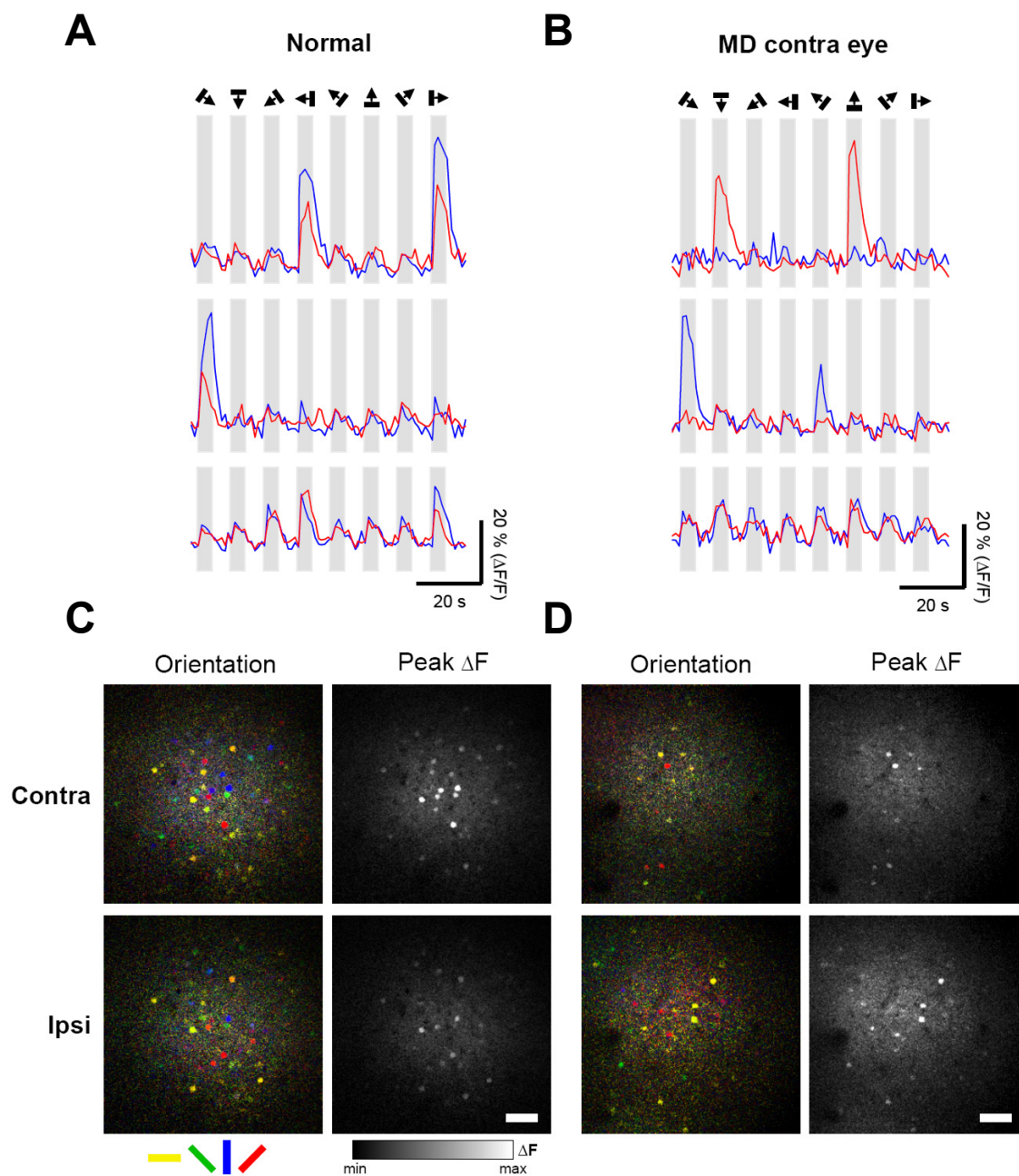


Figure 4.8. Imaging orientation selectivity in mouse visual cortex. (A,B) Averaged (8-10 repetitions) calcium transients in response to stimulation of the contralateral (blue traces) and ipsilateral eye (red traces), for three differently tuned cells in normal (A) and contralaterally deprived mice (B). Stimuli were gratings, moving in eight different directions, as depicted above the plots. Grey bars indicate stimulation periods. (C,D) Pixel-based maps of orientation preference (left panels) and response magnitude (right panels) for the contralateral (top) and ipsilateral (bottom) eye in layer 2/3 of a normal mouse (C) and following MD of the contralateral eye (D). Orientation preference of every pixel is colour-coded as indicated below. Scale bars, 50 μm .

Interestingly, after five to seven days of MD, OSI values of deprived eye responses remained within the same range after MD, despite weaker responsiveness (Fig 4.9A). Neither the proportion of orientation selective cells responding to either eye nor the mean OSI was significantly different from those in normal mice (Fig 4.9B,C, $p > 0.1$).

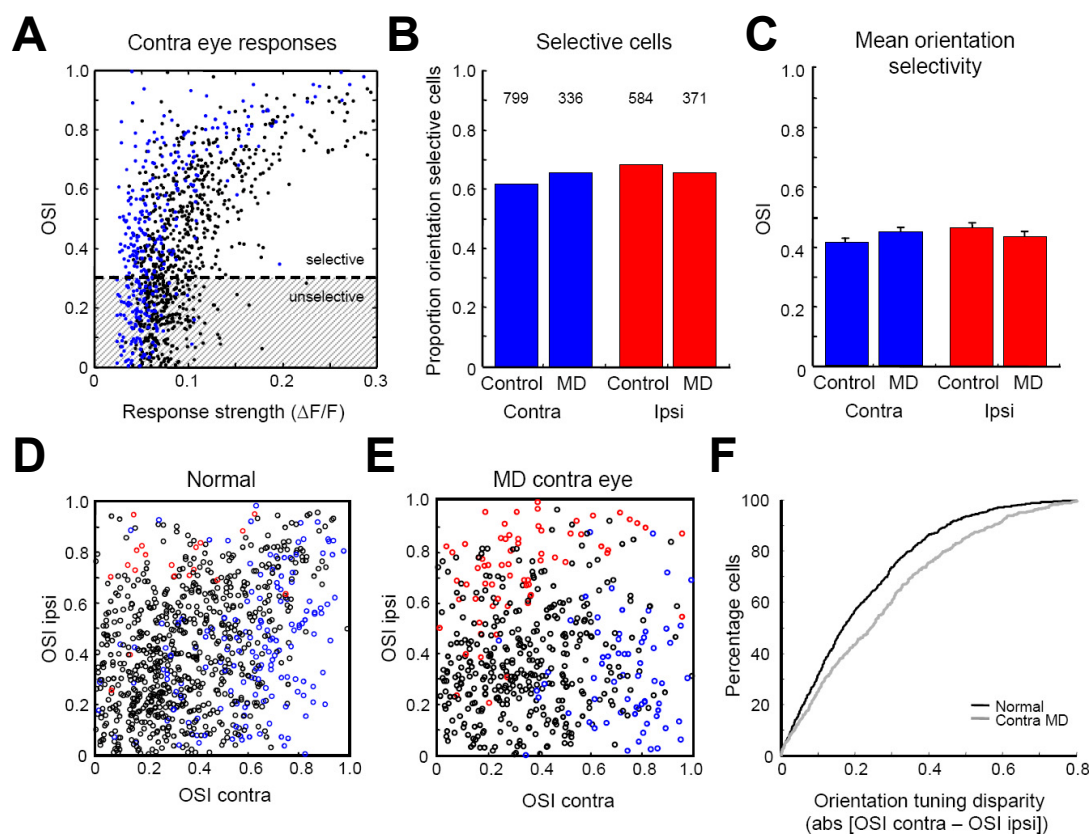


Figure 4.9. Changes in orientation tuning after contralateral MD. (A) Orientation selectivity index (OSI), plotted against response strength for contralateral eye stimulation in normal mice (black dots) and after contralateral eye MD (blue dots). Responses with OSI < 0.3 are defined as not selective for orientation. (B) Proportion of orientation selective neurons (OSI > 0.3) for each eye out of the cells responding significantly ($p < 0.01$) to stimulation of that eye, in normal ($n = 2$) and deprived animals ($n = 3$). Number of responsive cells is depicted above each bar. (C) Mean OSI values of all significantly responding neurons. Error bars indicate SEM. (D,E) OSI values of both eyes plotted against each other, for each neuron responding significantly to at least one eye, in normal mice (D) and following MD (E). Data points are colour-coded according to the cells' OD, divided equally in three classes, cells dominated by the ipsilateral eye (red circles), binocular (black circles), and dominated by the contralateral eye (blue circles). (F) Cumulative histogram of the absolute differences between the OSI-values for stimulation of contra- and ipsilateral eye, for all neurons responding significantly to at least one eye in normal (black line) and deprived mice (grey line).

The lack of significant degradation of deprived-eye orientation selectivity was not expected, given earlier studies claiming a loss of orientation tuning after MD (Shatz and Stryker 1978, Sherman and Spear 1982). We therefore explored our dataset further, by comparing orientation selectivity measured through the deprived and the non-deprived eye for each significantly responsive cell (Fig 4.9D), and investigated how this relationship varied with OD.

In normal animals, the majority of cells were driven substantially by both eyes, and in a large fraction of these the contralateral and ipsilateral responses were similarly selective for oriented gratings. After contralateral eye MD, however, this relationship was dramatically altered. Overall, the number of cells with similar orientation selectivity for both eyes greatly diminished (Fig 4.9E), as the differences in orientation disparity increased in comparison to normal animals (Fig 4.9F, $p < 10^{-5}$). Although this result can be partly explained by an increased presence of predominantly monocular cells after MD (OD score > 0.67 or < 0.33), the disparity between deprived and non-deprived eye OSI values became greater even for binocular cells (OD score > 0.33 and < 0.67 , k-s test, $p < 0.05$). Specifically, there was a decreased proportion of binocular cells which were highly orientation selective for both eyes (Fig. 4.9E). This seemed to be at least partly due to a gain in binocular neurons which were selective for orientation for the deprived eye, but not for the non-deprived eye, since the mean OSI of binocular neurons was significantly lower for stimulation of the non-deprived eye after MD ($p < 10^{-3}$), but not for stimulation of the deprived eye ($p = 0.8$).

4.5. Discussion

4.5.1. Imaging calcium transients in mouse binocular visual cortex

In this study, we used fluorometric calcium imaging *in vivo* to assess the functional properties of neurons in the visual cortex by monitoring the changes in somatic calcium concentration associated with neuronal activity (Smetters et al. 1999). Although this is only an indirect measure of neuronal spiking, several studies have demonstrated that the observed somatic calcium transients reflect suprathreshold, not subthreshold activity and reliably report action potential firing (Smetters et al. 1999, Mao et al. 2001). Moreover, the amplitude of somatic calcium responses seems to be a good indicator for the firing rate of a given cell (Kerr et al.

2005, Mao et al. 2001). Therefore, calcium imaging provides a suitable method for monitoring the spiking activity of large populations of neurons.

A possible limitation of our method could arise from the low temporal resolution of data acquisition (approximately 1 Hz frame rate), as this might result in the omission of an initial, transient peak of the response. However, we presented stimuli over a prolonged time period (4 s), which evoked strong, sustained responses in the visual cortex. When taking example traces with faster imaging rate (0.1 Hz), we did not observe a substantially different visual response shape. We therefore do not consider the temporal resolution to be of concern, especially since our results on eye-specific responses, OD and orientation selectivity are highly comparable to those from studies using electrophysiological single-unit recordings (Dräger 1975, Gordon and Stryker 1996).

At the same time, our approach offers several advantages over conventional methods for quantifying and mapping visually-evoked neuronal activity. First, the responsiveness of up to hundreds of cells can be visualised simultaneously (at $\sim 1 \mu\text{m}$ resolution), which permits the mapping of different functional properties (OD, orientation selectivity, retinotopy) on a fine spatial scale at different depths below the cortical surface. Second, the activity of single neurons can be compared to that of the surrounding neuropil, permitting simultaneous measurement of pre- and post-synaptic activity. Third, since this method can detect the responses of all cells within a given cortical region, it avoids sampling errors inherent to recordings with microelectrodes. This further allows the quantification of the proportions of responsive and unresponsive cells for any given stimulus. Applying *in vivo* calcium imaging to mouse binocular cortex, which contains a highly diverse mixture of neurons with different functional properties in close proximity, enabled us to directly compare visual responses in neighbouring cells.

4.5.2. Organisation and specificity of functional properties

In contrast to many higher mammals, the primary visual cortex of rodents has not been shown to have a columnar organization of OD and orientation tuning (Dräger 1974, Schuett et al. 2002, Van Hooser et al. 2005). In this study we could demonstrate that, even on a fine spatial scale, a systematic columnar arrangement of neurons with different functional

properties does not exist in the mouse, although we did observe a bias for clustering of OD. Whereas functional maps based on cortical columns may serve to minimize wiring (Koulakov and Chklovskii 2001, Swindale et al. 2000), the fact that some highly visual mammals lack OD or orientation columns (Murphy and Berman 1979, Adams and Horton 2003, Van Hooser et al. 2005) implies that functional maps are not essential for effective processing of visual information. Indeed, our results make it evident that neurons in mouse visual cortex can be functionally highly differentiated with respect to both their neighbours and the surrounding neuropil (Figure 4.5.). Considering that neuropil responses to a large degree represent the activity of presynaptic structures (Kerr et al. 2005), our results indicate that 1) the functional property of a neuron is not simply a reflection of the average functional attributes of the surrounding inputs, and 2) the spatial clustering of neurons responding to similar visual features is not necessary for functional specificity. In this respect, the spatial organization of orientation preference in mouse visual cortex resembles that of pinwheel centres in the cat – where neurons with disparate orientation tuning are located in close proximity, receiving the majority of their input from neurons with different preferred orientations (Bonhoeffer and Grinvald 1991, Maldonado et al. 1997). Since connectivity in the cortex is predominantly local, sharp tuning in individual neurons must arise by either intrinsic computation of diverse inputs (Schummers et al. 2002) or very precise connectivity (to similarly tuned neurons) within the local network. This specificity is all the more remarkable given that dendritic and axonal fields of neurons in mouse visual cortex can extend over distances up to 500 μm (Antonini et al. 1999, Holtmaat et al. 2005). The mouse therefore provides a useful model for investigating how precise (functional) connections are formed during development and how they are altered by experience.

4.5.3. Homeostatic OD plasticity

Previous studies have shown that brief experience of MD causes a strong shift in the number of neurons preferring one eye or the other (Wiesel and Hubel 1963, Gordon and Stryker 1996). At the level of the entire network, this shift is explained by a reduction of deprived-eye responses and an increase of non-deprived eye responses (Frenkel and Bear 2004, see also Chapter 3), which likely arises from the loss and gain of synaptic drive from the two eyes (Heynen et al. 2003, Mataga et al. 2004). It is still largely unresolved which mechanisms act on

individual cells or even individual synapses during OD plasticity, and whether these apply equally to the entire population of neurons in the binocular cortex. We found that the nature of MD-induced effects seemed to be dependent on the proportion of inputs a neuron receives from each eye. In cells with substantial input from the eye that had remained open, responses to the deprived eye were weakened, probably due to a competitive situation arising from the altered binocular input. In contrast, the responses of cells receiving dominant or exclusive input from the deprived eye were strengthened by deprivation.

Which mechanisms could account for the increase of visual drive in cells responding predominantly to the deprived eye? It is very likely that these cells had received the majority of their inputs from the deprived eye also before MD, and that they remained predominantly monocular following MD, as the relatively weak drive from the non-deprived eye was not sufficient to shift their OD substantially in favour of that eye. The reduced drive from the deprived eye may have been expected to cause a long-lasting depression of responsiveness through Hebbian mechanisms, as proposed by earlier work (Heynen et al. 2003); however, we found the opposite to be true. Our results are consistent with the notion that enhanced responses of monocular neurons subserving the deprived eye most likely arose from compensative, homeostatic mechanisms, triggered to prevent the total loss of connectivity that might have emerged from Hebbian plasticity alone (Desai 2003). Indeed, in neural preparations whose activity had been globally manipulated, there is growing evidence supporting the existence of homeostatic processes acting to alter the overall synaptic strength or intrinsic excitability (Turrigiano and Nelson 2004, Burrone and Murthy 2003), or to modify the threshold for plasticity at individual synapses (Bienenstock et al. 1982, Bear 1995, Abraham and Bear 1996). In ex-vivo visual cortex after deprivation, these mechanisms may counteract the loss of activity through the amplification of synaptic drive (Desai et al. 2002) or the facilitation of further synaptic strengthening by promoting the induction of LTP in favour of LTD (Kirkwood et al. 1996). Although we cannot distinguish between these alternatives, our findings strongly suggest that homeostatic plasticity operates in binocular cortex during MD. As such, they lend additional support for theoretical frameworks based on combined homeostatic and Hebbian rules, which have been put forward to explain how MD shifts OD in neurons receiving substantial input from each eye (van Rossum et al. 2000, Bear 2003).

Results from a previous study seem at apparent odds with our findings, since they indicate that 24 hours of MD lead to a reduction of deprived-eye response which is correlated with the expression of LTD in the monocular cortex (Heynen et al. 2003). However, since homeostatic changes appear to develop over prolonged deprivation periods (> 1 day, Turrigiano and Nelson 2004), it is plausible that the scaling up of deprived eye responses is preceded and even promoted by their earlier depression. Further experiments are needed to establish the time course of homeostatic changes in vivo, and how they interact with Hebbian rules during development and during experience-dependent plasticity of cortical circuits.

4.5.4. MD-induced changes in orientation tuning

The maturation and maintenance of orientation selectivity in the visual cortex depends crucially on normal visual experience after eye-opening (Crair et al. 1998, Chapman et al. 1999, White et al. 2001). Thus, it is not surprising, that prolonged MD during this period results in irreversibly degraded orientation tuning of the deprived eye (Shatz and Stryker 1978, Sherman and Spear 1982, Liao et al. 2004). The most sensitive period for OD plasticity occurs later in development, when other functional properties like orientation tuning are already largely mature. Previous studies did not systematically examine how MD induced during this period affects orientation selectivity and its relationship to the magnitude of eye-specific responses. We found that the induction of a short-term MD, which results in saturated OD shifts, does overall not lead to reduced orientation selectivity for either eye. The removal of salient, high-contrast information and the changes in neuronal firing pattern induced by eye-lid suture do therefore not per se degrade selectivity of responses at this late stage in development, nor does the weakening of deprived-eye responses. This indicates that the loss of inputs alone does not necessarily affect the computation of response selectivity. Instead, our data suggest that under specific conditions (as outlined below) the newly gained functional input from the open eye after MD might be non-selective, since in neurons which are binocular after MD, orientation tuning through the non-deprived eye is degraded. These neurons presumably were dominated by the deprived, contralateral eye before MD, and thus for the most part ($\sim 80\%$) received only weak, poorly selective input from the non-deprived eye. In contrast, gained input seemed to be more selective in neurons that already had substantial input from the same eye before, since cells that are dominated by the open eye after MD (and thus presumably were binocular

before the OD shift) did not show degraded orientation tuning through that eye. While these results are preliminary since the sample size is very low (2 normal and 3 deprived mice), they suggest that the reorganization of inputs can be accompanied by a degradation of functional properties. It remains to be seen if the newly gained input stays unspecific, or whether it acquires tuning with prolonged exposure to orientated features in the visual environment.

An MD study in cats (Crair et al. 1997) is consistent with our results in reporting that strongly weakened deprived-eye responses still showed orientation tuning. However, the authors also found that in small remaining cortical regions still responding strongly to the deprived eye, orientation selectivity of that eye was significantly degraded. This was, to a smaller extent, also true for non-deprived eye responses in these regions. We do not find degraded tuning in neurons which are still strongly driven by the deprived eye. However, this discrepancy could be due to the distinctly different visual cortex organization in the two species, as the patches of poorly tuned neurons in the cat study are located at specific positions in the orientation map of V1, namely the pinwheel centres, which are known to contain cells with broader tuning (Crair et al. 1997).

4.5.5. General conclusions

In this Chapter we have provided evidence in support of homeostatic changes regulating neuronal responsiveness in vivo during experience-dependent plasticity. Together with previous findings in this field, our results give credence to the idea that OD shifts induced by MD are likely mediated both by Hebbian and homeostatic rules. Future studies are required to reveal the exact mechanisms of how these rules are implemented at the level of individual cells and synapses.

5. Overview and Outlook

In this thesis, I addressed several aspects of development and plasticity in the mouse visual system, in particular concentrating on the role of neuronal activity in the initial formation of neuronal circuits and their subsequent experience-driven adaptations. Even though the early phase of visual system development is independent of sensory input, intrinsically generated neuronal activity has been shown to be important for setting up functionally meaningful connections. Later on, sensory-evoked activity is capable of sculpting neuronal circuits, especially in the cerebral cortex, thereby providing a powerful means to allow the brain to adapt to changing environments and to benefit from past experiences. It is still largely unresolved, however, to what extent activity influences the formation of neuronal networks, and especially, by which mechanisms neuronal spiking exerts its influence at different time points in development and throughout life. Moreover, it remains unclear how experience-induced adaptations of cortical circuits affect subsequent cortical function and plasticity.

To address these questions, I took advantage of two well established model systems in mice - topographic map formation in superior colliculus (SC) and ocular dominance (OD) plasticity in binocular visual cortex. Below, I summarize my main findings and point out some of the remaining open questions.

The role of retinal activity on retinotopic map formation

During retinotopic map formation in the SC, refinement of the initially diffuse retinocollicular projections has been demonstrated to be dependent on spontaneously generated, correlated activity in the retina (McLaughlin et al. 2003b). It remained open, however, if the lack of anatomical refinement caused by an early, transient disruption of correlated retinal ganglion cell (RGC) firing yields any consequences on functional connectivity. The work described in Chapter 2, together with a study by Chandrasekaran et al. (2005), showed that the anatomically unrefined projections in mice lacking retinal waves ($\beta 2^{-/-}$ mice) indeed caused functionally less precise mapping. Moreover, these functional deficits were not compensated after eye opening by experience-dependent refinement. Adapting intrinsic optical imaging to obtain functional maps from the SC additionally enabled me to examine the role of patterned RGC

activity for the overall retinotopic organization. I found that the lack of retinal waves not only led to local defects but also resulted in global distortions of the entire retinotopic map. The map of visual space was expanded anteriorly and compressed posteriorly, possibly caused by the initial, non-uniform ingrowth of RGC axons in combination with the lack of refinement. These results indicate that patterned neuronal activity is more influential in topographic map formation than previously thought, not only governing local refinement, but also shaping the gross organization.

Below I list several related questions that are particularly interesting and require further study:

- It would be interesting to examine whether retinal spiking is also important for the overall retinotopic organization in other visual areas like the LGN and the visual cortex, or if neuronal activity is particularly influential in SC development.
- Since molecular guidance signals and neuronal activity act jointly in setting up functional maps and circuits, a direct interaction between the two cues is conceivable. Ephrins and Eph receptors have been shown to be important for synapse formation and synaptic plasticity (Drescher 2000, Grunwald et al. 2004) and thus could play a role not only in axon guidance but also in functional circuit maturation. Conversely, neuronal activity could influence guidance cue expression and interaction. This could be investigated, for instance, by disrupting neuronal activity in restricted regions of the retina, to determine if the expression or function of different guidance molecules is altered in either RGCs or target structures.
- Once topographic maps are set up in midbrain and thalamus, they are thought to be relatively rigid and unsusceptible to visual experience later in life to ensure reliable sensory transmission. This actually not been examined in detail, in contrast to the cerebral cortex, where experience-dependent reorganization of topographic maps can take place also in adulthood (Buonomano and Merzenich 1998). It would be interesting to revisit plasticity of topographic representations at the subcortical level in greater detail to explore their potential for reorganization (e.g. following retinal lesions). Intrinsic optical imaging in the SC provides a well suited method for such a study.

Ocular dominance plasticity

The binocular representation in visual cortex seems to be far more susceptible to altered experience than retinotopic organization. Hence, by far the most important model for experience-dependent plasticity in the visual system is ocular dominance (OD) plasticity. Monocular deprivation (MD) strongly shifts OD of cortical neurons towards the open eye, most probably due to altered activity at deprived-eye synapses. Despite decades of research on this topic, surprisingly little is known about precisely how MD changes eye-specific responsiveness in the cortex. I examined this question in greater detail in Chapters 3 and 4. Intrinsic signal imaging enabled me to reliably assess the changes in the absolute magnitude of eye-specific responses, which underlie the deprivation-induced OD shifts. I found that brief MD in juvenile mice primarily led to weakening of deprived-eye population responses, consistent with previous studies (Chapter 3). Employing *in vivo* two-photon calcium imaging to monitor cortical responsiveness to visual stimulation at the single cell level (Chapter 4) provided the means to examine the MD-induced changes in greater detail and to gain insight into the cellular mechanisms underlying OD plasticity. Recording responses of thousands of individual neurons in the binocular cortex revealed that most cells changed their absolute responsiveness, shifting the OD towards the open eye. A small fraction of neurons, however, which received exclusive or dominant input from the deprived eye, did not lose this input, but showed even stronger responses to deprived eye stimulation after MD. This finding suggests that homeostatic changes act in monocular neurons to prevent the total loss of synaptic drive that might arise from Hebbian mechanisms. Binocular neurons, on the other hand, maintain their responsiveness in a different way, by shifting their responsiveness towards the stronger, non-deprived eye. The significant synaptic rewiring associated with OD shifts raises the question whether other functional properties in binocular cortex are also altered by MD. I explored this question by assessing orientation selectivity for each eye separately after deprivation. Binocular neurons seemed to be particularly affected, since strong concurrent orientation selectivity was lost in binocular cells after MD. Specifically, tuning of non-deprived eye responses seemed to be compromised in these cells, suggesting that the gain of non-deprived eye input following MD is non-specific. The weakening of inputs from the deprived eye, however, did not result in degraded orientation selectivity of responses to that eye (Chapter 4).

Adult plasticity

Intrinsic signal imaging as well as multi-unit recordings revealed extensive OD plasticity also in adult mice (Chapter 3). Both methods yielded very similar results, thus demonstrating once more that optical imaging of intrinsic signals faithfully reports spiking activity of neuronal populations. Interestingly, MD effects in adults seemed to be mediated by different mechanisms than in juvenile animals, since adult MD resulted primarily in a strengthening of non-deprived eye responses.

Intrinsic imaging in animals with restored binocular vision a few weeks after deprivation showed complete recovery of cortical responses in juvenile as well as in adult mice. Remarkably, when a second MD was induced several weeks later, OD shifts occurred faster and were more persistent than in response to the first deprivation, independent of age (Chapter 3). Since this enhancement of plasticity was specific to repeated closure of the same eye, it seems that the initial experience of MD leaves a lasting trace in the altered cortical connections. These results suggest that previous experiences can specifically expand the capacity of mature cortical circuits for change, thereby improving adaptation to similar experiences in the future.

Important questions concerning juvenile and adult OD plasticity still remain open or are brought up by the findings presented in this thesis:

- What happens in the monocular part of the mouse visual cortex after MD? Do cortical responses scale up there, too? What is the time course of homeostatic mechanisms and is homeostasis preceded by depression of deprived-eye responses?
- How is the computation of functional properties like orientation selectivity changed by the cortical reorganization following altered experience? Addressing this question might also shed light on how such properties evolve during development.
- Applying *in vivo* calcium imaging to assess adult OD plasticity and recovery from MD will provide further insights into the age-dependent mechanisms and effects on functional properties of individual cells.
- What is the nature of the permanent trace that seems to be established in cortical circuits by prior experience? The initial MD could lead to the formation of new connections,

which are maintained but functionally silenced or masked after restoring binocular vision, and as such may provide the substrate for future OD shifts. Repeated in vivo two-photon imaging of synaptic structures in the same animal during MD, recovery and second deprivation would be one approach to examine this theory.

The mouse will continue to serve as an effective model for investigating cortical plasticity. In particular, the rapid development of sophisticated imaging methods in combination with the still advancing transgenic technology will provide the means to answer many of the above questions in the near future. Understanding exactly how experiences influence and shape the circuits involved in sensory processing will hopefully also help to shed light on the mechanisms of learning and memory.

6. *References*

- Abraham WC, Bear MF (1996) Metaplasticity: the plasticity of synaptic plasticity. *Trends Neurosci* 19 (4), 126-130
- Adams DL, Horton JC (2003) Capricious expression of cortical columns in the primate brain. *Nat Neurosci* 6 (2), 113-114
- Antonini A, Fagiolini M, Stryker MP (1999) Anatomical correlates of functional plasticity in mouse visual cortex. *J Neurosci* 19 (11), 4388-4406
- Antonini A, Stryker MP (1993) Rapid remodeling of axonal arbors in the visual cortex. *Science* 260 (5115), 1819-1821
- Bansal A, Singer JH, Hwang BJ, Xu W, Beaudet A, Feller MB (2000) Mice lacking specific nicotinic acetylcholine receptor subunits exhibit dramatically altered spontaneous activity patterns and reveal a limited role for retinal waves in forming ON and OFF circuits in the inner retina. *J Neurosci* 20 (20), 7672-7681
- Bear MF (1995) Mechanism for a sliding synaptic modification threshold. *Neuron* 15 (1), 1-4
- Bear MF (2003) Bidirectional synaptic plasticity: from theory to reality. *Philos Trans R Soc Lond B Biol Sci* 358 (1432), 649-655
- Bear MF, Rittenhouse CD (1999) Molecular basis for induction of ocular dominance plasticity. *J Neurobiol* 41 (1), 83-91
- Beaver CJ, Fischer QS, Ji Q, Daw NW (2002) Orientation selectivity is reduced by monocular deprivation in combination with PKA inhibitors. *J Neurophysiol* 88 (4), 1933-1940

- Bi GQ, Poo MM (1998) Synaptic modifications in cultured hippocampal neurons: dependence on spike timing, synaptic strength, and postsynaptic cell type. *J Neurosci* 18 (24), 10464-10472
- Bienenstock EL, Cooper LN, Munro PW (1982) Theory for the development of neuron selectivity: orientation specificity and binocular interaction in visual cortex. *J Neurosci* 2 (1), 32-48
- Bonhoeffer F, Huf J (1982) In vitro experiments on axon guidance demonstrating an anterior-posterior gradient on the tectum. *EMBO J* 1 (4), 427-431
- Bonhoeffer T (1996) Neurotrophins and activity-dependent development of the neocortex. *Curr Opin Neurobiol* 6 (1), 119-126
- Bonhoeffer T, Grinvald A (1991) Iso-orientation domains in cat visual cortex are arranged in pinwheel-like patterns. *Nature* 353 (6343), 429-431
- Bonhoeffer T, Grinvald A (1996) Optical imaging based on intrinsic signals: The Methodology. (3), 55-97
- Brown A et al. (2000) Topographic mapping from the retina to the midbrain is controlled by relative but not absolute levels of EphA receptor signaling. *Cell* 102 (1), 77-88
- Buonomano DV, Merzenich MM (1998) Cortical plasticity: from synapses to maps. *Annu Rev Neurosci* 21 149-186
- Burrone J, Murthy VN (2003) Synaptic gain control and homeostasis. *Curr Opin Neurobiol* 13 (5), 560-567
- Butts DA (2002) Retinal waves: implications for synaptic learning rules during development. *Neuroscientist* 8 (3), 243-253

6. References

Cang J, Kaneko M, Yamada J, Woods G, Stryker MP, Feldheim DA (2005a) Ephrin-as guide the formation of functional maps in the visual cortex. *Neuron* 48 (4), 577-589

Cang J, Renteria RC, Kaneko M, Liu X, Copenhagen DR, Stryker MP (2005b) Development of precise maps in visual cortex requires patterned spontaneous activity in the retina. *Neuron* 48 (5), 797-809

Celikel T, Szostak VA, Feldman DE (2004) Modulation of spike timing by sensory deprivation during induction of cortical map plasticity. *Nat Neurosci* 7 (5), 534-541

Chandrasekaran AR, Plas DT, Gonzalez E, Crair MC (2005) Evidence for an instructive role of retinal activity in retinotopic map refinement in the superior colliculus of the mouse. *J Neurosci* 25 (29), 6929-6938

Changeux JP, Danchin A (1976) Selective stabilisation of developing synapses as a mechanism for the specification of neuronal networks. *Nature* 264 (5588), 705-712

Chapman B, Godecke I, Bonhoeffer T (1999) Development of orientation preference in the mammalian visual cortex. *J Neurobiol* 41 (1), 18-24

Chen L, Yang C, Mower GD (2001) Developmental changes in the expression of GABA(A) receptor subunits (alpha(1), alpha(2), alpha(3)) in the cat visual cortex and the effects of dark rearing. *Brain Res Mol Brain Res* 88 (1-2), 135-143

Cheng HJ, Nakamoto M, Bergemann AD, Flanagan JG (1995) Complementary gradients in expression and binding of ELF-1 and Mek4 in development of the topographic retinotectal projection map. *Cell* 82 (3), 371-381

Cline HT, Constantine-Paton M (1989) NMDA receptor antagonists disrupt the retinotectal topographic map. *Neuron* 3 (4), 413-426

Crair MC, Gillespie DC, Stryker MP (1998) The role of visual experience in the development of columns in cat visual cortex. *Science* 279 566-570

Crair MC, Ruthazer ES, Gillespie DC, Stryker MP (1997) Relationship between the ocular dominance and orientation maps in visual cortex of monocularly deprived cats. *Neuron* 19 (2), 307-318

Cynader M, Mitchell DE (1980) Prolonged sensitivity to monocular deprivation in dark-reared cats. *J Neurophysiol* 43 (4), 1026-1040

Dani JA (2001) Overview of nicotinic receptors and their roles in the central nervous system. *Biol Psychiatry* 49 (3), 166-174

Darian-Smith C, Gilbert CD (1994) Axonal sprouting accompanies functional reorganization in adult cat striate cortex. *Nature* 368 737-740

DeBello WM, Feldman DE, Knudsen EI (2001) Adaptive axonal remodeling in the midbrain auditory space map. *J Neurosci* 21 (9), 3161-3174

Desai NS (2003) Homeostatic plasticity in the CNS: synaptic and intrinsic forms. *J Physiol Paris* 97 (4-6), 391-402

Desai NS, Cudmore RH, Nelson SB, Turrigiano GG (2002) Critical periods for experience-dependent synaptic scaling in visual cortex. *Nat Neurosci* 5 (8), 783-789

Di Cristo G et al. (2001) Requirement of ERK activation for visual cortical plasticity. *Science* 292 (5525), 2337-2340

Dräger UC (1974) Autoradiography of tritiated proline and fucose transported transneuronally from the eye to the visual cortex in pigmented and albino mice. *Brain Res* 82 284-292

6. References

- Dräger UC (1975) Receptive fields of single cells and topography in mouse visual cortex. *J Comp Neurol* 160 (3), 269-290
- Dräger UC (1978) Observations on monocular deprivation in mice. *J Neurophysiol* 41 (1), 28-42
- Dräger UC, Hubel DH (1976) Topography of visual and somatosensory projections to mouse superior colliculus. *J Neurophysiol* 39 (1), 91-101
- Drescher U (2000) Excitation at the synapse: Eph receptors team up with NMDA receptors. *Cell* 103 (7), 1005-1008
- Drescher U, Kremoser C, Handwerker C, Loschinger J, Noda M, Bonhoeffer F (1995) In vitro guidance of retinal ganglion cell axons by RAGS, a 25 kDa tectal protein related to ligands for Eph receptor tyrosine kinases. *Cell* 82 (3), 359-370
- Dufour A et al. (2003) Area specificity and topography of thalamocortical projections are controlled by ephrin/Eph genes. *Neuron* 39 (3), 453-465
- Etienne AS, Maurer R, Seguinot V (1996) Path integration in mammals and its interaction with visual landmarks. *J Exp Biol* 199 (Pt 1), 201-209
- Fagiolini M, Fritschy JM, Low K, Mohler H, Rudolph U, Hensch TK (2004) Specific GABAA circuits for visual cortical plasticity. *Science* 303 (5664), 1681-1683
- Fagiolini M, Hensch TK (2000) Inhibitory threshold for critical-period activation in primary visual cortex. *Nature* 404 183-186
- Feldheim DA, Kim YI, Bergemann AD, Frisen J, Barbacid M, Flanagan JG (2000) Genetic analysis of ephrin-A2 and ephrin-A5 shows their requirement in multiple aspects of retinocollicular mapping. *Neuron* 25 (3), 563-574

- Feldheim DA et al. (1998) Topographic guidance labels in a sensory projection to the forebrain. *Neuron* 21 (6), 1303-1313
- Feller MB (2002) The role of nAChR-mediated spontaneous retinal activity in visual system development. *J Neurobiol* 53 (4), 556-567
- Feller MB, Wellis DP, Stellwagen D, Werblin FS, Shatz CJ (1996) Requirement for cholinergic synaptic transmission in the propagation of spontaneous retinal waves. *Science* 272 (5265), 1182-1187
- Fischer QS et al. (2004) Requirement for the RIIbeta isoform of PKA, but not calcium-stimulated adenylyl cyclase, in visual cortical plasticity. *J Neurosci* 24 (41), 9049-9058
- Flanagan JG, Vanderhaeghen P (1998) The ephrins and Eph receptors in neural development. *Annu Rev Neurosci* 21 309-345
- Frenkel MY, Bear MF (2004) How monocular deprivation shifts ocular dominance in visual cortex of young mice. *Neuron* 44 (6), 917-923
- Frisen J, Yates PA, McLaughlin T, Friedman GC, O'Leary DD, Barbacid N (1998) Ephrin-A5 (AL-1/RAGS) is essential for proper retinal axon guidance and topographic mapping in the mammalian visual system. *Neuron* 20 (2), 235-243
- Froemke RC, Dan Y (2002) Spike-timing-dependent synaptic modification induced by natural spike trains. *Nature* 416 (6879), 433-438
- Galli L, Maffei L (1988) Spontaneous impulse activity of rat retinal ganglion cells in prenatal life. *Science* 242 (4875), 90-91
- Gianfranceschi L, Fiorentini A, Maffei L (1999) Behavioural visual acuity of wild type and bcl2 transgenic mouse. *Vision Res* 39 (3), 569-574

6. References

Gnuegge L, Schmid S, Neuhauss SC (2001) Analysis of the activity-deprived zebrafish mutant macho reveals an essential requirement of neuronal activity for the development of a fine-grained visuotopic map. *J Neurosci* 21 (10), 3542-3548

Gordon JA, Stryker MP (1996) Experience-dependent plasticity of binocular responses in the primary visual cortex of the mouse. *J Neurosci* 16 (10), 3274-3286

Grinvald A, Lieke E, Frostig RD, Gilbert CD, Wiesel TN (1986) Functional architecture of cortex revealed by optical imaging of intrinsic signals. *Nature* 324 (6095), 361-364

Grubb MS, Rossi FM, Changeux JP, Thompson ID (2003) Abnormal functional organization in the dorsal lateral geniculate nucleus of mice lacking the beta 2 subunit of the nicotinic acetylcholine receptor. *Neuron* 40 (6), 1161-1172

Grubb MS, Thompson ID (2003) Quantitative characterization of visual response properties in the mouse dorsal lateral geniculate nucleus. *J Neurophysiol* 90 (6), 3594-3607

Grunwald IC et al. (2004) Hippocampal plasticity requires postsynaptic ephrinBs. *Nat Neurosci* 7 (1), 33-40

Grutzendler J, Kasthuri N, Gan WB (2002) Long-term dendritic spine stability in the adult cortex. *Nature* 420 (6917), 812-816

Guillery RW (1972) Binocular competition in the control of geniculate cell growth. *J Comp Neurol* 144 (1), 117-129

He HY, Hodos W, Quinlan EM (2006) Visual deprivation reactivates rapid ocular dominance plasticity in adult visual cortex. *J Neurosci* 26 (11), 2951-2955

Hensch TK (2005) Critical period plasticity in local cortical circuits. *Nat Rev Neurosci* 6 (11), 877-888

- Hensch TK, Fagiolini M, Mataga N, Stryker MP, Baekkeskov S, Kash SF (1998) Local GABA circuit control of experience-dependent plasticity in developing visual cortex. *Science* 282 (5393), 1504-1508
- Heynen AJ, Yoon BJ, Liu CH, Chung HJ, Haganir RL, Bear MF (2003) Molecular mechanism for loss of visual cortical responsiveness following brief monocular deprivation. *Nature Neuroscience* 6 (8), 854-862
- Hindges R, McLaughlin T, Genoud N, Henkemeyer M, O'Leary DD (2002) EphB forward signaling controls directional branch extension and arborization required for dorsal-ventral retinotopic mapping. *Neuron* 35 (3), 475-487
- Holtmaat AJ et al. (2005) Transient and persistent dendritic spines in the neocortex in vivo. *Neuron* 45 (2), 279-291
- Huang ZJ et al. (1999) BDNF regulates the maturation of inhibition and the critical period of plasticity in mouse visual cortex. *Cell* 98 (6), 739-755
- Hubel DH, Wiesel TN (1970) The period of susceptibility to the physiological effects of unilateral eye closure in kittens. *J Physiol* 206 (2), 419-436
- Hubel DH, Wiesel TN (1977) Functional architecture of macaque monkey visual cortex (Ferrier Lecture). *Proc R Soc Lond B* 198 1-59
- Hubel DH, Wiesel TN, LeVay S (1977) Plasticity of ocular dominance columns in monkey striate cortex. *Philos Trans R Soc Lond B Biol Sci* 278 (961), 377-409
- Hübener M (2003) Mouse visual cortex. *Curr Opin Neurobiol* 13 (4), 413-420
- Huberman AD, McAllister AK (2002) Neurotrophins and visual cortical plasticity. *Prog Brain Res* 138 39-51

6. References

Huberman AD, Murray KD, Warland DK, Feldheim DA, Chapman B (2005) Ephrin-As mediate targeting of eye-specific projections to the lateral geniculate nucleus. *Nat Neurosci* 8 (8), 1013-1021

Huberman AD, Stellwagen D, Chapman B (2002) Decoupling eye-specific segregation from lamination in the lateral geniculate nucleus. *J Neurosci* 22 (21), 9419-9429

Huberman AD, Wang GY, Liets LC, Collins OA, Chapman B, Chalupa LM (2003) Eye-specific retinogeniculate segregation independent of normal neuronal activity. *Science* 300 (5621), 994-998

Kalatsky VA, Stryker MP (2003) New paradigm for optical imaging: temporally encoded maps of intrinsic signal. *Neuron* 38 (4), 529-545

Kerr JN, Greenberg D, Helmchen F (2005) Imaging input and output of neocortical networks in vivo. *Proc Natl Acad Sci U S A* 102 (39), 14063-14068

Kind PC, Mitchell DE, Ahmed B, Blakemore C, Bonhoeffer T, Sengpiel F (2002) Correlated binocular activity guides recovery from monocular deprivation. *Nature* 416 (6879), 430-433

Kirkwood A, Rioult MC, Bear MF (1996) Experience-dependent modification of synaptic plasticity in visual cortex. *Nature* 381 (6582), 526-528

Knudsen EI (1998) Capacity for plasticity in the adult owl auditory system expanded by juvenile experience. *Science* 279 1531-1533

Knudsen EI (2002) Instructed learning in the auditory localization pathway of the barn owl. *Nature* 417 (6886), 322-328

Kobayashi T, Nakamura H, Yasuda M (1990) Disturbance of refinement of retinotectal projection in chick embryos by tetrodotoxin and grayanotoxin. *Brain Res Dev Brain Res* 57 (1), 29-35

- Koulakov AA, Chklovskii DB (2001) Orientation preference patterns in mammalian visual cortex: a wire length minimization approach. *Neuron* 29 (2), 519-527
- Krahe TE, Medina AE, Bittencourt-Navarrete RE, Colello RJ, Ramoa AS (2005) Protein synthesis-independent plasticity mediates rapid and precise recovery of deprived eye responses. *Neuron* 48 (2), 329-343
- Krakauer JW, Ghez C, Ghilardi MF (2005) Adaptation to visuomotor transformations: consolidation, interference, and forgetting. *J Neurosci* 25 (2), 473-478
- Kuhl PK (2004) Early language acquisition: cracking the speech code. *Nat Rev Neurosci* 5 (11), 831-843
- LeVay S, Stryker MP, Shatz CJ (1978) Ocular dominance columns and their development in layer IV of the cat's visual cortex: A quantitative study. *J Comp Neurol* 179 223-244
- Levi DM (2005) Perceptual learning in adults with amblyopia: a reevaluation of critical periods in human vision. *Dev Psychobiol* 46 (3), 222-232
- Liao DS, Krahe TE, Prusky GT, Medina AE, Ramoa AS (2004) Recovery of cortical binocularity and orientation selectivity after the critical period for ocular dominance plasticity. *J Neurophysiol* 92 (4), 2113-2121
- Liao DS, Mower AF, Neve RL, Sato-Bigbee C, Ramoa AS (2002) Different mechanisms for loss and recovery of binocularity in the visual cortex. *J Neurosci* 22 (20), 9015-9023
- Lickey ME, Pham TA, Gordon B (2004) Swept contrast visual evoked potentials and their plasticity following monocular deprivation in mice. *Vision Research* 44 (28), 3381-3387
- Linden DC, Guillery RW, Cucchiari J (1981) The dorsal lateral geniculate nucleus of the normal ferret and its postnatal development. *J Comp Neurol* 203 (2), 189-211

6. References

Linkenhoker BA, der Ohe CG, Knudsen EI (2005) Anatomical traces of juvenile learning in the auditory system of adult barn owls. *Nature Neuroscience* 8 (1), 93-98

Maldonado PE, Gödecke I, Gray CM, Bonhoeffer T (1997) Orientation selectivity in pinwheel centers in cat striate cortex. *Science* 276 1551-1555

Mandolesi G, Menna E, Harauzov A, von Bartheld CS, Caleo M, Maffei L (2005) A role for retinal brain-derived neurotrophic factor in ocular dominance plasticity. *Curr Biol* 15 (23), 2119-2124

Mangini NJ, Pearlman AL (1980) Laminar distribution of receptive field properties in the primary visual cortex of the mouse. *J Comp Neurol* 193 (1), 203-222

Mao BQ, Hamzei-Sichani F, Aronov D, Froemke RC, Yuste R (2001) Dynamics of spontaneous activity in neocortical slices. *Neuron* 32 (5), 883-898

Markram H, Lubke J, Frotscher M, Sakmann B (1997) Regulation of synaptic efficacy by coincidence of postsynaptic APs and EPSPs. *Science* 275 (5297), 213-215

Marks MJ, Whiteaker P, Grady SR, Picciotto MR, McIntosh JM, Collins AC (2002) Characterization of [(125) I]epibatidine binding and nicotinic agonist-mediated (86) Rb(+) efflux in interpeduncular nucleus and inferior colliculus of beta2 null mutant mice. *J Neurochem* 81 (5), 1102-1115

Masino SA, Kwon MC, Dory Y, Frostig RD (1993) Characterization of functional organization within rat barrel cortex using intrinsic signal optical imaging through a thinned skull. *Proc Natl Acad Sci U S A* 90 (21), 9998-10002

Mataga N, Mizuguchi Y, Hensch TK (2004) Experience-dependent pruning of dendritic spines in visual cortex by tissue plasminogen activator. *Neuron* 44 (6), 1031-1041

- Mataga N, Nagai N, Hensch TK (2002) Permissive proteolytic activity for visual cortical plasticity. *Proc Natl Acad Sci U S A* 99 (11), 7717-7721
- McCormick DA, Trent F, Ramoa AS (1995) Postnatal development of synchronized network oscillations in the ferret dorsal lateral geniculate and perigeniculate nuclei. *J Neurosci* 15 (8), 5739-5752
- McGee AW, Yang Y, Fischer QS, Daw NW, Strittmatter SM (2005) Experience-driven plasticity of visual cortex limited by myelin and Nogo receptor. *Science* 309 (5744), 2222-2226
- McGonigle BO, Flook J (1978) Long-term retention of single and multistate prismatic adaptation by humans. *Nature* 272 (5651), 364-366
- McLaughlin T, Hindges R, O'Leary DD (2003a) Regulation of axial patterning of the retina and its topographic mapping in the brain. *Curr Opin Neurobiol* 13 (1), 57-69
- McLaughlin T, Torborg CL, Feller MB, O'Leary DD (2003b) Retinotopic map refinement requires spontaneous retinal waves during a brief critical period of development. *Neuron* 40 (6), 1147-1160
- Meister M, Wong RO, Baylor DA, Shatz CJ (1991) Synchronous bursts of action potentials in ganglion cells of the developing mammalian retina. *Science* 252 (5008), 939-943
- Metin C, Godement P, Imbert M (1988) The primary visual cortex in the mouse: receptive field properties and functional organization. *Exp Brain Res* 69 (3), 594-612
- Mioche L, Singer W (1989) Chronic recordings from single sites of kitten striate cortex during experience-dependent modifications of receptive-field properties. *J Neurophysiol* 62 (1), 185-197
- Mitchell DE, Cynader M, Movshon JA (1977) Recovery from the effects of monocular deprivation in kittens. *J Comp Neurol* 176 (1), 53-63

6. References

Morris R (1984) Developments of a water-maze procedure for studying spatial learning in the rat. *J Neurosci Methods* 11 (1), 47-60

Mower AF, Liao DS, Nestler EJ, Neve RL, Ramoa AS (2002) cAMP/Ca²⁺ response element-binding protein function is essential for ocular dominance plasticity. *J Neurosci* 22 (6), 2237-2245

Mower GD (1991) The effect of dark rearing on the time course of the critical period in cat visual cortex. *Brain Res Dev Brain Res* 58 (2), 151-158

Mui SH, Hindges R, O'Leary DD, Lemke G, Bertuzzi S (2002) The homeodomain protein Vax2 patterns the dorsoventral and nasotemporal axes of the eye. *Development* 129 (3), 797-804

Muir DW, Mitchell DE (1973) Visual resolution and experience: acuity deficits in cats following early selective visual deprivation. *Science* 180 (84), 420-422

Muir-Robinson G, Hwang BJ, Feller MB (2002) Retinogeniculate axons undergo eye-specific segregation in the absence of eye-specific layers. *J Neurosci* 22 (13), 5259-5264

Murphy EH, Berman N (1979) The rabbit and the cat: a comparison of some features of response properties of single cells in the primary visual cortex. *J Comp Neurol* 188 (3), 401-427

Naeff B, Schlumpf M, Lichtensteiger W (1992) Pre- and postnatal development of high-affinity [³H]nicotine binding sites in rat brain regions: an autoradiographic study. *Brain Res Dev Brain Res* 68 (2), 163-174

Nägerl UV, Eberhorn N, Cambridge SB, Bonhoeffer T (2004) Bidirectional activity-dependent morphological plasticity in hippocampal neurons. *Neuron* 44 (5), 759-767

- Ohki K, Chung S, Ch'ng YH, Kara P, Reid RC (2005) Functional imaging with cellular resolution reveals precise micro-architecture in visual cortex. *Nature* 433 (7026), 597-603
- Oray S, Majewska A, Sur M (2004) Dendritic spine dynamics are regulated by monocular deprivation and extracellular matrix degradation. *Neuron* 44 (6), 1021-1030
- Pang PT et al. (2004) Cleavage of proBDNF by tPA/plasmin is essential for long-term hippocampal plasticity. *Science* 306 (5695), 487-491
- Penn AA, Riquelme PA, Feller MB, Shatz CJ (1998) Competition in retinogeniculate patterning driven by spontaneous activity. *Science* 279 (5359), 2108-2112
- Pham TA et al. (2004) A semi-persistent adult ocular dominance plasticity in visual cortex is stabilized by activated CREB. *Learning & Memory* 11 (6), 738-747
- Pham TA, Impey S, Storm DR, Stryker MP (1999) CRE-mediated gene transcription in neocortical neuronal plasticity during the developmental critical period. *Neuron* 22 (1), 63-72
- Philpot BD, Espinosa JS, Bear MF (2003) Evidence for altered NMDA receptor function as a basis for metaplasticity in visual cortex. *J Neurosci* 23 (13), 5583-5588
- Picciotto MR et al. (1995) Abnormal avoidance learning in mice lacking functional high-affinity nicotine receptor in the brain. *Nature* 374 (6517), 65-67
- Pizzorusso T, Medini P, Berardi N, Chierzi S, Fawcett JW, Maffei L (2002) Reactivation of ocular dominance plasticity in the adult visual cortex. *Science* 298 (5596), 1248-1251
- Pizzorusso T, Medini P, Landi S, Baldini S, Berardi N, Maffei L (2006) Structural and functional recovery from early monocular deprivation in adult rats. *Proc Natl Acad Sci U S A*
- Prusky GT, Douglas RM (2003) Developmental plasticity of mouse visual acuity. *Eur J Neurosci* 17 (1), 167-173

6. References

- Rao Y, Fischer QS, Yang Y, McKnight GS, LaRue A, Daw NW (2004) Reduced ocular dominance plasticity and long-term potentiation in the developing visual cortex of protein kinase A RII alpha mutant mice. *Eur J Neurosci* 20 (3), 837-842
- Renger JJ, Hartman KN, Tsuchimoto Y, Yokoi M, Nakanishi S, Hensch TK (2002) Experience-dependent plasticity without long-term depression by type 2 metabotropic glutamate receptors in developing visual cortex. *Proc Natl Acad Sci U S A* 99 (2), 1041-1046
- Rittenhouse CD, Shouval HZ, Paradiso MA, Bear MF (1999) Monocular deprivation induces homosynaptic long-term depression in visual cortex. *Nature* 397 (6717), 347-350
- Rossi FM, Pizzorusso T, Porciatti V, Marubio LM, Maffei L, Changeux JP (2001) Requirement of the nicotinic acetylcholine receptor beta 2 subunit for the anatomical and functional development of the visual system. *Proc Natl Acad Sci U S A* 98 (11), 6453-6458
- Rubin BD, Katz LC (1999) Optical imaging of odorant representations in the mammalian olfactory bulb. *Neuron* 23 (3), 499-511
- Ruthazer ES, Akerman CJ, Cline HT (2003) Control of axon branch dynamics by correlated activity in vivo. *Science* 301 (5629), 66-70
- Sanes JR, Yamagata M (1999) Formation of lamina-specific synaptic connections. *Curr Opin Neurobiol* 9 (1), 79-87
- Sawtell NB, Frenkel MY, Philpot BD, Nakazawa K, Tonegawa S, Bear MF (2003) NMDA receptor-dependent ocular dominance plasticity in adult visual cortex. *Neuron* 38 977-985
- Schmitt AM, Shi J, Wolf AM, Lu CC, King LA, Zou Y (2006) Wnt-Ryk signalling mediates medial-lateral retinotectal topographic mapping. *Nature* 439 (7072), 31-37
- Schuett S, Bonhoeffer T, Hübener M (2001) Pairing-induced changes of orientation maps in cat visual cortex. *Neuron* 32 (2), 325-337

- Schuett S, Bonhoeffer T, Hübener M (2002) Mapping retinotopic structure in mouse visual cortex with optical imaging. *J Neurosci* 22 (15), 6549-6559
- Schummers J, Marino J, Sur M (2002) Synaptic integration by V1 neurons depends on location within the orientation map. *Neuron* 36 (5), 969-978
- Shatz CJ, Stryker MP (1978) Ocular dominance in layer IV of the cat's visual cortex and the effects of monocular deprivation. *J Physiol (Lond)* 281 267-283
- Sherman SM, Spear PD (1982) Organization of visual pathways in normal and visually deprived cats. *Physiol Rev* 62 (2), 738-855
- Shiosaka S, Yoshida S (2000) Synaptic microenvironments--structural plasticity, adhesion molecules, proteases and their inhibitors. *Neurosci Res* 37 (2), 85-89
- Simon DK, O'Leary DD (1991) Relationship of retinotopic ordering of axons in the optic pathway to the formation of visual maps in central targets. *J Comp Neurol* 307 (3), 393-404
- Simon DK, O'Leary DD (1992) Development of topographic order in the mammalian retinocollicular projection. *J Neurosci* 12 (4), 1212-1232
- Simon DK, Prusky GT, O'Leary DD, Constantine-Paton M (1992) N-methyl-D-aspartate receptor antagonists disrupt the formation of a mammalian neural map. *Proc Natl Acad Sci U S A* 89 (22), 10593-10597
- Smetters D, Majewska A, Yuste R (1999) Detecting action potentials in neuronal populations with calcium imaging. *Methods* 18 (2), 215-221
- Sperry R (1963) Chemoaffinity in the orderly growth of nerve fiber patterns and connections. *Proc Natl Acad Sci* 50 703-710

6. References

- Stellwagen D, Shatz CJ (2002) An instructive role for retinal waves in the development of retinogeniculate connectivity. *Neuron* 33 (3), 357-367
- Stosiek C, Garaschuk O, Holthoff K, Konnerth A (2003) In vivo two-photon calcium imaging of neuronal networks. *Proc Natl Acad Sci USA* 100 (12), 7319-7324
- Swindale NV, Shoham D, Grinvald A, Bonhoeffer T, Hübener M (2000) Visual cortex maps are optimized for uniform coverage. *Nat Neurosci* 3 (8), 822-826
- Tagawa Y, Kanold PO, Majdan M, Shatz CJ (2005) Multiple periods of functional ocular dominance plasticity in mouse visual cortex. *Nat Neurosci* 8 (3), 380-388
- Taha S, Hanover JL, Silva AJ, Stryker MP (2002) Autophosphorylation of alpha CaMKII is required for ocular dominance plasticity. *Neuron* 36 (3), 483-491
- Thompson I, Holt C (1989) Effects of intraocular tetrodotoxin on the development of the retinocollicular pathway in the Syrian hamster. *J Comp Neurol* 282 (3), 371-388
- Torborg CL, Hansen KA, Feller MB (2005) High frequency, synchronized bursting drives eye-specific segregation of retinogeniculate projections. *Nat Neurosci* 8 (1), 72-78
- Torii N, Kamishita T, Otsu Y, Tsumoto T (1995) An inhibitor for calcineurin, FK506, blocks induction of long-term depression in rat visual cortex. *Neurosci Lett* 185 (1), 1-4
- Trachtenberg JT et al. (2002) Long-term in vivo imaging of experience-dependent synaptic plasticity in adult cortex. *Nature* 420 (6917), 788-794
- Tribollet E, Bertrand D, Marguerat A, Raggenbass M (2004) Comparative distribution of nicotinic receptor subtypes during development, adulthood and aging: an autoradiographic study in the rat brain. *Neuroscience* 124 (2), 405-420

- Turrigiano GG, Nelson SB (2004) Homeostatic plasticity in the developing nervous system. *Nat Rev Neurosci* 5 (2), 97-107
- Van Hooser SD, Heimel JAF, Chung S, Nelson SB, Toth LJ (2005) Orientation selectivity without orientation maps in visual cortex of a highly visual mammal. *J Neurosci* 25 (1), 19-28
- van Rossum MC, Bi GQ, Turrigiano GG (2000) Stable Hebbian learning from spike timing-dependent plasticity. *J Neurosci* 20 (23), 8812-8821
- Wagor E, Mangini NJ, Pearlman AL (1980) Retinotopic organization of striate and extrastriate visual cortex in the mouse. *J Comp Neurol* 193 (1), 187-202
- Watanabe M, Kobayashi Y, Inoue Y, Isa T (2005) Effects of local nicotinic activation of the superior colliculus on saccades in monkeys. *J Neurophysiol* 93 (1), 519-534
- Weliky M, Bosking WH, Fitzpatrick D (1996) A systematic map of direction preference in primary visual cortex. *Nature* 379 (6567), 725-728
- White LE, Coppola DM, Fitzpatrick D (2001) The contribution of sensory experience to the maturation of orientation selectivity in ferret visual cortex. *Nature* 411 (6841), 1049-1052
- Wiesel TN, Hubel DH (1963) Single cell responses in striate cortex of kittens deprived of vision in one eye. *J Neurophysiol* 26 1003-1017
- Williams SE et al. (2003) Ephrin-B2 and EphB1 mediate retinal axon divergence at the optic chiasm. *Neuron* 39 (6), 919-935
- Willshaw DJ, von der Malsburg C (1976) How patterned neural connections can be set up by self-organization. *Proc R Soc Lond B Biol Sci* 194 (1117), 431-445
- Wong RO (1999) Retinal waves and visual system development. *Annu Rev Neurosci* 22 29-47

6. References

Wong RO, Chernjavsky A, Smith SJ, Shatz CJ (1995) Early functional neural networks in the developing retina. *Nature* 374 (6524), 716-718

Wong WT, Myhr KL, Miller ED, Wong RO (2000) Developmental changes in the neurotransmitter regulation of correlated spontaneous retinal activity. *J Neurosci* 20 (1), 351-360

Xu W et al. (1999) Multiorgan autonomic dysfunction in mice lacking the beta2 and the beta4 subunits of neuronal nicotinic acetylcholine receptors. *J Neurosci* 19 (21), 9298-9305

Yang Y, Fischer QS, Zhang Y, Baumgartel K, Mansuy IM, Daw NW (2005) Reversible blockade of experience-dependent plasticity by calcineurin in mouse visual cortex. *Nat Neurosci* 8 (6), 791-796

Yates PA, Roskies AL, McLaughlin T, O'Leary DD (2001) Topographic-specific axon branching controlled by ephrin-As is the critical event in retinotectal map development. *J Neurosci* 21 (21), 8548-8563

Yoshimura Y, Ohmura T, Komatsu Y (2003) Two forms of synaptic plasticity with distinct dependence on age, experience, and NMDA receptor subtype in rat visual cortex. *J Neurosci* 23 (16), 6557-6566

Yuste R, Nelson DA, Rubin WW, Katz LC (1995) Neuronal domains in developing neocortex: mechanisms of coactivation. *Neuron* 14 (1), 7-17

Zheng J, Lee S, Zhou ZJ (2006) A transient network of intrinsically bursting starburst cells underlies the generation of retinal waves. *Nat Neurosci* 9 (3), 363-371

Zhou Q, Homma KJ, Poo MM (2004) Shrinkage of dendritic spines associated with long-term depression of hippocampal synapses. *Neuron* 44 (5), 749-757

Zhou ZJ, Zhao D (2000) Coordinated transitions in neurotransmitter systems for the initiation and propagation of spontaneous retinal waves. *J Neurosci* 20 (17), 6570-6577

Publications based on the work in this thesis

Hofer SB, Mrsic-Flogel TD, Bonhoeffer T, Hübener M

Lifelong learning: ocular dominance plasticity in mouse visual cortex

Current Opinion in Neurobiology, review, in press

Hofer SB, Mrsic-Flogel TD, Bonhoeffer T, Hübener M (2006)

Prior experience enhances plasticity in adult visual cortex.

Nature Neuroscience, 9 (1): 127-132

Mrsic-Flogel TD, **Hofer SB**, Creutzfeldt C, Cloez-Tayarani I, Changeux JP, Bonhoeffer T, Hübener M (2005)

Altered map of visual space in the superior colliculus of mice lacking early retinal waves

Journal of Neuroscience, 25 (29): 6921-6928

Curriculum vitae

Personal Data

Name:	Sonja Hofer
Date of birth:	April 30 th , 1977
Place of birth:	Munich, Germany
Citizenship:	German

Education

11/2002 -	PhD under the supervision of PD Dr. Mark Hübener and Prof. Dr. Tobias Bonhoeffer, Max-Planck-Institute of Neurobiology
04/2001 - 04/2002	Diploma Thesis with Prof. Dr. Georg Klump, Technical University of Munich and University of Oldenburg: "Comodulation masking release and auditory grouping: a physiological study on signal detection in narrow-band noise in the auditory forebrain of European starlings"
11/1996 - 04/2002	Undergraduate study in Biology at the Technical University of Munich, major subject: Zoology, minor subjects: Biochemistry, cell biology, behavioral ecology degree: diploma (final grade: 1.0, "with distinction")
1996	Abitur (High-School Diploma) at Unterhaching Gymnasium, Germany (final grade: 1.1)

Teaching, Professional Experience

08/2002 – 10/2002	Research Assistant at the Department of Zoophysiology and Behavior, University of Oldenburg
05/2002 - 07/2002	Teaching Assistant at the Department of Zoology, Technical University of Munich

Grants, Awards

07/2006	FENS Forum 2006, travel grant
06/2003	CSHL, travel grant
12/2002	Junior Scientist Award, 2 nd place, NeuroNord Conference
04/1999 - 04/2002	Scholarship of the "Studienstiftung des deutschen Volkes"

List of publications

Hofer SB, Mrsic-Flogel TD, Bonhoeffer T, Hübener M. Lifelong learning: ocular dominance plasticity in mouse visual cortex. Current Opinion in Neurobiology, in press

Hofer SB, Mrsic-Flogel TD, Bonhoeffer T, Hübener M (2006). Prior experience enhances plasticity in adult visual cortex. Nature Neuroscience 9 (1): 127-132

Mrsic-Flogel TD, **Hofer SB**, Creutzfeldt C, Cloez-Tayarani I, Changeux JP, Bonhoeffer T, Hübener M (2005). Altered map of visual space in the superior colliculus of mice lacking early retinal waves. Journal of Neuroscience, 25 (29): 6921-6928

Hofer SB, Klump GM (2003). Within- and across-channel processing in auditory masking: A physiological study in the songbird forebrain. Journal of Neuroscience, 23(13): 5732-5739

Gehr DD, **Hofer SB**, Marquardt D, Leppelsack HJ (2000). Functional changes in field L complex during song development of juvenile male zebra finches. Developmental Brain Research, 125 (1-2): 153-165